Influence of Plant Water Relation on Ecosystem Function under Water Stress

Dissertation

zur Erlangung des akademischen Grades doctor rerum naturalium

(Dr. rer. nat.)

vorgelegt dem Rat der Chemisch-Geowissenschaftlichen Fakultät der

Friedrich-Schiller-Universität Jena

von

MSc. Sisay Girma Tessema

geboren am 13.05.1979 in Arsi, Ethiopia

Gutachter:

1.

2.

Tag der öffentlichen Verteidigung:

Zusammenfassung: Fokus der vorliegenden Arbeit ist die Wechselwirkung von Biodiversität und oberflächennahen Grundwasserunter Trockenstress (Evapotranspiration¿ Niederschlag), wobei das Arbeitsgebiet, ein großmaßstäblich angelegtes Feldexperiment zur Biodiversität (Jena Experiment), zunächst im Hinblick auf Hydrogeologie und hydrochemische Prozesse im Grund- und Bodenwasser untersucht wird. Das Testfeld umfasst zum einen vier Blöcke (Blick I, II, III und IV), welche wiederum in Plots mit unterschiedlicher Biodiversität (Spezies und funktionelle Gruppen) unterteilt sind, und zum anderen Grundwassermessstellen. Bevor auf einen Zusammenhang zur Biodiversität eingegangen wird, wird zunächst die räumliche und jahreszeitliche Variation (Einfluss von Trockenstress) der hydrochemischen Zusammensetzung des Grundwassers, sowie den Einfluss des nahegelegenen Flusses Saale auf das Grundwasserbetrachtet.

Für die Interpretation der hydrogeochemischen Daten wurden statistische Methoden angewandt auf deren Basis fünf vorherrschende Faktoren identifiziert, zu denen sich ca. 90% der Varianz des hydrogeochemischen Datensatzes der der kalten Jahreszeit zugeordneten Monate (März, April, November) und der der warmen Jahreszeit zugeordneten Monate (Juni, August) zuordnen lassen. Weiterhin resultierte die Faktorenanalyse in einer 43%igen Varianz im Datensatz der kalten Monate und 53% der Varianz im Datensatz der warmen Monate welche den Hauptkat- und anionen zugeordnet werden kann, was wiederum auf Interaktionen des Grundwassers mit dem Aquifermaterial hindeutet. Weitere 15% bzw. 19% der Varianz in den kalten bzw. warmen Monaten gehen auf Redox und redoxsensitive Elemente zurück. Hydrogeochemische Modellierungen mit PHREEQC zeigten dass die mit Röntgendiffraktometrie nachgewiesenen Minerale Calcit, Dolomit, Quarz und Siderit für die Änderung der hydrochemischen Zusammensetzung des Grundwassers herangezogen werden können.

Die Betrachtung der räumlichen Verteilung der hydrogeochemischen Ergebnisse zeigte, dass speziell die Plots BIIIA02 und BIIIA13 in Block III sich von den anderen Plots

unterscheiden. Texturzusammensetzungen von Proben, die verschiedenen Bohrungen auf dem Testfeld entnommen wurden, weisen darauf hin, dass die unterste beprobte Schicht in Block III hauptsächlich aus kiesigen Sand besteht, was wiederum zu einer geringeren Verweilzeit und weniger gelöste Inhaltsstoffe führt. Der Vergleich der chemischen Zusammensetzung des Untersuchungsgebietes mit Grundwasser, welches aus verschiedenen geologischen Einheiten stammt, zeigt, dass das Grundwasser der meisten Plots im Untersuchungsgebiet die hydrochemische Signatur des Oberen Buntsandsteins wiederspiegelt.

Der Vergleich der verschiedenen Jahreszeiten zugeordneten Datensätze zeigt eine saisonal und räumlich abhängige Grundwasserzusammensetzung hinsichtlich der Elemente Ba, B, Fe, Mn, U, V, Zn, Sr, Ni, HCO_3^- und DOC. Die Hauptwassertypen im Untersuchungsgebiet lassen sich den geologischen Einheiten zuordnen; bspw. Ca-Mg-HCO_3^- (in den Plots B3A02, B3A13 im Muschelkalk), Ca-Mg-SO_4^{2-} und Ca-Mg-Cl- in allen anderen Plots und Grundwässern des Buntsandsteins. Die Untersuchung von Wasserstoff- und Sauerstoffisotopen im Grundwasser deutete auf eine Anreicherung im Block III (besonders in den Plots B3A02, B3A13) hin. Eine mögliche Ursache könnte das Fällen von Calcite durch die Reaktion von Calcium mit isotopischleichtem Wasser und Kohlenstoffdioxid sein. Des Weiteren wurde eine Abreicherung von Sauerstoff- und Wasserstoffisotopen in der kalten Jahreszeit beobachtet.

Bevor die Wechselwirkung von Biodiversität und Boden- und Grundwasser betrachtet wurde, wurde zunächst der Einfluss von weiteren Faktoren (bspw. des nahegelegenen Flusses Saale, eines unterirdisch verlaufenden Abflussrohrs und des Niederschlag s) bewertet. Dazu wurden hydrochemische Modellierungen mit PHREEQC, Zeitreihenanalyse und der Verwendung von Chlorid als hydrologischen Tracer herangezogen. Die Ergebnisse der PHREEQC-Modellierungen zeigten, dass kein signifikanter Einfluss der Saale auf die Grundwasserchemie im Untersuchungsgebiet vorliegt. Bei zunehmend influenten Verhältnissen steigen jedoch die Konzentrationen von Fe,

K, Ca, Cl^-, Mg, Mn, SO_4^{2-} und NO_3^- im Grundwasser signifikant an. Die Vermutung einer bestehenden Wechselwirkung des künstlich angelegten Wasserkanals mit dem Grundwasser und dem damit verbundenen hydrogeochemischen Einfluss des Kanals auf das Grundwasser wurde basierend auf den Tracerstudien mit Chlorid nicht bestätigt.

Zur Untersuchung der Wechselwirkung von Biodiversität und Boden- und Grundwasser wurdeChlorid als hydrologischer Tracer herangezogen. Durch die Betrachtung des vertikalenChloridtransports unter Trockenstress konnte keine konkrete Korrelation zwischen der Biodiversität der Pflanzen und dem Wasserfluss der ungesättigten Zone nachgewiesen werden, allerdings jedoch eine positive Korrelation des LAI (leafareaindex) und der Chloridakkumulation. Der Zusammenhang von LAI und Diversität wurde bereits in vorangegangenen Studien nachgewiesen. Ein höherer LAI und eine hochgewachsenere Vegetation verringern die Oberfläche der Pflanze und verstärken die Evapotranspiration. Plots mit einer höheren Evaporation zeigten wiesen auch eine höhere Akkumulation von Chlorid nahe der Oberfläche auf. Des Weiteren konnte basierend auf den Ergebnissen des Chloridtransports in der ungesättigten Zone festgestellt werden, dass Plots mit einem höheren Anteil an funktionellen Gruppen (hier: höhere Diversität) und Plots in denen sowohl tief- als auch flachwurzelnde Pflanzen vorkamen mehr Chlorid in den oberflächennahen Schichten akkumulieren.

Summary: In this thesis we study the interaction between biodiversity and near surface groundwater, during water stress by first characterizing the study area in terms of groundwater and soil water geochemical processes and hydrogeology in a large-scale biodiversity experiment (the Jena experiment). We also investigated the spatial and seasonal variation of groundwater chemical composition and the effect of the river Saale on the groundwater of the main experimental field by taking water stress into account before relating to diversity. The experimental field is constructed in four blocks (block I, II, III and IV) which contain several plots over which different plant diversity (species and functional group diversity) are grown and groundwater wells are also located as well.

Characterization of the groundwater hydrochemical data using statistical technique shows that there are five dominant factors that account for about 90% of the variation of the chemical data set in the cold season (March, April, November) and the warm season (June, August). Factor analysis results showed that 43% of the variation in the cold season and 53% of the variation in the warm season of the groundwater hydrochemical data is due to major cations and anions. This reveals groundwater-geological matrix interaction. Redox- and redox-sensitive elements are the next important factors and account for 15% and 19% variation in cold season and warm season, respectively. The hydrochemical modeling using PHREEQC results showed that calcite, dolomite, quartz, and siderite are reactive minerals and are responsible for changes in chemical composition. X-ray diffraction was used to validate the result from PHREEQC.

The spatial variation of the groundwater chemical composition of the experimental field was analyzed and the result showed that sampled plots (BIIIA02, BIIIA13) in block III have relatively different chemical composition from other plots. From textural composition of the boreholes in the experimental field we observed that the lower layer of block III are mainly gravely sand, and showed lower dissolved solids concentration since the hydraulic residence time is low. The comparison of chemical

composition of the groundwater of our study area with the groundwater hosted in various hydrogeologic formation shows that, the groundwater in most of the plots of the study area have similar hydrochemical signature with the Upper Buntsandstein.

The hydrochemical data of the two seasons (cold and warm season) were also compared and the results showed that, the groundwater chemistry of the study area varied seasonally and spatially in terms of some parameters such as mainly metals (Ba, B, Fe, Mn, U, V, Zn, Sr, Ni), HCO_3 and DOC. Graphical technique (using AquaChem) results show that the groundwater type of the study area are Ca-Mg-HCO_3 (in plots BIIIA02, BIIIA13 and in the Muschelkalk hydrogeologic unit) and Ca-Mg-SO_4 and Ca-Mg-Cl in all other plots and groundwater in the Buntsandstein hydrogeologic unit. Hydrogen and oxygen isotope of the groundwater results also shows that most of the ground waters in wells of block III specially plots BIIIA13 and BIIIA02 are more enriched than that in other plots. This could be because calcium precipitates by reacting with lighter water and carbon dioxide to form calcite. We also observed that, in depletion of oxygen and hydrogen isotopes occurs during the cold season.

Before studying the interaction of biodiversity on subsurface water, we investigated the effect external factors (nearby river Saale, precipitation and an underground channel) on the groundwater of the study area. Hydrogeochemical modeling using PHREEQC, time series analysis and chloride (hydrological tracer) were used to investigate the effects. PHREEQC results show that there is no significant effect of the river on the groundwater chemistry of the study area at mean river flow. However, Fe, K, Ca, Cl, Mg, Mn, SO_4^{2-} and NO_3^- concentrations of the groundwater are predicted to increase significantly when the influx of the river increases toward the groundwater of the study area. Chloride concentration (used as hydrologic tracer) measured at the inlet of the channel and in groundwater shows that the channel did not leak and therefore has no effect on the groundwater.

Chloride was used as a hydrological tracer to study the interaction between biodiversity and subsurface water. The upward chloride transport during water stress, could not show a clear correlation between the aboveground diversity and water flow in the unsaturated zone. However, we could see a positive correlation of LAI (leaf area index) and chloride accumulation. Previous studies already showed that the LAI is positively correlated with diversity. The higher LAI and taller vegetation heights reduced surface and aerodynamic resistance to flow of water vapor which in turn increased the rate of evapotranspiration. Plots with a higher rate of evapotranspiration show a higher accumulation of more chloride near the surface of the earth. We could also observe from the results of chloride transport in the unsaturated zone, that plots with more plant functional groups (higher diversity) and those with a mixture of deep and shallow roots accumulate more chloride near the ground surface.

Contents

Abbreviation	**Description**
ICP-OES	Inductively Coupled Plasma Optical Emission Spectrometry
ICP-MS	Inductively Coupled Plasma Mass Spectrometry
TLUG	Thüringer Landesanstalt für Umwelt und Geologie
SI	Saturation Index
IAP	Ion Activity Product
DOC	Dissolved Organic Carbon $[mg/L]$
TOC	Total Organic Carbon $[mg/L]$
XRD	X-ray Diffraction
CCF	Cross Correlation Function
ACF	Auto Correlation Function
ET	Evapotranspiration [mm/day]
EC	Electrical Conductivity [μS/cm]
LAI	Leaf Area Index [m^2 leaf area/m^2 Soil surface]
LAI_{active}	Active Leaf Area Index [m^2 leaf area/m^2 Soil surface]
VSMO	Vienna Standard Mean Ocean Water
GMWL	Global Meteoric Water Line
TDS	Total Dissolved Solids $[mg/L]$
RH	Relative Humidity [%]
CEC	Cation Exchange Capacity
UTM	Universal Transverse Mercator

List of Figures

List of Tables

Chapter 1

Introduction

1.1 Motivation

Surface temperature of the globe is projected to increase by 1.4-5.8°C by 2100, in reaction to the rise in concentration of the greenhouse gases in the atmosphere (Houghton et al. 2001). Climate change affects the ecosystem in which all plants and animals live and therefore, loss of biodiversity as a result. Loss of biodiversity is one of the big problem mankind increases during the last century (McLaren 2006). Recent biodiversity extinction rate is 100 to 1000 faster than at prehuman level (Pimm et al. (1995)). There is a concern that species loss has an effect on ecosystem processes and functioning (Tilman and Downing (1994)). Species-poor ecosystems may perform (in terms of productivity, nutrient and water use) differently or less efficiently than the species-rich system from which they are derived (Zedler et al. (2001)). This concern has motivated research to focus on how biodiversity loss affects ecosystem functioning.

Studies on different aspects of biodiversity have been conducted by many researchers in the last decades. Biodiversity has been shown to affect ecosystem functions (McGrady-Steed et al. (1997), Tilman et al. (1997)). It has an effect on element cycles, carbon storage (Fornara and Tilman 2009, Steinbeiss et al. 2008) and water storage in soil (http://ec.europa.eu/environment/soil 2010). Palmborg et al. (2005),

Oelmann et al. (2007) showed that the nitrate pool in general decreased with increasing species richness. However, some functional groups might also increase the nitrogen content (Palmborg et al. 2005). Productivity (plant biomass) increases as the species richness (measure of diversity) increases (Marquard et al. 2009, Tilman et al. 1997, Cardinale et al. 2006).

Diversity affects also water movement in the soil. There are times when the resources (e.g. water) are limited and out of reach for plant community. During water stress plants might take up water from shallow groundwater. However the way they take is dependent up on the above ground species composition, richness as well as functional group type. The water consumption pattern changes if the community is diverse. The composition of the above ground plants can also affect the rate of evapotranspiration, which determines the rate of groundwater upward flow during water stress. However, how the diversity influences resource consumption is studied only for some resources, such as nitrate and phosphate. Most of the biodiversity studies focus on aboveground systems. Preliminary studies on the below ground system were also made by Mirgorodsky (2007), Steinbeiss (2006), Kreutziger (2006). In our study we will focus on the linkage between below-ground and above-ground system and see if the plant diversity affects water and nutrient transport from shallow groundwater during water stress in a large grassland experimental field, the Jena experiment. This work involves the characterization of the subsurface in terms of the geochemical background, geology and hydrogeology and then study the effect of hydrological features (river Saale and channel) on the ground water of the study area. Finally it investigates how the above and below below-ground system are related specially, on the effect of level of plant diversity on the subsurface water under stress condition.

Biodiversity improves local climate (http://www.cbd.int/climate/intro.shtml 2010) as well as nutrient and water consumption during water stress.

1.2 Objectives

In this study we investigated the effect of biodiversity on subsurface water at Jena experimental site. However, it is difficult to study the effect of biodiversity on belowground system when the complex interaction between groundwater, river water, and soil water are still unknown. There is also a channel which goes underground to the experimental field and carries water from the river to the field.

We first characterize the subsurface system in terms of physico-chemical, hydrogeological, hydrogen and oxygen isotope, soil texture and other hydrological features. Difference in diversity might result in differences in transport of solutes from the groundwater to the near surface. Therefore, to compare the effect of difference level of diversity on the transport of solute, the background hydrogechemical should be understood. We will then see if the hydrological features in the study area (river Saale and channel from river Saale to the study area) have an effect on the groundwater of the study area. We finally study how the flow of water change with biodiversity level using chloride transport in the unsaturated zone.
We will use different hydrogeochemical modeling, statistical techniques, graphical methods, and groundwater flow modeling to characterize hydrogeology of the study area. To study the effect of river Saale and channel on the groundwater of the study area we will use chloride as a tracer and PHREEQC hydrochemical modeling to study the effect at mean river flow and predict the effects at higher flow season. PHREEQC, a hydrogeochemical model (Pankhurst and Appelo (2009)) is a package designed to perform a wide variety of low temperature aqueous geochemical calculations. The objective of this thesis is therefore,:

- To characterize the subsurface water of the study area in terms of hydrogeochemical, geological and hydrological properties. This enables us to understand the background property before investigating its relationship with above ground biodiversity. To interpret the groundwater chemical composition, we used multivariate techniques, PHREEQC (hydrogeochemical modeling) and graphical methods.

- To assess the seasonal variability of the groundwater physico-chemical properties (such as major cations and anions and trace elements). These elements (e.g. chloride) will be used as tool to relate biodiversity and subsurface water.

- To study whether water from river Saale (as influx from river and through artificial channel from the river) has effect on the groundwater of the study area.

- Study the relationship of level of plant diversity and the shallow groundwater of the study area. We will use evapotranspiration (using Penman-Monteith equation) and precipitation to find out the time of the net flow in the unsaturated zone. Then we will study chloride ion accumulation and transport in response to different diversity level.

1.3 Thesis organization

Chapter two introduces the theoretical background of biodiversity and to principles governing the hydrogeochemical processes in the groundwater and surface water. Concepts of biodiversity, and mechanisms responsible for relationship between biodiversity and ecosystem function is explained in this chapter. Thermodynamic principles and some of the main geochemical processes (ion-exchange, carbonate reactions) and principles of hydrogeochemical modeling using PHREEQC are also presented in Chapter two. Water isotopes and use of chloride as hydrological tracer to understand the water flow in unsaturated zone is also discussed in this chapter.

Chapter three gives a description of the study area (Jena biodiversity experiment). It describes the study area in terms of geography, climate, hydrogeology, soil type, and geological settings. Some aspects of hydrology important for this study are also covered in this chapter. It also explains the experimental design of the biodiversity experiment.

Chapter four focuses on the material and methods of hydrogeochemical modeling (using PHREEQC), field sampling and measurement and methods used for analysis

in the laboratory. Introduction to geochemical data interpretation using multivariate statistical techniques is covered in this chapter. Description of data preparation for interpretation using statistical techniques and methods to analyze multivariate statistical methods are also explained in this chapter.

Chapter five deals with the characterization of the study area by using hydrochemical modeling, multivariate statistical techniques, and graphical methods. We used factor analysis to find out what controls the groundwater geochemical process of the study area. We also interpreted groundwater chemical composition data from TLUG (Thüringer Landesanstalt für Umwelt und Geologie) and compare the result with the result of our study. This helped us to identify in which hydrogeologic units our study area located. Seasonal variation of the groundwater of the study area is also interpreted. Water types, mechanisms controlling the water types in the groundwater of the study area are also discussed in this chapter.

Chapter six of the thesis discusses the hydrological features affecting the groundwater of the study area. These are the channel from the river and river Saale itself. We study by using PHREEQC, hydrogeochemical modeling and natural tracer (chloride ion) to see if the channel and river Saale have an effect on the groundwater of the study area. We also used PHREEQC to predict the effect of Saale when the flow in the river is higher than mean flow.

Chapter seven deals with the relationship between level of diversity and shallow groundwater under water stress. We used chloride measurement at different depth in the soil and see if there is difference in accumulation due to difference in diversity level. We also used one dimensional vertical flow model to see if level of diversity and groundwater are related. Chloride was assumed as a conservative ion, and was used to study the water flow and solute transport pattern in the unsaturated zone. We estimated the chloride profile by solving diffusion convection equation analytically.

Chapter eight deals with the overall discussion based on previous chapters mainly chapter five, six and seven. We also discussed here some of the limitation of the study and recommendations for further work.

Chapter 2

Theoretical background

2.1 Biodiversity

The definition of biodiversity according to Article 2 contained in Convention on Biological Diversity (http://www.cbd.int/doc/legal 1992) is "the variability among living organisms from all sources including, inter alia, terrestrial, marine and other aquatic ecosystems and the ecological complexes of which they are part: this includes diversity within species, between species and of ecosystems".

To understand the effect of change of biodiversity and to use for applications (such as comparing systems in terms of diversity level), one has to measure biodiversity. But from the definition we can see that it is difficult to have a specific definition or formula to measure biodiversity. According to Gaston and Spicer (2006), there is no single overall measure of biodiversity; rather there are multiple measures of different facets, because the variety of life can be expressed in a multiplicity of ways. Species richness (the number of species in a given site or habitat) and evenness (measure of the relative abundance of the different species making up the richness of an area) (Purvis and Hector 2000, Pimm et al. 1995) are the main measures of biodiversity. However, species richness has become the common currency of much of the study of biodiversity, and has proven valuable for many heuristic and practical purposes although it has some significant limitations (Gaston and Spicer 2006). As

species richness and evenness increases, diversity also increases (Tilman et al. 1997, McGrady-Steed et al. 1997). To measure diversity we can use Simpson's diversity index (Simpson 1949), which takes into account both species richness and evenness.

Biodiversity has been shown to affect ecosystem functions (McGrady-Steed et al. 1997, Tilman et al. 1997). Ecosystem functioning is a broad term that encompasses a variety of phenomena, including ecosystem properties (rates of processes, e.g. fluxes of material and energy among compartments), ecosystem goods (direct market value, e.g. food, construction materials, medicine, tourism, recreation, etc), and ecosystem service (maintaining hydrologic cycle, regulating climate, pollination, storage and cycling of nutrients) (Hooper et al. 2005). According to a study by Shahid et al. (1994) three mechanisms have been proposed to explain why there should be a relationship between biodiversity and ecosystem functioning:

- **Sampling effect:** if in a regional part of large number of species, some have strong impacts on ecosystem processes, then the more species that are drawn from this pool to form a local assemblage the greater probability that some of these strongly impacting species will be included.

- **Species complementarities:** if species differ in their resource use, then more species that are drawn from this pool to form a local assemblage the greater the probability that some of this strongly impacting species will be included. Complementarily results from reduced interspecies competition through niche partitioning (Hooper et al. 2005). According to the same author, if species use different resources, or the same resource at different times or different points in space, more of the total available resource are expected to be used by the community. Niche is a species' way of life in a community and includes everything that affects its survival and reproduction, such as how much resource is needed, how much space it requires and the temperature it can tolerate (Miller and Spoolman 2009).

- **Positive interactions:** increasing number of species in a local assemblage could result in increase in the number of mutual (when both get benefit from

the relation), facultative, or positive indirect effect among them, increasing ecosystem functioning. Such interaction occurs if certain species alleviate harsh environmental conditions or provide a critical resource for other species Bruno et al. (2003), Hooper et al. (2005). Different plant diversity with various functional groups in our study area might improve resource use during stress periods.

In practice, all three of these mechanisms may often be operating, with the research challenge being to find ways to determine their relative contribution to ecosystem functioning (Shahid et al. 1994, Hooper et al. 2005). Understanding the relationship between biodiversity and ecosystem functioning is, however, furthermore complicated by the temporal dynamics of ecological systems.

Effect of species diversity on ecosystem processes is the sum of the effects of individual plant species. For example, one or a few species may dominate nutrient uptake in more diverse communities, and have effects on the available pool similar to what they would have in monoculture (Hooper and Vitousek 1998, Hooper et al. 2005, Tilman and Wedin 1991). Therefore, it is important to consider the effect of each functional group separately.

2.2 Introduction to principles controlling the hydrogeochemical processes

Some of the basic concepts of thermodynamics in aqueous systems used for our investigation and main geochemical processes (ion-exchange, carbonate reactions) are presented in the following sections.

2.2.1 Thermodynamics of aqueous systems

Chemical equilibrium is the time invariant, most stable state of a closed system (the state of minimum Gibbs free energy) (Langmuir 1977). A system can be open

(where there is both mass and energy exchange), closed (energy exchange, but no mass exchange) or isolated where there is no exchange of mass and energy. Whether a system can be considered open or closed depends not only on the specific system under study, but also on both the rates of flux of matter in and out of a system and the time scale of interest (Langmuir 1977). For our study area the groundwater can be considered as a closed system since the rate of input of substances under consideration are very slow and the reaction rates are comparatively fast.
Thermodynamic principles are useful in correlating chemical processes with biological or physical processes (Hem 1989), for example for evaluating:

- Feasibility of various possible chemical processes in natural water systems.
- Predicting the actual dissolved concentration of reaction products that should be present in the water (equilibrium solute concentration), whether the aqueous species are naturally present or from anthropogenic addition.
- Predicting the direction in which chemical reaction may occur.

2.2.1.1 Gibbs free energy, Enthalpy

Gibbs free energy is a measure of driving energy of a reaction (Fetter 1994). At standard conditions, the Gibbs free energy of a reaction ΔG_r^O is the difference between the sum of the free energy of products and the reactants. It tells us the direction in which chemical reaction may go as:
$\Delta G_r^O > 0$ the reaction proceeds to the left
$\Delta G_r^O = 0$ the reaction is at equilibrium
$\Delta G_r^O < 0$ the reaction proceeds to the right
In this study, our systems (water bodies) are assumed to be in equilibrium. Therefore the Gibbs free energy of our system should be zero.

Enthalpy is the chemical energy content of a system at constant pressure and temperature. Enthalpy may be thought of as having two components, an internal component which is termed entropy ΔS, and a component that is or can become available externally which is termed free energy ΔG (Hem 1989). Therefore,

$\Delta G = \Delta H - T\Delta S$. By knowing the enthalpy of a reaction we can evaluate whether the increase in temperature and pressure has an effect on the reaction. From Le Chatelier's principle as stated in Smith (2004), "perturbation of a system at equilibrium will cause the equilibrium position to change in such a way as to tend to remove the perturbation". Therefore knowing the enthalpy of a reaction we can evaluate how the seasonal variation (change in increase or decrease of temperature and pressure) changes the chemical composition of the water body. Most of the carbonates have an exothermic heat of dissolution, therefore their solubility decreases with increasing temperature (Langmuir 1977); and as a result less concentration of the elements making up these minerals.

2.2.1.2 Activity and strength of ions

In solution which is not dilute, ions interact electrostatically with each other (Appelo and Postma 1994). As a result, the activity decreases with increasing ionic strength and it is always lower than the concentration, for that reason the ions are charged and oppositely charged ions interact with each other to reduce the available charge (Merkel et al. 2005). Therefore, the ion activity coefficient, which is ion-specific correction factor, is used to describe the influence of the interaction. Activity coefficients may vary, but if ion i is present at trace concentration, and there are no other ions present, then the value approaches 1 (Appelo and Postma 1994). The interactions are modeled by using activity coefficients to adjust molal or molar concentrations to effective concentration. It is calculated as $a_i = \gamma(\frac{C_i}{C_i^o})$ where γ is the activity coefficient, a is activity, and C_i and C_i^o are the molal concentration and concentration at standard state respectively.

Debye-Hückel theory is used to calculate activity coefficients for solutes. To calculate the activity coefficients the ionic strength, I is calculated first as shown below:

$$I = \frac{1}{2} \sum m_i \cdot z_i^2 \tag{2.1}$$

Where z_i is the charge number of ion I, and m_i is the molality of i. The ionic strength of fresh water is normally less than 0.02 while sea water has an ionic strength of about 0.7. A highly saline environment, like the Dead Sea, has an ionic strength of 9.4 (Appelo and Postma (1994)). The calculation of ionic strength must take into account all major ions, such as:

$$\mathrm{I} = \frac{1}{2}[\mathrm{M}_{\mathrm{Na^+}} + 4\mathrm{M}_{\mathrm{Ca^{2+}}} + 4\mathrm{M}_{\mathrm{Mg^{2+}}} + \mathrm{M}_{\mathrm{HCO_3^-}} + \mathrm{M}_{\mathrm{Cl^-}} + 4\mathrm{M}_{\mathrm{SO_4^{2-}}}]$$

The most accurate values of ionic strengths is obtained by total water analysis which includes all ionic species. If complete analysis is not made, ionic strengths can also be estimated from total dissolved solids (TDS) according to Langmuir (1977) as follows:

$\mathrm{I} \approx 2{*}10^{-5}{*}\mathrm{TDS}$ ($\frac{\mathrm{mg}}{\mathrm{L}}$) NaCl solution

$\mathrm{I} \approx 2.5{*}10^{-5}{*}\mathrm{TDS}$ ($\frac{\mathrm{mg}}{\mathrm{L}}$) "Average" water

$\mathrm{I} \approx 2.8{*}10^{-5}{*}\mathrm{TDS}$ ($\frac{\mathrm{mg}}{\mathrm{L}}$) $Ca(HCO_3)_2$ water

Then the activity coefficients can be calculated by using the Debye-Hückel equation as below for I<0.1 (Langmuir 1977)

$$log\gamma_i = -\frac{AZ_i^2\sqrt{I}}{1 + Ba_i\sqrt{I}} \tag{2.3}$$

where A and B are temperature dependent constants; at 25°C, A=0.5085 and B=0.3285*1010/m. a_i is ion size parameter and is the measure of the effective diameter of the hydrated ion. For ionic strengths greater than 0.1 the following modified Debye-Hückel equation is proposed Pankhurst and Appelo (2009).

$$log\gamma_i = -\frac{AZ_i^2\sqrt{I}}{1 + Ba_i\sqrt{I}} + b_i I, \tag{2.4}$$

where a_i and b_i are ion specific fit parameters.

Davis equation is used for higher ionic strength (I between 0.1 and about 0.7

mol/Kg) models (Langmuir 1977).

$$log\gamma_i = -Az_i^2(\frac{I^{0.5}}{1+I^{0.5}} - 0.3I). \tag{2.5}$$

2.2.1.3 Common ion effect

A mineral in the groundwater is generally less soluble if the water contains an ion which is the same as one of the constituent ions of that mineral. This is known as the common ion effect. Groundwater and surface water generally contain ions from many sources, so it is important to consider common ion effects when interpreting the concentration of ions in the groundwater. The common ion effect of gypsum ($CaSO_4 \cdot 2H_2O$) dissolution and calcite ($CaCO_3$) precipitation is often accompanied by dolomite ($CaMg(CO_3)_3^{+2}$) dissolution, leading to the increase in Mg^{2+} in the groundwater (Sharif et al. 2008).

2.2.2 Ion exchange processes

Ion exchange is a reversible chemical reaction where an ion from solution is exchanged for a similarly charged ion attached to an immobile solid particle. Both cation exchange and anion exchange can occur, but in some neutral soils cation exchange is the dominant process (Fetter 1994). According Appelo and Postma (1994), Fetter (1994), although all soils and sediments have some ion exchange capacity, ion exchange site is found primarily on clays and soil organic material and metal oxy-hydroxides, . A general ordering of cation exchangeability for common ions in groundwater is often (Fetter 1994):

$Na^+ > K^+ > Mg^{2+} > Ca^{2+}$

2.2.3 Carbonate reactions

Carbonate minerals do react quite readily with water, and they play an important role in the evolution of many groundwater systems (Hem 1989). Usually, the car-

bonate rocks have high porosity and low permeability (Appelo and Postma 1994). Dolomite, calcite, magnesite, rhodochrosite, siderite are the main carbonate minerals that form groundwater aquifers. Calcite and magnesite are the most soluble carbonate minerals and the groundwater containing these minerals contains dissolved Ca, Mg, and carbonate ions.

2.2.4 Processes controlling groundwater and surface water chemical composition

The geochemical behavior and chemical and isotopic properties of natural waters are related to their location in the hydrosphere and can be grouped, that is, as precipitation, stream flow, soil water, groundwater, and ocean water (Langmuir (1977)). Water in these systems has different chemical composition.

Controls on the subsurface: The composition of subsurface water is complex and a function of many variables as follows (Langmuir 1977):

- Recharge composition (influenced by chemistry of precipitation), leaching of salts, weathering of soil material
- A minerologic and petrologic composition of subsurface rocks. Among the most soluble rocks are halites (NaCl), gypsum ($CaSO_4.H_2O$), and carbonate rocks such as limestones ($CaCO_3$).
- Hydrogeologic properties (hydraulic conductivity and porosity) of rocks or soil material have strong influence on the water/rock interaction. High groundwater flow velocities usually imply groundwater that is relatively low in dissolved solids because of the short rock contact time and high water/rock ratios, and vice versa (Langmuir 1977). The hydrogeologic properties of some common materials are shown in Fig. 2.1. Intrinsic permeability represent the size and interconnectedness of the pores in the porous medium while hydraulic conductivity is a measure of the porous media ability to transmit water under a given hydraulic gradient. The hydraulic conductivity represents both the properties

of the porous medium as wells as the properties of the fluid flowing through the porous medium.

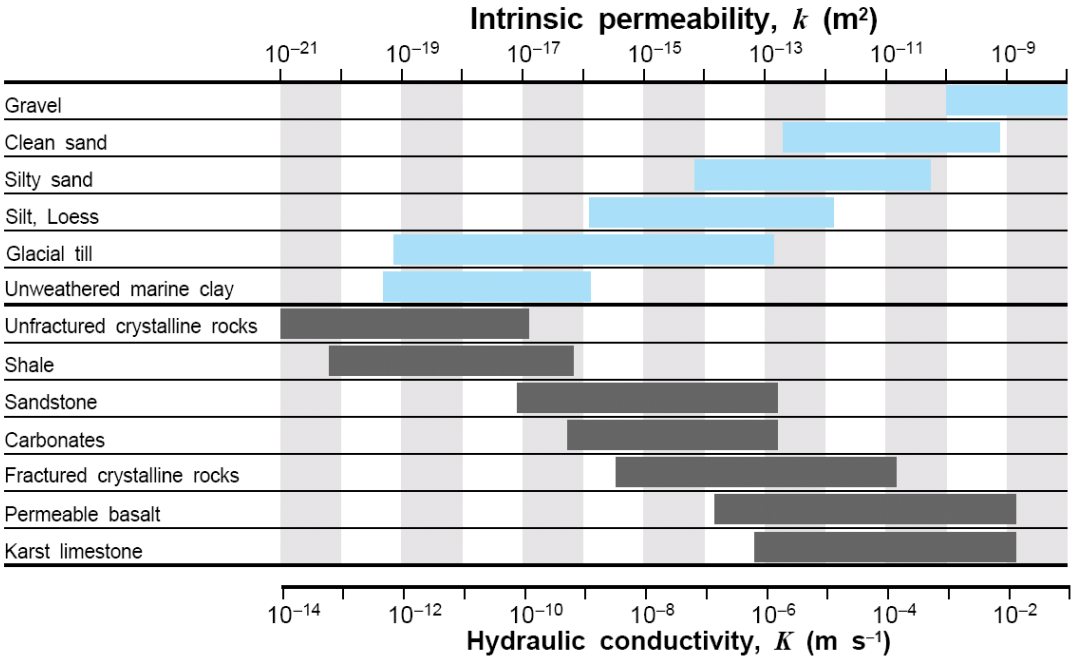

Fig. 2.1 Ranges of intrinsic permeability and hydraulic conductivity for a variety of rocks (gray bars) and sediments (blue bars) from (Hornberger et al. 1998)

Atmospheric carbon dioxide is one of the factors which controls the acidity of water that infiltrates and that in turn controls mineral weathering processes (Stumm and Morgan (1994)). Root respiration in areas with dense vegetation releases CO_2 to the soil environment; which results in increased weathering of minerals (Williams et al. 2003). Organic matter decay, and acidic parent material also contribute to acidity.

Controls on soil moisture chemical composition: The chemistry of soil water depends on local climate, the geologic matrix forming the soil material and also other geochemical processes. In high rainfall climates, where evapotranspiration rates are low, the soils are quartz-sand rich and deficient in weathering minerals (as they have been wash out) and therefore, the chemistry of soil water may resemble

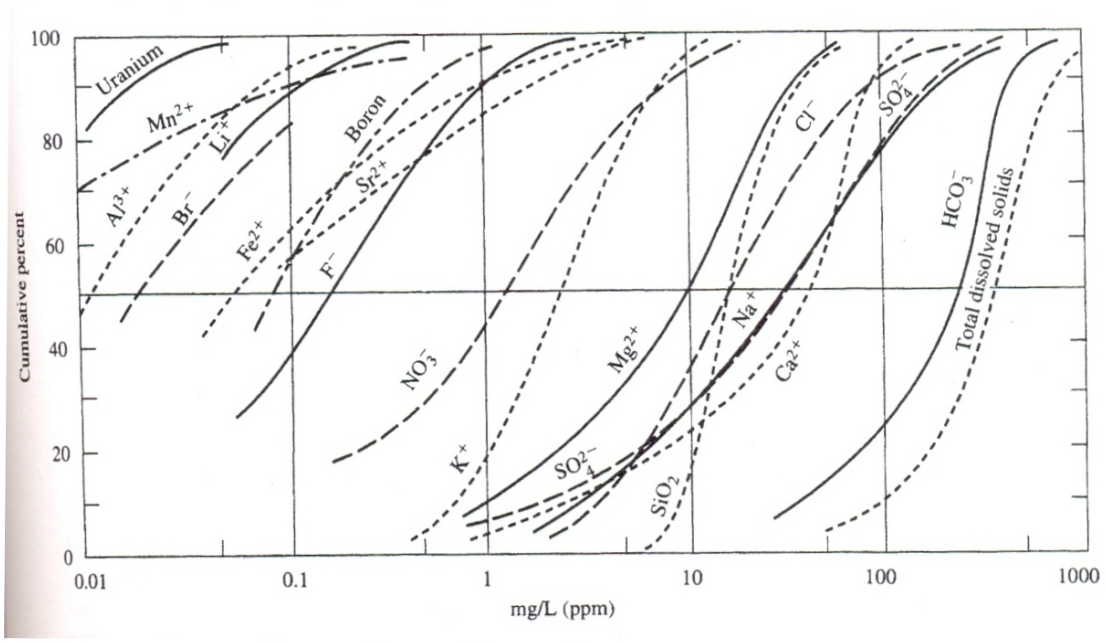

Fig. 2.2 Cumulative percentages showing the frequency distribution of various constituents in potable (chiefly surface-) water (Langmuir 1977)

that of local precipitation (Langmuir 1977). From Figures 2.2 and 2.3 we can see

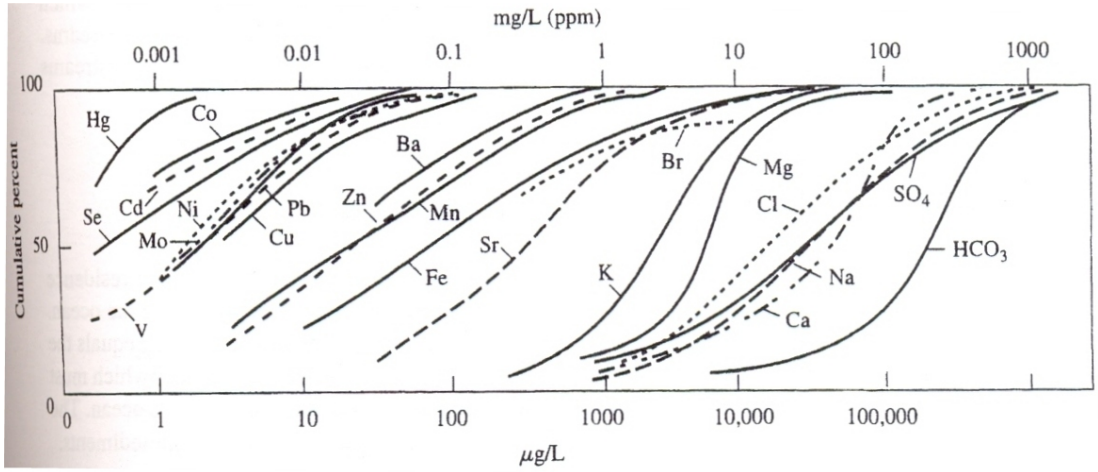

Fig. 2.3 Cumulative percentages of some major and trace elements in groundwater Langmuir (1977).

the order of abundance in the average groundwater and surface water. Calcium and HCO_3^- are predominant chemicals in most of the surface and groundwater.

We can use the thermodynamic principles and geochemical processes mentioned in this section to setup hydrogeochemical modeling. The next section deals with the principles and introduction to formulation of hydrogeochemical modeling using PHREEQC.

2.3 Hydrogeochemical modeling

2.3.1 Overview

PHREEQC 2.16.03 biogeochemical model (Pankhurst and Appelo 2009) is a free software package designed to perform a wide variety of low temperature aqueous geochemical calculations based on an ion-association aqueous model. The acronym PHREEQC stands for PH (pH), RE (redox), EQ (equilibrium), and C (program written in C). PHREEQC is based on principles of conservation of mass and minimum free energy at equilibrium. PHREEQC rewrites all chemical equations in terms of master species. Species are the molecular entities, such as the gases CO_2 and O_2 in a gas, or the electrolytes Na^+ and SO_4^{-2} in aqueous solution that exist within a phase (Bethke 2008). The species present in aquatic system can be divided into master/primary species and the secondary species. Master species are one of the form of aqueous species associated with each element, activities of the hydrogen ion, aqueous electron, and water. The number of master species, N_m is equal to the total number of species in the system minus the number of independent reactions. The number of secondary species, N_s is equal to the difference between the number of master species and total number of species in the system.

Governing equations

The overall chemical composition of a system can be described in terms of a set of one or more master species (chemical components). The first step is to identify independent reactions and master species (A^m). Independent reactions are reactions formed from primary species (master species). The next step is to write

a mass-action equation for each independent reaction identified. Then, governing mass balance equation can be derived using mass action equation formulated. The secondary species (A_i) is written in terms of master species (A^m)for a given reaction:

$$A_i = \sum_{j=1}^{N_m} (v_{ij} A_j)^m \tag{2.6}$$

where A_i and A_j^m are the chemical formula for the secondary and master species, v_{ji} are the stoichiometric coefficients in the reaction, and N_m is the number of aqueous master species. The mass-action equation of the corresponding reaction is:

$$K_i^l = a_i^l \prod_{j=1}^{N_m} (a_i^m)^{-v_{ji}^l} \tag{2.7}$$

where, K_i^l thermodynamic equilibrium constant, a_i^m is the activity of the ion, m and l are master and secondary aqueous species. The equilibrium constant K, depending on the type of reaction, could be solubility product (if the reaction is dissolution or precipitation), complexation constant (if complexation or dissolution of complex), distribution/selectivity coefficient (if sorption) or stability constant if redox reaction. Equilibrium among aqueous species in an ion-association model requires that all mass-action equations for aqueous species are satisfied (Pankhurst and Appelo 2009). Equation 2.7 can then be rewritten as:

$$c_i^l = \frac{K_i^l \prod_{j=1}^{N_m} (a_i^m)^{v_{ji}^l}}{\gamma_i^l} \tag{2.8}$$

And the mass balance equation is written for each master species from the reaction and mass-action equation as follow:

We can define the concentration C_m of a master species as:

$$C_m = c_m + \sum_{j=1}^{N_{sat}} (v_{ji} c_i)^m \tag{2.9}$$

mass balance equation for the above is:

$$M_i = m_{H2O} C_i = m_{H2O}(c_i + \sum_{j=1}^{N_{sat}} v_{ji} c_i) \tag{2.10}$$

Then inserting *equation* (2.8) in *equation* (2.10), will give us:

$$M_i = m_{H2O} C_i = m_{H2O}(c_i + \sum_{j=1}^{N_{sat}} v_{ji} \frac{\mathrm{K_i^l} \prod_{\mathrm{j=1}}^{\mathrm{N_m}} (\mathrm{a_i^m})^{\mathrm{v_{ji}^l}}}{\gamma_\mathrm{i}^\mathrm{l}}) \tag{2.11}$$

Charge balance: The ionic species in an electrolyte solution remain charge balanced on a macroscopic level (Bethke 2008). The electoneutrality can be expressed by the condition of charge balance among the species in a solution according to:

$$\sum_i (z_i M_i) = 0 \tag{2.12}$$

where z_i is charge of the ion and M_i is the mole of master species m.
Therefore by using *equation* (2.11) and *equation* (2.12) and forming number of equations equal to the number of master species (components), the systems of equations can then be solved. A Newton-Raphson formulation is used in PHREEQC to iteratively arrive at a solution to the equations.

Saturation Index

Saturation indices (S.I.) of all the minerals were calculated to see the saturation state of the mineral. The saturation index of particular mineral is calculated as:

$$S.I. = \log \frac{IAP(T)}{K_{SP}(T)} \tag{2.13}$$

Where, IAP (T) is ion activity product of the given mineral as a function of temperature (T) and K_{sp} (T) is the solubility product (sp) of the mineral as a function of temperature. Saturation indexes in the ranges of ±0.5 are assumed to be in equilibrium with the ground water (Appelo and Postma 1994).

When the mineral is in equilibrium with the aqueous solution then SI=0, when the

water is undersaturated with respect to the mineral, SI<0 and when the water is supersaturated with respect to the mineral, SI>0.

One of the objective of geochemical modeling is investigating speciation, that is calculating the concentration and form in which the elements exist in the water. We can also calculate the saturation state of existing minerals with respect to water.

2.4 Hydrological tracers

There are different methods to study the water flow pattern in the unsaturated zone. Kirchner et al. (2010) used hydrogen and oxygen isotopes for tracing mixing processes. Chloride is also widely used in hydrology as a natural tracer (Scanlon 1991, Kirchner et al. 2010). Barnes and Allison (1988) and others used chloride as tracer to solve and understand some hydrological problems such as tracing the source of water and studying the interaction of surface water and groundwater. In our study we used the chloride ion to study the flow of water in the unsaturated zone.

The main source of chloride in the soil are rainwater, air pollution, nearby road (deicing salts during winter), shallow groundwater with higher chloride, accumulation in soil during upward flow (Jacques et al. 2008), fertilization and irrigation. The possible sources of chloride in the soil of our study area are: rainwater, upward flow of groundwater and deicing salt from the adjacent road to the experimental field.

Geochemical, biological and physical processes might affect the concentration of chloride in the soil. The main specific processes are geochemical reactions, adsorption on the soil material, uptake by plants, and evapotranspiration of the water. More detail is given in the following sections.

Geochemical process

Chlorine is extremely reactive, unstable and exists in nature as chloride. Chloride (chlorine, which gained one electron) is negatively charged, most stable, and unreactive. Therefore geochemical reactions affect the chloride concentration to a

negligible amount.

Soil particles are predominantly negatively charged; therefore, chloride ion tends to be repelled from mineral surfaces contained in many soil particles (Bohn et al. 1979). Some soil particles carry positive charges. For example, oxide surfaces (notably Fe- and Al-oxide/hydroxide) and edges of clay minerals are likely to be positively charged at pH value below seven (Bolt and Bruggenwert 1978). According to an experimental study by Bolt and Bruggenwert (1978), the order of preference for adsorption is:

$$SiO_4^{4+} > PO_4^{3-} >> SO_4^{2-} > NO_3^- \approx Cl^-$$

As a result, SO_4^{2-} and Cl^- ions are often not adsorbed even if only very low concentration of PO_4^{3-} ions is present. In a system free of PO_4^{3-} ion adsorption of Cl^- and/or SO_4^{2-} may occur, at least when the pH does not exceed a value of 6 (Bolt and Bruggenwert 1978). The pH value in the soil water of our study area is always neutral to basic. There were also SO_4^{2-} ions in soil water in all measured samples. We therefore assume that chloride is therefore not readily adsorbed on the soil complexes. Because of this, chloride moves readily with soil water.

Biological processes

Chloride is not much affected chemically by soil organisms (opposed to NO_3^- and SO_4^{2-}). There are some studies done on formation (incorporation of chloride) and mineralization (release of chloride) of organic chlorine which takes place in soil (White and Broadley (2001)). But the significance of this process is not well studied. Chloride is also an essential micronutrient for higher plants and minimal requirement for crop plants (White and Broadley 2001). We assumed for the study area that the chloride uptake is low as the plants are mainly grass types.

Physical processes

According to a study by White and Broadley (2001) the movement of chloride within soil is determined by water fluxes and in particular, the relationship between pre-

cipitation and evapotranspiration. Detail of chloride movement in the unsaturated zone is discussed in Chapter 7, Section 7.1.3.

2.4.1 Hydrogen and oxygen isotopes

Hydrogen and oxygen and other elements, exist in nature with different mass numbers called isotopes. Due to the difference in mass, the isotopes behave differently in physical, chemical and biological processes Appelo and Postma (1994). Some of these properties are differences in diffusion velocity, binding energies, and collision frequencies with molecules (http://www.iaea.org 2011). These processes change (fractionate) the ratio of heavy isotope to light isotope. The resulting variation in ration is important in hydrology.

Because the variation in isotopic abundance is small, isotopic ratio of a sample, R_{sample} is given with respect to standards (e.g. VSMOW) as δ values (Cook and Herczeg 2000).

$$\delta = \frac{R_{sample} - R_{standard}}{R_{standard}} * 1000 \tag{2.14}$$

where R_{sample} and $R_{standard}$ are the ratio of heavy to light isotope of sample water and standard water respectively. Since the δ value is smaller, it is usually multiplied by 1000 for convenience. Positive value of δ signifies enrichment of ^{18}O and ^{2}H while negative values indicate a depletion of heavier isotopes. The standard value is ocean isotope and has a value of $\delta^{18}O$ of approximately 0.

Chapter 3

Description, Geology and Hydrogeology of the Study Area

3.1 Geography and climate

3.1.1 Geography

The Jena biodiversity experimental field is located in the northern part of Jena along river Saale in Thuringia, Germany (between 50°57'03"N, 11°37'14"E and 50°57'07"N, 11°37'40"E), and between 137 and 139 m above sea level at eastern and western part of the study area respectively. The main experiment field is located at about 40 to 70 meter distance west of river Saale which flows from south to north Fig. 3.1. The study area is located in low lying Thurigian basin, but the site is characterized by plain topography with almost the same topography in the main experimental area. At the western side of the study area there is a main road (Wiesenstrasse) that receives de-icing salt during the winter seasons. Before the experimental setup the study area was mainly used as an agricultural area (Roscher et al. 2004). There were also events of flooding since the setup of the experiment, in 2003 and 2011.

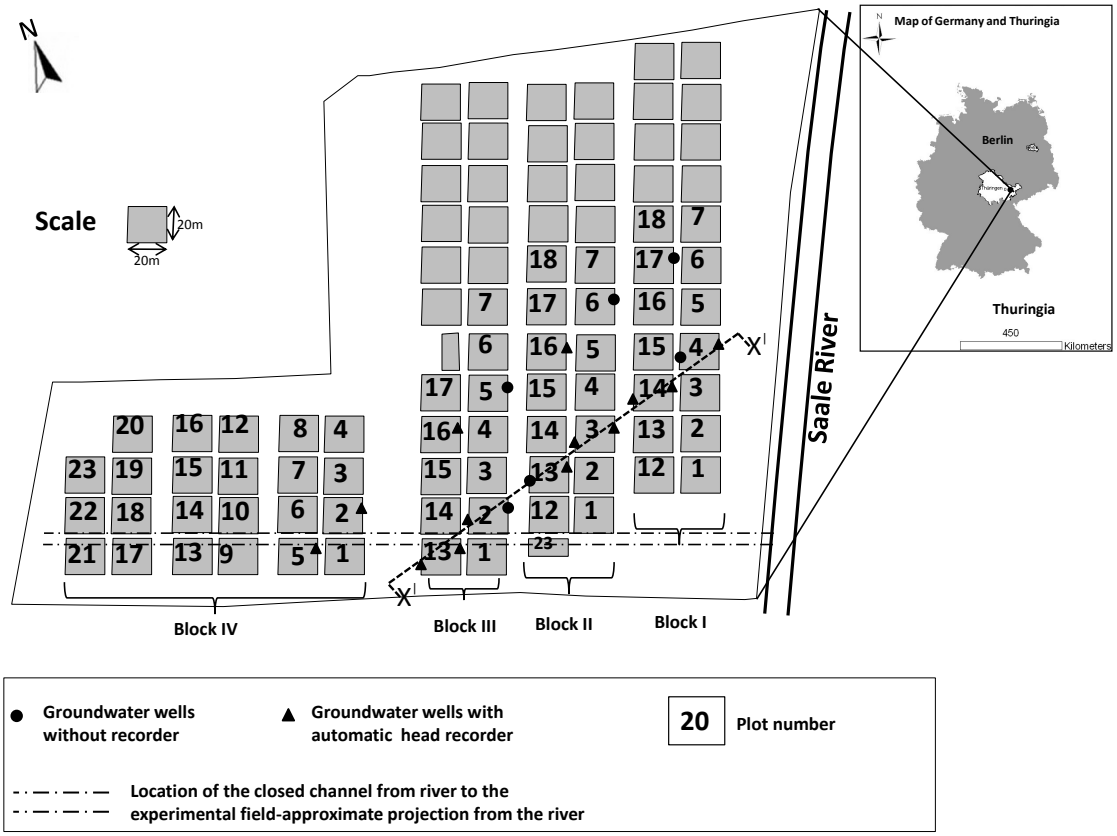

Fig. 3.1 Study area of Jena experimental field and location of the groundwater wells within the field and other hydrological features (river Saale and a channel). The soil texture along the line X-X was also made will be discussed in Chapter 5

3.1.2 Climate

According to Köppen-Geiger climate classification system, our study area (also whole Germany) lays in the Cfb-climate zone (Kottek et al. 2006). This zone is characterized by warm temperate, fully humid and warm summer.

The area around Jena has a mean annual rainfall of 587 mm and a mean temperature of 9.3°C based on data from 1961-1990 (Kluge and Müller-Westermeier 2000). The average annual rainfall of the site (Jena experiment) based on 8 years data (2003-2010) is 533mm. The mean monthly precipitation of the study area is indicated in Fig. 3.2 for the years 2003-2010. The highest average monthly precipitation was recorded in August and the lowest rainfall was recorded in February. Rainfall is higher during late spring and summer but generally low during the winter time.

Evapotranspiration (ET)

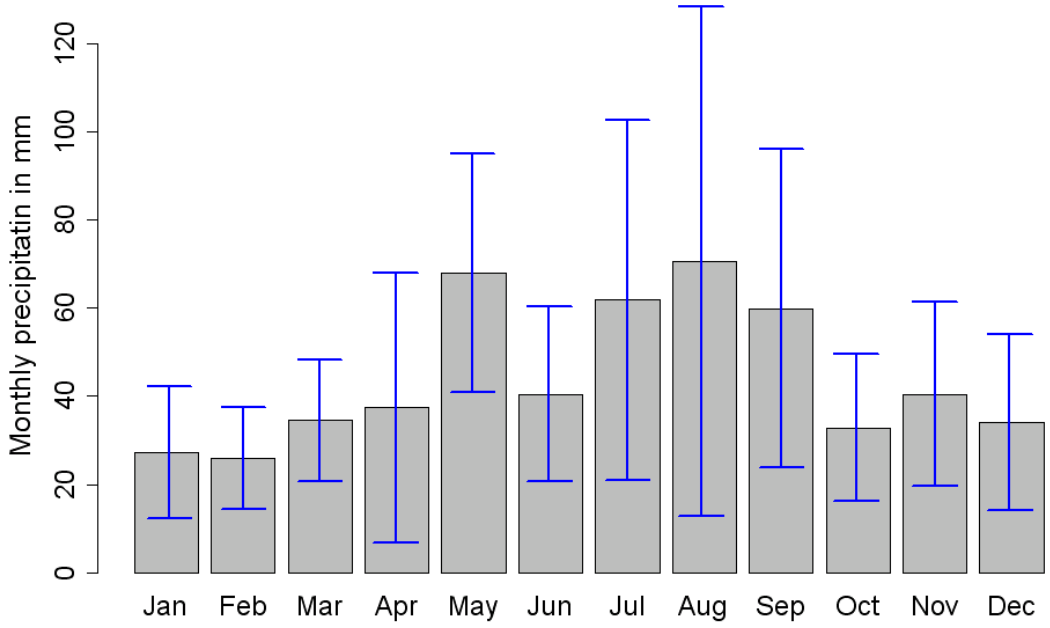

Fig. 3.2 Monthly precipitations (in mm) of the study area from the years 2003-2010. The bar on each plot is the standard deviation.

Water is lost on the one hand from the soil surface by evaporation and on the other hand from the plant by transpiration. The combination of both fluxes is known as evapotranspiration (Allen et al. 1998). The rate of evapotranspiration is a function of four factors (Allen et al. 1998); soil moisture, plant type, stage of development and weather (solar radiation, wind speed, humidity, temperature).

Relative humidity: is defined as the ratio of the partial pressure of water vapor to saturated vapor pressure of water at a given temperature. The relative humidity shows diurnal variation (for two days-July1-2/2010) as shown in Fig. 3.3. We can see from the graph that the relative humidity is higher in the morning and low during the day time. It is an important climatic variable and it affects the rate of evapotranspiration in an area since the rate of evaporation is high when the relative humidity is low.

The wind speed is also an important climatic variable and it is generally low during the summer time. Net radiation is higher in summer (June, July, and August)

causing high evaporation occurs during this time.

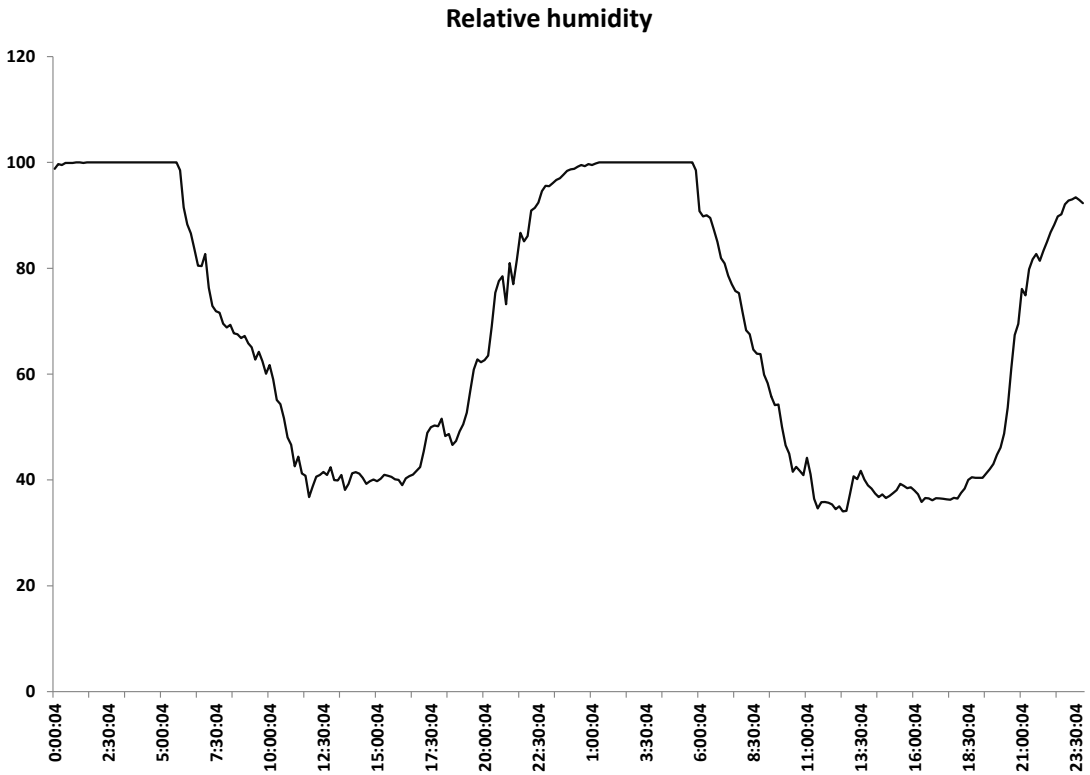

Fig. 3.3 Diurnal variation of relative humidity in the study area, July 1-2/2010

3.2 Experimental design

The Jena experiment is constructed in 4 blocks each with different number of plots. The reason why it is divided in blocks is to account for the effect of difference in soil heterogeneity (Roscher et al. 2004). Because of the flooding effect the soil varies as we go farther from the river. There are 86 plots (20m by 20m) with different level of species richness (1, 2, 4, 8, 16, and 60) and functional group richness (1, 2, 3, and 4). The species mixtures are made from a pool of 60 different species while the functional groups are legumes, tall herbs, short herbs and grasses. The experiment design is shown in Fig. 3.4. To maintain the species diversity level plots were regularly weeded during the experimental time.

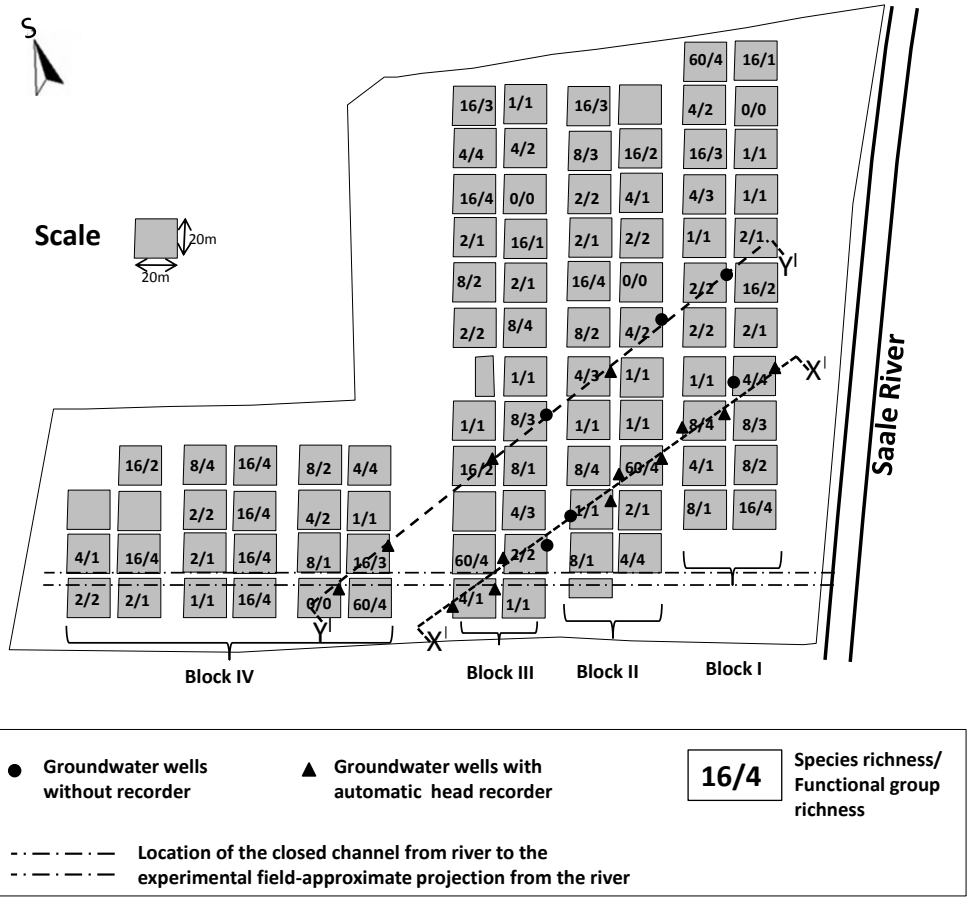

Fig. 3.4 Experimental design showing plot and block arrangement. The first number in the plot indicates the number of species types in the plot and the second number indicates the number of the functional groups types in the mixture forming the plot.

3.3 Geological and Hydrogeological setting

3.3.1 Geological setting

The main geological (lithological) units near Jena area are: Buntsandstein, Muschelkalk and Keuper which belong to the Germanic Trias (Seidel 2003). In addition, alluvial deposits are also the major component of the site as the study area is located along the river. The characteristic of each of the geologic unit is a as follow:

Buntsandstein: The Buntsandstein predominantly consists of sandstone layers of the Lower Triassic series and is one of three characteristic Triassic units (together with the Muschelkalk and Keuper that form the Germanic Trias Supergroup (Aigner and Bachmann 1992). It is mainly divided in to three layers; Upper, Mid-

dle and Lower Buntsandstein. The facies of the Lower and Middle Buntsandstein fluctuates between fluvial sandstones and lacustrine deposits (Gaupp et al. 1998). The Upper Buntsandstein (Röt formation) is dominated by mudstone facies ranging from shallow-marine dolomitic clay stones to sabkha-mudpalin environments (Gaupp et al. 1998).

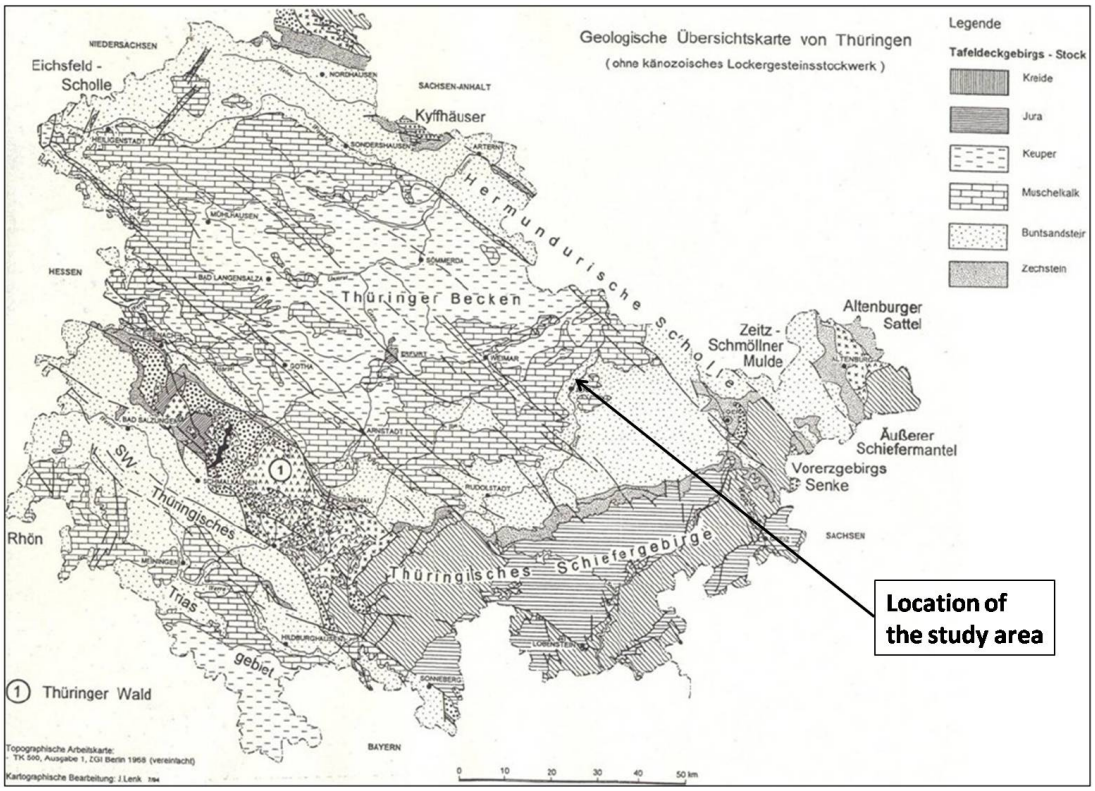

Fig. 3.5 Geological map of the study and nearby area (Seidel 2003)

.

Muschelkalk:

The Muschelkalk is marked by prevailing marine environment and is subdivided in to three units which reach a total thickness of about 250 meters; Lower, Middle and Upper Muschelkalk units.

Lower Muschelkalk: Jena formation which is about 120m thick is located in this unit. It is thinny bedded marly limestone, so called "Wellenkalke" displaying a wealth of sedimentary structures and rich trace fossil communities (Hagdorn et al. 1998). The lower Muschelkalk (Jena formation) of Thuringian basin consists of mainly of micritic limestones with different types of diagenetic bedding (wavy-, flaser-, and

nodular structures) (Gaupp et al. 1998).

Middle Muschelkalk**:** Karlstadt formation is in this unit. This formation is up to 15m thick dolomite and dolomitic marls with stromatolities and low diversity benthic communities dominated by the bivalve Neoschizodus orbicularis. The subsequent evaporates (gypsum, anhydrite, and halite) of the Heibronn formation have been dissolved in the subsurface (Hagdorn et al. 1998). Evaporites such as dolomitic marls, gypsum and even rock salt, dominate the middle Muschelkalk (Gaupp et al. 1998).

Upper Muschelkalk: Trochitenkalk formation of up to 40m thick is in this formation. This formation is limestone and partly dolomites (in marginal positions) (Hagdorn et al. 1998). The upper Muschelkalk limestones and marl of Thuringia were deposited in an open marine environment (Gaupp et al. 1998).

Keuper: is defined as the upper most unit of the Triassic (von Alberti 1834). Outcrops of Keuper occur only in the mountainous regions of middle and southern Germany (Bachmann 1998). According this author the most important area of this crops in Germany are Osnabrück-Weser Mountains, Thuringian basin, Trier-Bitburg basin and parts of Baden-Württemberg and Franconia. This unit is found near Cospeda, and it might interact and attribute some properties to nearby Muschelkalk geologic units.

3.3.2 Chemical properties of the groundwater

The Muschelkalk groundwater is of the Ca-Mg-SO_4-(HCO_3) type, while the Buntsandstein groundwater is of the Na-HCO_3-Cl-(SO_4) type (Gimmi and Waber 2004). The Muschelkalk groundwater composition is dominated by alkaline earth elements while that of Buntsandstein has high ratio of alkaline to alkaline earth elements and high content of fluoride and lithium (Gimmi and Waber 2004).

According to a study by Bruelheide and Udelhoven (2005) average pH values decreased in the sequences of soil whose parent material are from, Muschelkalk, Upper Buntsandstein, and Middle Buntsandstein. They also found the same pattern in

exchangeable calcium; however, exchangeable Al, Fe, and Mn showed increasing values. The same author also reported that Mg and K showed highest value in soil with geologic substrates from middle and Upper Buntsandstein.
Keuper groundwater is of Na-SO4-(Cl) type with sulphate as the dominant anion and less chloride content (Gimmi and Waber 2004).

3.3.3 Occurrence and movement of the groundwater

Groundwater stores and moves in a geologic formation called aquifer (Fetter 1994). An aquifer could be confined (artesian) types, unconfined or perched types. Confined aquifers are overlain by impermeable or semi-permeable confining layers (Babar 2005) while unconfined aquifers have no confining layers between zone of saturation and land surface (Babar 2005). Perched aquifer is a saturation zone with in the zone of aeration that overlies a confining layer. The upper surface of an unconfined aquifer is at atmospheric pressure, and it also receive recharge directly from the surface water. Groundwater of the study area is located in an unconfined aquifer and the water table fluctuates between about 40 cm (during spring recharge) to 270 cm (in summer) (depth to water table) based on water table measurement in 2010.

Groundwater movement

The velocity of groundwater movement is governed by hydraulic head gradient hydraulic conductivity, porosity, and other aquifer and water properties. We can use Darcy's Law and conservation of mass to describe groundwater flow in hydro-geologic environments.

Hydraulic head

The hydraulic head in a groundwater system is measured as the height above a reference level. It is the sum of the pressure from the weight of overlying water (pressure head), and the potential energy resulting from elevation (elevation head). The hydraulic head in an incompressible fluid is given by:

$$h = \frac{\mathrm{u}^2}{2g} + \frac{\mathrm{p}}{\rho g} + z \tag{3.1}$$

Where u is the fluid velocity. In porous media the groundwater moves slowly, and the velocity term ($\frac{u^2}{2g}$) can be ignored and the resulting equation is:

$$h = \frac{p}{\rho g} + z \tag{3.2}$$

Therefore, if we know the height of mean sea level, then we can calculate the pressure head as:

H (water pressure head) $= h - z$

Groundwater always moves in the direction of decreasing total head (elevation head + water pressure head). Groundwater flow gradient in our study area is higher in summer season than in wet season (Fig. 3.6). We could also see that the hydraulic gradient is higher in the summer than in other periods. Therefore, the flow velocity will be higher. This might result in low total dissolved solids in summer as a result of small contact time between water and geologic material.

Hydraulic conductivity: is the measure of porous medium ability to transmit

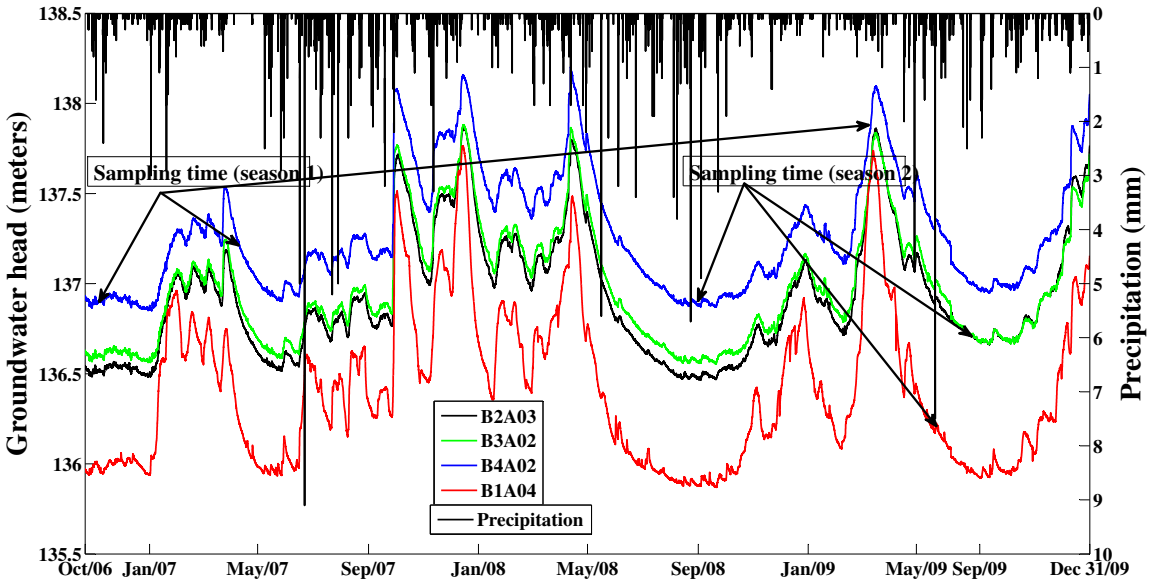

Fig. 3.6 Dynamics of groundwater level and precipitation from 2006-2009, during two sampling periods; Season 1(**November/2006, April/2007, March/2009**), and Season 2 (**August/2008, June/2009, August/2009**)

water when there is hydraulic gradient.

Porosity: is defined as the ratio of volume of voids to the total volume of the soil. It depends on the grain size distribution and the depth (compaction effect).

Equations of groundwater flow The groundwater flow equation is based on Darcy's law and the continuity equation. Darcy found that the total discharge Q (in a cylindrical volume of sand, with a cross-sectional area = A and length = L) is directly proportional to the cross-sectional area A and to hydraulic head difference between the two columns (Δh) and inversely proportional to the length L.

$$Q = -\mathrm{KA}(\frac{\mathrm{dh}}{\mathrm{dl}}). \tag{3.3}$$

Where K [L T^{-1}]is a constant of proportionality and it is called the hydraulic conductivity. The negative sign indicates that flow is in the direction of decreasing hydraulic head.

The continuity equation describes conservation of fluid mass during flow through porous media. According to this law, the rate of mass accumulation= Rate of mass inflow-Rate of mass outflow. Therefore, by using Darcy's law and the continuity equation we can derive the equation the for groundwater flow.

3.3.4 Groundwater-surface water interaction

Streams can be connected to the groundwater system (gaining stream, losing stream) by a continuous saturated zone (Fig. 3.7 A and B) or they can be disconnected from the groundwater system by an unsaturated zone (Fig. 3.7 C). The groundwater of the study area is connected with the river Saale which looks as type A and B depending on the water level in the river.

3.3.5 Hydrological features of the investigation area

River Saale and the artificial channel from the river interact with the groundwater of our study area during higher discharge of river Saale. However, how and when

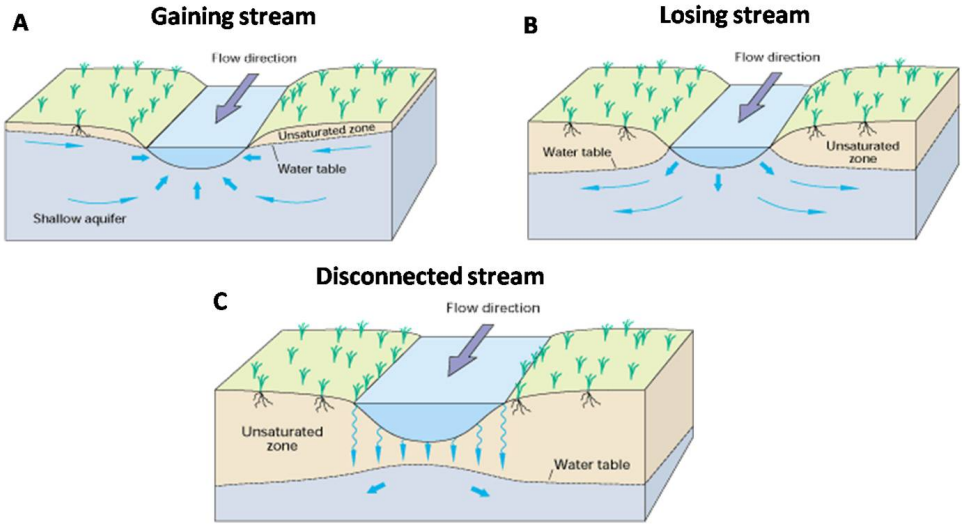

Fig. 3.7 Interaction of groundwater and stream (Winter et al. 1998)

they affect the groundwater of the study area was not studied. Groundwater and river water interact in different ways. We can see in the Fig. 3.7 that the river flows to the groundwater during low water table and the groundwater flow to the river during the low river discharge. The channel caries water always from the river toward the experimental field. The flow in the channel is proportional to the river flow rate. It is suspected that the channel might have contact with the groundwater of the study area. The map of the water table in March-2009 shows that the flow direction is from southwest to northeast direction (Fig. 3.8). River Saale with a catchment area of 24079 km^2 originates at a height of 705 m above sea level near the Big Waldstein in the Fichtelgebirge Mountains and flows into the Elbe after 427 km (Zerling et al. 2003). The catchment is characterized by shale bed rock in upland regions, porous sandstone of its forelands, karstic limestone bordering the Thuringian basins formations, the Keuper landscape and low land sediments of Börde region (Bongartz et al. 2007).

The Thuringian basin is a depression in the central and northwest part of Thuringia in Germany which is crossed by several rivers. Saale River is one of it. The basin is surrounded by a wider outer girdle of limestone (Muschelkalk) ridges and to the southwest by Thuringian forest and to the southeast by sharply divided terraces (the llm-Saale and Ohrdruf Muschelkalk plateau, and Saale Elster Buntersandstein plateau.

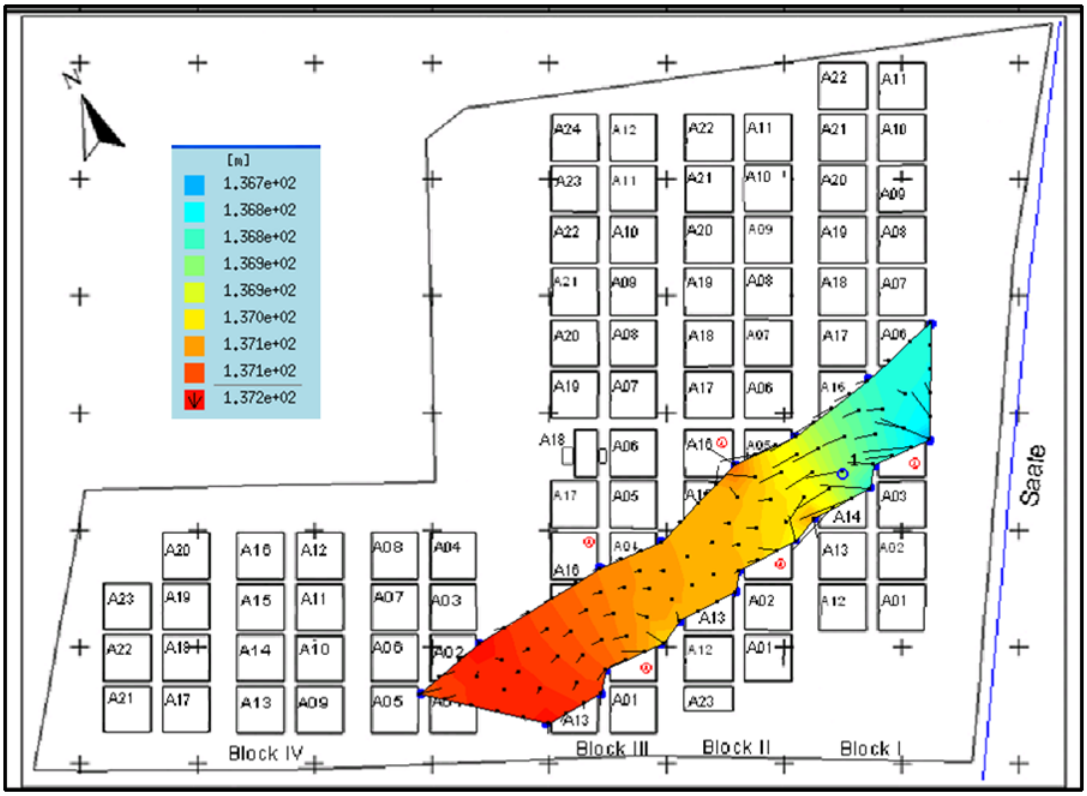

Fig. 3.8 Flow direction of groundwater in the study area in March-2009. The flow direction is based on linear interpolation between close groundwater heads indicated in dots.

3.3.6 Soil types

The upper layer of the studied area consists of mainly alluvial materials. Silty loam, loam, gravel and sand are the major texture of this layer. The texture of the upper layer varies from loam in block I to silty loam in block II and block III of the experimental field. In contrast, the lower horizon is composed mainly of sand and gravel material. The sand content is higher near the river and decreases with distance from the river, while the gravely material is higher in plots of Block III. The texture of soil of the study area is shown in Fig. 5.2.

Significance of soil texture: soil texture is important since it influences many processes and properties in the soil such as soil water movement, solute movement, organic matter storage, hydraulic conductivity and others. Some of the properties influenced by soil texture are:

1. Water holding capacity
2. Organic matter content
3. Cation exchange capacity (CEC)
4. pH buffering capacity and
5. Aeration are some of the important ones

Sandy soils (such as the lower layer of block I and block II of our study area) are low in organic matter content and fertility , low in ability to retain moisture and nutrients, low in cation exchange capacity (CEC). CEC is the degree to which a soil can adsorb and exchange cations. Soil particles and organic particles have negative charges on their surfaces. They have high permeability and allow rapid movement of water and air.

Silty and clayey soil (such as the top layer of the block III and block IV of the main experimental field) are capable of retaining moisture and nutrient, have high cation exchange capacity, contain more organic matter (Neufeldt et al. 2002), and less permeable to water and air.

We can also interpret soil from its color. According to study by Troeh and Thompson (2005) the coloring of soil is due to organic matter content,climate, soil drainage, and soil mineralogy.

Soils which contain hematite red color, hydrated ferric oxide are red brown and ferrous oxide are gray color (Troeh and Thompson 2005). Geothites have yellow color indicating moderate drainage and aeration (Schaetzl and Anderson 2005). Soils containing organic matter and manganese compounds have dark and grey dark color (Fisher et al. 2000, Yerima and Ranst 2005) and soils with calcium carbonate have whitish color (Yerima and Ranst 2005). The top layer of most of the locations at the study site are generally brown color indicating that it contains hydrated ferric oxide. Some locations, for example B1A17 and B3A16 are dark brown indicating high content of organic material compared to other locations. The different color of the soil profile in the study area and the material they contain for some plots are given in Appendix B.

Chapter 4

Materials and Methods

4.1 Field measurement and sampling procedure

4.1.1 Groundwater

21 groundwater wells in June 2006 were installed along transect lines X-X and Y-Y as shown in the Fig. 3.4. The wells are distributed in all the blocks. Their geographic location and altitude are shown in Table 4.1. Groundwater samples from 19 groundwater wells of biodiversity experiment area (Fig. 3.1) were collected in November 2006, April 2007, August 2008, March 2009, June 2009, August 2009, May 2010 (twice), and August 2010. There are wells which did not have water (usually in summer when the water table is low) in some periods of the year and samples for chemical analysis could not be collected from these wells. Twelve groundwater wells are equipped with automatic hydraulic head data loggers and recorded small fluctuations of piezometric heads every 15 minutes since 2006. The groundwater wells are designated as BIVA02E, BIVA05E, BIIIA13E, BIIIA13W, BIIIA05E, BIIIA02E, BIIIA02W, BIIIA16E, BIIA06E, BIIA13E, BIIA13W, BIIA03E, BIIA03W, BIIA16E, BIA17E, BIA14E, BIA14W, BIA04E and BIA04W. The first character and Roman number in the name of the wells indicate the block to which it belongs and the last character and number indicate the plot number in the block (for example, BIVA02

is plot number 2 in fourth block). The letter E (East) and W (West) indicates the relative direction of the well in the plot. In this study only groundwater wells which had water in all the sampling periods are used for investigation. The location of the plots and blocks are indicated in Fig. 5.1.

Table 4.1 Geographic location of the groundwater wells in the study area. The latitude and longitude are in UTM (Universal Transverse Mercator)

Name of the wells	Latitude	Longitude
BIA04E	0684445	5647631
BIA04W	0684422	5647628
BIA14E	0684414	5647618
BIA14W	0684390	5647617
BIA17E	0684438	5647687
BIIA16E	0684368	5647664
BIIA03E	0684371	5647608
BIIA03W	0684350	5647607
BIIA13E	0684343	5647598
BIIA13W	0684323	5647588
BIIA06E	0684396	5647675
BIIIA16E	0684297	5647647
BIIIA02E	0684306	5647592
BIIIA02W	0684284	5647586
BIIIA05E	0684332	5647656
BIIIA13E	0684274	5647577
BIIIA13W	0684254	5647575
BIVA05E	0684201	5647602
BIVA02E	0684234	5647621

4.1.2 Soilwater, rainwater and river Saale

Soil water samples were collected from plots at 20, and 30 cm depth in block I, 10, 20, 30, and 60 cm depth in block II, 20, and 30 cm depth in block III in March 2009. We also collected sample for chloride analysis from these depths in June, July, August, September and October 2010. Suction plates for soil water sampling were installed by group of Dr. Gerd Gleixner, Max-Planck Institute of Biogeochemistry. Location of the suction plates in the experimental field from which we took sample is shown in Fig. 7.3. Rain water was collected from the three blocks (Block I, Block II and Block III) in March 2009. River Saale water sample were also collected from

two points (from upstream and downstream of the study area) in March 2009 when the river flow is high. The sample from river was used to study the effect of river and channel from the river on the groundwater of the study area.

4.2 Sampling procedure

The water samples were filtered in the field using glass fiber prefilters (Millipore, Germany) and cellulose acetate filters (Sartorius, Germany) with a pore size of $0.45\mu m$. Parameters that were measured and recorded on spot using portable equipments were pH, temperature, EC, Eh, and oxygen concentration. Temperature was measured by using an external thermocouple (WTW Wissenschaftlich Technische Werkstätten, Germany). Electrical conductivity (EC), pH, Redox potential (Eh) and oxygen concentrations were measured using portable LF320, pH320, and Oxygen meters (WTW Wissenschaftlich Technische Werkstätten, Germany). The water samples for cation analysis were stabilized by adding nitric acid (65%, Baker Ultrex, USA). Acidification stops most bacterial growth, block oxidation reactions, and prevents adsorption and precipitation of cations (Appelo et al 2009). Some volume of the samples remained unacidified for determination of anions by ion chromatography, photometry and titration. The samples were then stored at 6°C until analysis.

4.3 Analysis of samples and analytical methods used

Each sample of the groundwater, soil water and river water was analyzed for major cations and anions, trace elements, including rare earth elements. Ground water and river Saale were also analyzed for HCO_3^- and dissolved organic carbon (DOC) . Rain water was analyzed for major cations and anions (except HCO_3^-). HCO_3^- analysis was not made for rainwater and soil water, because there was no enough volume in the sample.

Different analytical methods were used to determine the chemical analysis of groundwater, soilwater, river water and rainwater in the study area. These are inductively coupled plasma mass spectrometry (ICP-MS), inductively coupled plasma atomic emission spectroscopy (ICP-OES), ion-chromatography, atomic absorption spectroscopy (AAS), photometer and titration.

Inductively coupled plasma optical emission spectrometry (ICP-OES) (Spetroflame, Germany) is a multi-element method and was used to measure the major cations. Calcium, K, Mg, Mn, Na, P, S, Si, and Sr. It is a type of emission spectroscopy that uses the inductively coupled plasma to produce excited atoms and ions that emit electromagnetic radiation at wavelengths characteristic of a particular element (http://en.wikipedia.org/wiki/ICP-MS). The intensity of this emission is indicative of the concentration of the element within the sample.

Inductively coupled plasma mass spectrometry (ICP-MS))(X-Series II, Thermo Fisher Scientific, Germany) is a method featuring high multi-element capacity and detection limits in the ng/ L range (Merten and Büchel 2004) and was used measure trace elements (Al, As, B, Ba, Cd, Co, Cr, Cs, Cu, Fe, Li, Mn, Ni, Pb, U, V and Zn and rare earth elements). The instrument employs a plasma (ICP) as the ionization source and a mass spectrometer (MS) analyzer to detect the ions produced. Detail of the procedure on ICP-MS and ICP-OES is explained in Merten et al. (2005).

Chloride, NO_3^-, and SO_4^{2-} were determined using ion chromatography (DX-120, Dionex, Germany). Ion-exchange chromatography retains solute molecules on the column based on ionic interactions. The stationary phase surface displays ionic functional groups (R-X) that interact with solute ions of opposite charge. This type of chromatography is further subdivided into cation exchange chromatography and anion exchange chromatography. The ionic compound consisting of the cationic species M^+ and the anionic species B^- can be retained by the stationary phase [wex].

Hydrogen bicarbonate (HCO_3^-) was analyzed by titration (Titrino, Metrohm, Germany).

X-ray diffraction technique (XRD): is a non-destructive analytical technique which reveals information about the crystallographic structure, chemical composition, and physical properties of materials and thin films (He 2009). According to the same author this technique is based on observing the scattered intensity of an X-ray beam hitting a sample as a function of incident and scattered angle, polarization, and wavelength or energy. We analyzed the x-ray diffraction pattern of our samples, and then compared the result with XRD spectra of reference standard minerals. The measurements were made with in 2θ range of 3-70° and 0.02° steps. The instrument uses Cu Kα radiation.

The groundwater hydrochemical analysis data other than study area is from TLUG (Thüringer Landesanstalt für Umwelt und Geologie). The groundwater hydrochemical data of TLUG are sampled from Zwätzen (1.45km), Talstein (0.87 km), Löbstedt (0.74 km) and Kunitz (1.1 km), all of them from nearby study area and the distance indicated is from Jena experiment test site.

4.4 Statistical methods

4.4.1 Standardization and data preparation

The accuracy of chemical analysis can be estimated from the electrical balance since the sum of positive and negative charges in the water is equal (Appelo and Postma 1994):

$$Electrical\ balance\ \ (\%) = \frac{(\text{Sum cation} + \text{Sum anions})}{(\text{Sum cation} - \text{Sum anions})} * 100$$

where cations and anions are expressed as meq/L and inserted with their charge sign.

If the differences in electrical balance is in excess of 5%, the sampling analytical procedure should be examined (Appelo and Postma 1994). In our investigation the ion balances were calculated with major cation and anion and nearly all of the samples are within ±5% limit.

In order to evaluate the seasonal variation, the dataset was divided into two categories: April, November and March dataset as cold season and June and August as warm season. The cold season is characterized by relatively lower temperature, higher precipitation, shallower groundwater levels, while warm season is featured by higher temperature, relatively deeper groundwater levels and less precipitation (Fig. 3.6).

Before applying statistical models it is necessary to explore the data set to avoid common statistical problems. Some of the explorations could be to check for outliers, homogeneity of data, normality (based on the model type), and relationships between variables.

Outlier: is a value or measurement which is very small or large compared to the majority of the measurements or values. Boxplot and Cleveland dotplot (Zuur et al. 2010) are the common methods to visualize outliers in the data set. Cleveland dotplot is a graph in which the measurement value is plotted versus the order of measurement.

Homogeneity of variance: if the statistical problem involves analysis of variance (ANOVA) then the homogeneity of the data set is important (Zuur et al. 2010). We can transform the data set (example Z transformation) to remove the effect of variance difference. In this study before making multivariate statistical analysis each variable was standardized to avoid the problems of having one variable influencing the determination of factor loading.

Normality: to make comparison of variables (for example, t-test assumes normal distribution), we have to check normality of the data set. Histogram and QQ-plot were used to check for normality.

Correlations: some of the statistical models need some correlation among the data set. Factor analysis for example needs the variables to be correlated. We used Pearosn's formula to check correlation among multivariate data.

All calculations were performed using MATLAB version 7.6 (MatWorks, Inc, Natick, MA), and R statistical software (R-team).

4.4.2 Multivariate statistical techniques

There are different ways to interpret groundwater physico-chemical data. Common methods are multivariate statistical techniques, hydrochemical modeling (previous section) and graphical methods. Multivariate analysis can be used to identify the governing process through data reduction and classification. Multivariate statistical techniques such as factor analysis and cluster analysis can be performed to identify the most important factors which contribute to the underlying data structure and the similarities between the sampling points or between factors. Zeng and Todd (2005) used factor analysis to extract factors which contribute to the tributary water quality data. They also used factor analysis to extract the largest source of lake water quality variation. Suk and Lee (1999) used factor analysis and cluster analysis to characterize the groundwater hydrochemical system. They extracted factors from the groundwater physical and chemical data set and were used to explain the background hydrochemical processes. They also used cluster analysis using factor scores to divide the groundwater region into different zones of hydrochemical regimes. Several studies (Lee et al. 2001, Chen et al. 2007, Alther 1979, Momen et al. 1996, Olmez et al. 1994) have applied multivariate methods (factor analysis and cluster analysis) to groundwater chemical data in order to understand processes controlling groundwater hydrochemical composition.

4.4.2.1 Cluster analysis

Cluster analysis creates groups of objects that are similar compared to other objects or groups. There are various types of clustering: hierarchical, K-means clustering, overlapping clusters and fuzzy clusters. In this study hierarchical cluster analysis was used to create the groups. In this type of clustering we start with the whole data set and divide it into two based on a similarity measure (see below), then divide again until we reach a final object. It computes the similarity between all pairs of objects, and then it divides the groups by their similarity, and finally creates a hierarchical tree visualized as a dendrogram. There are also different choices to

form clusters in hierarchical cluster analysis; single linkage, average linkage, density linkage, ward's method, and others. In our study we used the single linkage method. In this linkage the distance between two clusters is computed as the distance between the two closest elements in the two clusters (Larose 2005). The disadvantage of using this linkage method is that, clusters may be forced together due to single element being close to each other, even though many of the other elements may be distant. Euclidean distance (Davis 1986) was used as a similarity measure. It measures the distance between the points in the multidimensional space according to:

$$d_{jk} = \sqrt{\frac{\sum_{k=1}^{m}(X_{ik} - X_{jk})^2}{m}}, \tag{4.1}$$

Where d_{jk} is Euclidean distance, X_{ik} and X_{jk} denotes the k^{th} variable measured on objects (sampling points) i and j. m is the number of variables measured. A low distance shows the objects are similar or have close similarity whereas a large distance indicates dissimilarity.

4.4.2.2 Factor analysis

Factor analysis is based on the assumption that variables which significantly correlate with each other are influenced by the same underlying factor. Factor analysis method can be divided into two broad classes, called R-mode (interrelations between variable) and Q-mode (relationship between objects) techniques (Davis 1986).

According to Dillon and Goldstein (1984) the basic factor analytic-model is usually expressed as:

$$X = \Lambda f + e \tag{4.2}$$

where, X= p-dimensional vector of observed responses, X'=(x_1,x_2,...,x_p), f=q-dimensional vector of unobservable variables called common factors, f'=(f_1,f_2,...,f_q), e= p-dimensional vector of unobservable variables called unique factors, e'=(e_1,e_2,...,e_p), and Λ=p×q matrix of unknown constants called factor loadings (l).

Factor loadings represent the extent to which each of the variables are related with

each of the factors.

$$\Lambda = \begin{pmatrix} l_{11} & l_{12} & \dots & l_{1q} \\ l_{21} & l_{22} & \dots & l_{2q} \\ \vdots & \vdots & \ddots & \vdots \\ l_{m1} & l_{m2} & \dots & l_{mq} \end{pmatrix} \tag{4.3}$$

Before performing factor analysis, standardization of raw data is required to remove the effect of difference in magnitude and in units. The Z-transformation is a common method to standardize raw data. The Z values are calculated as follows:

$$Z_i = \frac{X_i - \bar{X}}{S}$$

Where Z_i is the i^{th} standardized variable. X_i the i^{th} value of the variable X, $\overline{X}$ is the mean of the values of the variable X, and S is the standard deviation of the i^{th} variable.

4.4.3 Methods

To perform factor analysis, the raw data were first standardized using Z transformation as explained in *Section 4.4.2.2* to remove the effect of difference in values and units. Correlation coefficients were then calculated using Pearson's formula as follow:

$$r_{xy} = \frac{\sum_{i=1}(X_i - \overline{X})(Y_i - \overline{Y})}{\sqrt{\sum_{i=1} X_i - \overline{X})^2 * \sum_{i=1}(Y_i - \overline{Y})^2}} \tag{4.4}$$

where X_i and Y_i are the standardized variables and $\overline{X}$ and $\overline{Y}$ are their respective means. Eigenvalues were then calculated for the correlation matrix. Then eigenvalue of the factors and proportion of the variances associated with each factor were computed. The proportions are summed up to calculate cumulative eigenvalues. There are different ways to decide the number of factors to be extracted. These are; number of eigenvalues >1, scree plot, and percentage of variance explained.

In this study the number of factors extracted is based on criteria proposed by Kaiser (1959). According to this study only factors with eigenvalues that are greater than 1 are retained. We also draw scree plots to see if there is much difference and to see the result graphically. According to Scree test, the eigenvalues of the correlation matrix in descending order should be plotted, and then to use a number of factors equal to the number of eigenvalues that occur prior to the last major drop in eigenvalue magnitude (Zoski and Jurs 1996). Then the factors are rotated to get an easily interpretable result. In this study, Kaiser's varimax rotation scheme was used (Kaiser 1958). According to this study given a factor matrix with n tests and r factors, the varimax criteria requires that we make orthogonal rotation on this matrix such that,

$$\sum_s \left\{ n \sum_i (\frac{a_{is}^2}{h_i^2})^2 - (\sum_i \frac{a_{is}^2}{h_{is}^2})^2 \right\} \qquad is \;\; max, \tag{4.5}$$

where i=1, 2,..., n are tests on the s^{th} factor, a_{is} is the loading for i^{th} test and h_i^2 is the communality of the i^{th} test. Factor loadings with high values represent information on which the interpretation of factors are based and are bolded.

All calculations were performed using MATLAB version 7.6 (MatWorks, Inc, Natick, MA), and R (R-Team 2009) statistical software.

4.5 Implementations in PHREEQC

Speciation of the groundwater chemical composition

PHREEQC was used to speciate the groundwater composition and enable us to know which form of the element is dominant in the given environment. It also helps us to know the saturation state of the aqueous species with respect to available precipitates or minerals in the groundwater. The input of the PHREEQC is through KEYWORDS and associated data blocks. For example we use KEYWORD SOLUTION to specify the composition of our water sample. A full description of the

keywords are given in Pankhurst and Appelo (2009). An example of an input file is shown as follows: temp, pH, pe, redox, and units are important parameters and should always be included to specify a solution.

```
=====================================================================
Example of Input file format
TITLE [Comment]
SOLUTION [number][description]
    temp      6.6 #in degree centigrade
    pH        7.0
    pe        6.1
    redox     pe
    units     mg/l
    density   1 #kg/m3
    Alkalinity 461 as HCO3
    major cations and anions and other trace elements
   -water    1 # kg
EQUILIBRIUM_PHASES [number][description]
[Others] #can include different key words such as transport,
mix, and #so on based on the problem to be solved.
SAVE solution [number]
END
--------------------------------------
Example of some of the output file format
Distribution of species (Ca-ion)
                                  Log        Log      Log
Species           Molality    Activity   Molality Activity     Gamma
Ca                6.533e-03
Ca2+              5.521e-03   3.104e-03    -2.258    -2.508    -0.250
CaSO4             8.141e-04   8.190e-04    -3.089    -3.087     0.003
CaHCO3+           1.894e-04   1.640e-04    -3.723    -3.785    -0.063
```

```
CaCO3              7.679e-06   7.726e-06    -5.115    -5.112     0.003
Saturation indices (Ca containing minerals)
Phase            SI   log(IAP)  log(KT)
Calcite           0.16   -8.24   -8.40  CaCO3
Dolomite         -0.43  -17.06  -16.64  CaMg(CO3)2
Gypsum           -0.71   -5.31   -4.60  CaSO4:2H2O
================================================================================
```

Effect of river Saale on the groundwater chemical composition

We assumed that the groundwater at any place in the Jena experimental field should be a mixture of upstream groundwater (block IV) and river Saale water. The effect of river was investigated with PHREEQC by varying the presumed proportion of the river versus groundwater in the upstream (block IV). We calculated the mixing proportion in March 2009 by measured chloride concentration in river and groundwater in block IV, and obtained 55/45 (groundwater to river water). We used this proportion in PHREEQC to calculate all other concentrations and to determine other properties. We also predicted the chemical composition at low and high river flow seasons.

Effect of Channel on the groundwater of the study area

To study the effect of the channel and river on the groundwater chemistry of the study area we calculated the result of mixing of the channel and the river on the groundwater chemical composition. To know the proportion of river mixing we used chloride as a conservative element and calculate the proportion of groundwater and river.

Chapter 5

Hydrochemical characterization of groundwater system [1]

5.1 Introduction

This chapter deals with how hydrochemical modeling, graphical methods and different statistical techniques (factor and cluster analysis) were applied on a number of hydrochemical variables and ten sampling points (from six sampling campaigns) to understand the nature of geological and hydrochemical processes in a shallow groundwater aquifer of Jena biodiversity experimental field.

5.1.1 Investigation area

The geography, geology and hydrogeology of the of the study area and design of the experimental field is covered in *Sections 3.1* and *3.2*. The location of groundwater wells used to investigate the hydrogeochemical characterization are indicated in Fig. 5.1.

The study area and nearby area are located in Muschelkalk (Triassic lime-

[1]The content is based on the paper **under review**: Tessema S.G., Mirgorodsky D., Merten D., Hildebrandt A., Attinger S., Büchel G.: Hydrochemical characterization of groundwater system of biodiversity experimental field Jena/Germany, Env Geol.(2011)

Fig. 5.1 Groundwater wells in Jena biodiversity experiment field. The textural composition along transect line X-X is shown in Fig. 5.2. The numbers in the map shows plot number in a given block.

stone) or Upper Buntsandstein geological formations (Seidel 2003). The Muschelkalk mainly comprises carbonates and evaporites. According to the study by Voigt et al. (2005), groundwaters in Muschelkalk are characterized by higher Ca^{2+}, electrical conductivity, HCO_3^-, Mg^{2+}, and SO_4^{2-}. The same authors concluded that Upper Buntsandstein has relatively lower electrical conductivity. They observed that groundwater in carbonate rocks (Muschelkalk) differ from that of sand and sandstone with increased mineralization. The Buntsandstein predominantly consists of sandstone layers. The detail description of these and other geologic units and their chemical composition are discusses in Chapter 3.5.

The groundwater is hosted in an unconfined aquifer and the water table fluctuates between about 40 cm (in spring) to 270 cm (in summer) (depth to water table).

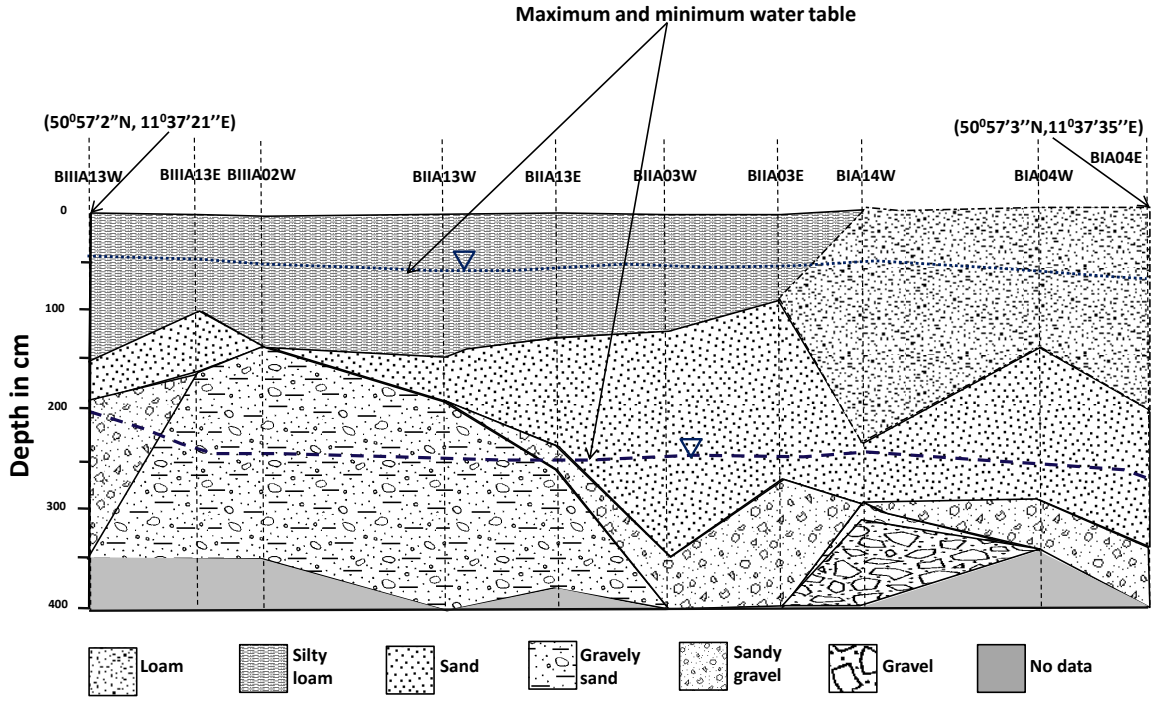

Fig. 5.2 Textural composition of the horizontal cross section of the study field along transect line X-X (transect line X-X is shown in the Fig. 5.1)

The contour map of the water table (Fig. 3.8) shows that the flow direction is from southwest to northeast direction. But the velocity field generally varies.

5.2 Results and discussion

In order to evaluate the seasonal variation, the dataset was divided into two categories: April, November and March dataset as cold season and June and August as warm season. The cold season is characterized by relatively lower temperature, higher precipitation, shallower groundwater levels, while warm season is featured by higher temperature, relatively deeper groundwater levels and less precipitation (Fig. 3.6).

Table 5.1 Cross correlation of variables of wet season (March-2009, April-2007, November-2006) groundwater samples. The values of the parameter at each sampling points are the average of 3 sampling campaigns. From the correlation we can see that there are some correlations among group of parameters, which shows that there are possible underlying processes. We used factor analysis to extract these processes.

Para.	T	EC	pH	Eh	O_2	B	Ba	Ca	Co	Cu	Fe	K	Li	Mg	Mn	Na	Ni	Si	Sr	U	V	Zn	Cl	SO_4	NO_3	HCO_3	DOC
T	1.0																										
EC	0.5	1.0																									
pH	-0.4	-0.4	1.0																								
Eh	0.1	0.3	0.1	1.0																							
O_2	0.0	0.2	0.8	0.1	1.0																						
B	0.6	1.0	-0.6	0.3	0.0	1.0																					
Ba	-0.2	-0.8	-0.2	-0.3	-0.6	-0.7	1.0																				
Ca	0.5	1.0	-0.2	0.4	0.4	0.9	-0.9	1.0																			
Co	0.4	-0.1	-0.5	-0.7	-0.5	0.0	0.5	-0.3	1.0																		
Cu	0.4	0.3	-0.3	0.5	0.0	0.4	-0.1	0.3	-0.3	1.0																	
Fe	-0.2	-0.4	0.1	-0.9	-0.1	-0.4	0.3	-0.5	0.7	-0.7	1.0																
K	0.5	0.8	-0.8	0.1	-0.3	0.9	-0.4	0.7	0.1	0.4	-0.3	1.0															
Li	0.4	0.7	-0.8	0.3	-0.4	0.9	-0.3	0.6	0.0	0.5	-0.4	1.0	1.0														
Mg	0.5	1.0	-0.6	0.2	0.0	1.0	-0.7	0.9	0.0	0.3	-0.3	0.9	0.8	1.0													
Mn	0.6	0.4	-0.3	0.0	-0.3	0.3	0.0	0.2	0.6	-0.2	0.2	0.2	0.1	0.3	1.0												
Na	0.5	1.0	-0.5	0.3	0.1	1.0	-0.8	1.0	-0.1	0.3	-0.4	0.9	0.8	1.0	0.3	1.0											
Ni	0.6	0.4	-0.5	0.1	-0.3	0.4	0.1	0.2	0.6	0.1	0.0	0.5	0.5	0.4	0.6	0.4	1.0										
S	0.6	1.0	-0.3	0.3	0.3	0.9	-0.8	1.0	-0.2	0.2	-0.4	0.7	0.6	0.9	0.3	1.0	0.4										
Si	0.2	0.6	0.1	0.8	0.2	0.5	-0.6	0.6	-0.6	0.3	-0.7	0.3	0.3	0.4	0.2	0.5	0.1	1.0									
Sr	-0.1	-0.1	0.0	-0.7	0.1	-0.1	0.2	-0.2	0.6	-0.6	0.7	-0.2	-0.3	0.0	0.3	-0.1	0.3	-0.6	1.0								
U	-0.5	-0.6	0.3	-0.1	-0.2	-0.6	0.3	-0.6	-0.1	-0.1	0.3	-0.4	-0.4	-0.6	-0.3	-0.6	-0.3	-0.1	-0.3	1.0							
V	-0.6	-0.7	0.6	-0.2	0.1	-0.7	0.4	-0.6	0.0	-0.3	0.4	-0.7	-0.7	-0.7	-0.4	-0.7	-0.3	-0.4	0.2	0.8	1.0						
Zn	0.1	0.4	0.0	0.3	0.2	0.4	-0.4	0.4	-0.2	0.4	-0.2	0.2	0.2	0.3	0.0	0.4	0.3	0.4	-0.1	0.3	0.2	1.0					
Cl	0.5	1.0	-0.6	0.3	0.0	1.0	-0.7	0.9	-0.1	0.3	-0.4	0.9	0.8	1.0	0.3	1.0	0.4	0.5	-0.2	-0.6	-0.7	0.3	1.0				
SO_4	0.6	1.0	-0.3	0.3	0.3	0.9	-0.8	1.0	-0.1	0.2	-0.4	0.8	0.6	0.9	0.3	1.0	0.4	0.5	0.0	-0.7	-0.6	0.4	0.9	1.0			
NO_3	0.3	0.6	-0.7	0.4	-0.2	0.7	-0.3	0.6	-0.3	0.8	-0.6	0.8	0.9	0.7	-0.1	0.7	0.2	0.3	-0.3	-0.5	-0.7	0.3	0.7	0.5	1.0		
HCO_3	-0.6	-1.0	0.3	-0.4	-0.3	-0.9	0.8	-1.0	0.2	-0.4	0.5	-0.8	-0.7	-0.9	-0.2	-1.0	-0.3	-0.5	0.2	0.6	0.6	-0.3	-0.9	-1.0	-0.6	1.0	
DOC	-0.4	-0.6	-0.2	-0.4	-0.3	-0.5	0.6	-0.6	0.1	0.1	0.2	-0.2	-0.1	-0.4	-0.7	-0.5	-0.2	-0.7	0.0	0.3	0.4	-0.4	-0.5	-0.6	0.0	0.5	1.0

(**Para.**=Parameter (variable measured), **DOC**=dissolved organic carbon)

Table 5.2 Descriptive statistics (range, arithmetic mean, standard deviation) of Cold season (March-2009, April-2007, November-2006) groundwater samples. The values of the parameter at each sampling points are the average of 3 sampling campaigns. The raw data is given in Appendix A

		Sampling Points										**Range**		**Mean**	
Para.	Unit	B4A02	B4A05	B3A13	B3A02	B2A13	B2A03	B1A14	B1A04	B2A16	B3A16	Min	Max	Mean	SD
pH		6.96	6.98	7.03	7.07	6.97	7.01	7.07	7.17	7.03	7.03	**6.96**	**7.17**	**7.03**	**0.06**
EC	[μS/cm]	1661	1630	1415	1302	1676	1689	1636	1555	1601	1548	**1302**	**1689**	**1571**	**124**
Eh	[mV]	423	427	437	397	453	460	483	453	360	337	**337**	**483**	**423**	**46**
T	[°C]	9.57	9.80	9.77	9.47	10.00	9.93	9.57	9.70	9.87	9.70	**9.47**	**10.00**	**9.74**	**0.17**
O_2	[mg/L]	3.96	4.44	3.97	3.80	4.20	4.17	4.55	6.31	4.55	4.55	**3.80**	**6.31**	**4.45**	**0.71**
B	[μg/L]	298	280	166	101	295	282	255	196	258	209	**101**	**295**	**234**	**64**
Ba	[μg/L]	77.6	80.4	103.9	104.4	84.4	75.8	73.0	68.1	76.2	89.7	**68.1**	**104.4**	**83.4**	**12.5**
Ca	[mg/L]	279	278	256	242	277	280	277	276	271	264	**242**	**280**	**270**	**12**
Co	[μg/L]	0.86	1.10	1.41	1.18	1.40	1.31	0.78	0.48	1.53	1.87	**0.48**	**1.87**	**1.19**	**0.40**
Cu	[μg/L]	0.96	1.60	1.09	0.90	1.23	1.04	0.93	1.03	0.89	0.55	**0.55**	**1.60**	**1.02**	**0.27**
Fe	[mg/L]	0.01	<6E-4	0.01	0.22	<6E-4	<6E-4	<6E-4	0.01	0.29	0.41	**<6E-4**	**0.41**	**0.10**	**0.15**
K	[mg/L]	5.75	4.93	1.98	1.00	5.90	4.10	3.57	1.60	4.39	2.80	**1.00**	**5.90**	**3.60**	**1.72**
Li	[μg/L]	21.63	20.23	10.57	7.10	22.23	15.77	13.97	6.80	13.73	9.93	**6.80**	**22.23**	**14.20**	**5.73**
Mg	[mg/L]	43.2	42.3	33.7	28.4	42.9	41.7	40.0	36.1	41.0	38.6	**28.4**	**43.2**	**38.8**	**4.8**
Mn	[μg/L]	375	494	903	525	1343	2761	873	129	1182	1591	**129**	**2761**	**1018**	**764**
Na	[mg/L]	56.9	54.6	38.7	26.3	57.7	55.7	53.4	46.0	51.1	46.3	**26.3**	**57.7**	**48.7**	**9.9**
Ni	[μg/L]	3.77	4.27	4.27	3.73	5.63	4.46	4.59	3.53	4.20	4.87	**3.53**	**5.63**	**4.33**	**0.61**
Si	[mg/L]	4.81	4.74	4.46	4.66	5.12	5.25	5.21	5.05	4.66	4.26	**4.26**	**5.25**	**4.82**	**0.33**
Sr	[mg/L]	3.43	3.32	1.88	1.50	3.41	3.05	2.84	1.92	2.95	0.88	**0.88**	**3.43**	**2.52**	**0.90**
U	[μg/L]	5.70	6.14	6.10	7.37	5.66	5.67	6.80	5.80	6.67	5.73	**5.66**	**7.37**	**6.16**	**0.59**
V	[μg/L]	4.65	5.05	5.50	5.70	4.60	4.45	5.75	5.20	5.30	5.35	**4.45**	**5.75**	**5.16**	**0.46**
Zn	[μg/L]	30.1	62.2	32.6	37.9	45.5	43.1	64.2	41.1	45.2	39.7	**30.1**	**64.2**	**44.2**	**11.2**
Cl	[mg/L]	104.1	93.6	60.1	36.0	100.6	98.6	88.0	72.4	88.3	71.9	**36.0**	**104.1**	**81.3**	**21.4**
SO_4	[mg/L]	445	430	343	249	463	468	444	425	434	403	**249**	**468**	**410**	**66**
NO_3	[mg/L]	16.17	19.30	4.37	1.26	13.50	9.63	5.7	4.00	2.03	1.29	**1.26**	**19.30**	**7.72**	**6.56**
HCO_3	[mg/L]	455	460	502	567	447	455	463	467	464	498	**447**	**567**	**478**	**36**
DOC	[mg/L]	6.34	6.12	6.55	6.55	5.95	4.50	5.35	5.60	5.90	5.88	**4.50**	**6.55**	**5.87**	**0.62**

(**SD**=standard deviation, **DOC**=dissolved organic carbon)

Table 5.3 Descriptive statistics (range, arithmetic mean, standard deviation) of Warm season (June-2009, August-2008, August-2009) groundwater samples. The values of the parameter at each sampling points are the average of 3 sampling campaigns. The raw data is given in Appendix A

		Sampling Points										**Range**		**Mean**	
Para.	Unit	B4A02	B4A05	B3A13	B3A02	B2A13	B2A03	B1A14	B1A04	B2A16	B3A16	Min	Max	Mean	SD
pH		7.01	7.06	7.09	7.15	7.67	7.09	7.60	7.27	7.14	7.18	**7.01**	**7.67**	**7.23**	**0.23**
EC	**[μS/cm]**	1592	1472	1276	1149	1627	1605	1611	1463	1638	1532	**1149**	**1638**	**1497**	**165**
Eh	**[mV]**	463	443	238	217	373	420	210	120	170	137	**120**	**463**	**279**	**132**
T	**[°C]**	16.7	17.1	16.7	17.4	17.2	17.2	17.7	14.4	16.8	17.2	**14.4**	**17.7**	**16.8**	**0.9**
O_2	**[mg/L]**	2.97	3.07	3.10	3.00	3.13	3.80	3.20	3.70	2.83	3.13	**2.83**	**3.80**	**3.19**	**0.31**
B	**[μg/L]**	209	186	141	71	236	160	215	14	196	160	**14**	**236**	**157**	**72**
Ba	**[μg/L]**	93	109	132	154	131	99	101	129	98	126	**93**	**154**	**117**	**20**
Ca	**[mg/L]**	271	256	233	224	274	284	281	303	285	268	**224**	**303**	**268**	**24**
Co	**[μg/L]**	0.85	1.12	1.32	0.85	5.05	1.17	1.46	< 0.1	1.21	1.22	**0.85**	**5.05**	**1.58**	**1.31**
Cu	**[μg/L]**	0.71	0.65	$<$ 0.20	0.38	0.57	0.42	0.35	$<$ 0.20	0.30	$<$ 0.20	$<$ **0.20**	**0.71**	**0.37**	**0.25**
Fe	**[mg/L]**	0.02	0.03	0.17	0.32	0.09	0.02	0.15	0.15	0.39	0.43	**0.02**	**0.43**	**0.18**	**0.15**
K	**[mg/L]**	5.87	3.86	2.70	1.13	6.26	5.30	4.81	1.20	5.10	3.32	**1.13**	**6.26**	**3.95**	**1.84**
Li	**[μg/L]**	21.3	13.67	11.21	4.17	22.50	19.60	16.90	4.66	15.66	7.89	**4.17**	**22.5**	**13.8**	**6.6**
Mg	**[mg/L]**	41.2	37.8	29.8	24.9	41.6	42.6	41.1	35.7	42.6	38.1	**24.9**	**42.6**	**37.6**	**5.9**
Mn	**[μg/L]**	139	117	246	114	397	1444	424	402	428	287	**114**	**1444**	**400**	**388**
Na	**[mg/L]**	54.6	41.9	31.1	17.7	54.9	48.9	52.8	40.6	50.3	43.7	**17.7**	**54.9**	**43.7**	**11.8**
Ni	**[μg/L]**	3.33	3.03	3.03	2.10	5.17	4.05	3.20	1.60	3.09	4.14	**1.60**	**5.17**	**3.27**	**1.02**
Si	**[mg/L]**	5.11	5.15	5.20	5.34	5.60	5.49	5.59	5.32	5.13	4.86	**4.86**	**5.60**	**5.28**	**0.24**
Sr	**[mg/L]**	1.18	0.80	0.41	0.41	1.21	1.65	0.96	1.66	1.03	0.72	**0.41**	**1.66**	**1.00**	**0.44**
U	**[μg/L]**	9.43	10.89	8.62	10.69	9.15	9.32	11.24	10.82	10.55	7.63	**7.63**	**11.24**	**9.83**	**1.18**
V	**[μg/L]**	0.95	0.99	0.62	1.04	0.76	0.91	0.93	2.16	0.77	0.82	**0.62**	**2.16**	**0.99**	**0.43**
Zn	**[μg/L]**	35.7	50.8	26.8	28.7	44.6	20.2	17.2	8.7	15.8	18.4	**8.7**	**50.8**	**26.7**	**13.5**
Cl	**[mg/L]**	90.1	56.8	37.1	5.2	88.5	80.0	83.3	51.5	84.8	57.4	**5.2**	**90.0**	**63.5**	**27.4**
SO_4	**[mg/L]**	412	308	229	139	437	434	421	384	417	336	**139**	**437**	**352**	**100**
NO_3	**[mg/L]**	10.23	59.45	2.90	0.27	13.80	10.75	5.00	1.70	0.83	0.90	**0.27**	**59.45**	**10.58**	**17.83**
HCO_3	**[mg/L]**	483	511	573	662	469	481	500	508	530	589	**469**	**662**	**531**	**60**
DOC	**[mg/L]**	2.97	3.24	3.21	4.80	2.50	3.10	4.13		3.37	4.40	**2.50**	**4.80**	**3.52**	**0.75**

(**SD**=standard deviation, **DOC**=dissolved organic carbon)

5.2.1 General groundwater chemistry

The chemical composition of the groundwater samples were divided into cold and warm seasons and then interpreted. The chemical and physical property data together with some descriptive statistics are given in Tab. 5.2 and Tab. A.1. The tables show the mean, standard deviation, minimum and maximum value of the data of cold and warm seasons respectively.

There are relatively higher total dissolved solids (measured in terms of electrical conductivity) values in all plots except plots BIIIA02 and BIIIA13 in block III. The electrical conductivity values range from 1148 to 1690 μS/cm. The pH values in both seasons are circum-neutral (6.96-7.23). The groundwater is always oxidizing (Eh is $>$ 330 mV in cold season and $>$ 110 mV in warm season) and also varied spatially. Oxygen concentration is higher in the cold season (3.80-6.31 mg/L) compared to warm season (2.83-3.80 mg/L). The temperature of the groundwater is higher in warm season than in cold season.

Dissolved organic carbon values are between 2.5 mg/L and 4.8 mg/L in warm season and 4.5 mg/L to 5.87 mg/L in cold season. The concentration of Fe is elevated in plots BIIIA02, BIIIA13 and BIIIA16 compared to other plots. It is also generally higher in warm season than in cold season. There is a big variation of NO_3^- in the groundwater. NO_3^- ranges from 0.27 mg/L to 59.45 mg/L. The NO_3^- concentration in Block IV (plots BIVA02 and BIVA05) was much higher than for other plots. In contrast, Plots BIIIA02, BIIIA13 and BIIIA16 have lowest NO_3^- concentration. There was lower concentration of Li and K in plots BIIIA02 (block III), BIIIA13 (block III) and BIA04 (block I) compared to other plots in both seasons. K and Li showed also spatial variation in a similar pattern. Sodium and Cl^- concentrations are higher in block IV, a block near the main road.

The total dissolved solid in the groundwater of the study area is mainly because of the high content of HCO_3^-, SO_4^{2-} and Ca. The order of concentration of the major cations and anions in the groundwater are: Ca>Na>Mg>K>Sr and HCO_3^->SO_4^{2-}>Cl^->NO_3^- respectively. The EC value is relatively lower in groundwater wells located in Block III (plots BIIIA02 and BIIIA13). According to study

by Langmuir (1977) zones with higher groundwater flow velocity will have lower dissolved solids because of shorter contact time between the rock and ground water and high water to rock ratio. The soil texture below plots BIIIA02 and BIIIA13 in Block III is mainly sandy gravel and gravely sand (Fig. 5.2) which has relatively higher hydraulic conductivity and therefore higher velocity which result in less contact time between geologic matrix and groundwater. The constant value of the pH suggests that the buffering capacity groundwater is good. This is because of the presence of the carbonate and bicarbonate minerals which have buffering capacity. The higher values of oxygen concentration in cold season is due to increase in solubility as temperature decreases. According to Tromans (1998) solubility of the oxygen in water generally decrease as the temperature increases over the temperature range of -13 to 77 °C.

The concentration of iron increases as the groundwater becomes anoxic (Chapelle 2000). Most of the groundwater wells in the experimental field however, are in oxidizing condition and the concentration of iron is low. The elevated iron concentration in plots BIIIA02, BIIIA13, and BIIIA16 of Block III and BIIA16 of block II could be related to the availability of reactive minerals containing iron. The hydrochemical modeling using PHREEQC also indicates that there is spatial variation of iron containing reactive mineral ($FeCO_3$). Those plots have saturation indices near zero with respect to siderite. The concentration of Fe is positively correlated with DOC in warm season (r=0.66) and HCO_3^-(r=0.69). Dissolved organic carbon and HCO_3^- are also positively correlated (r=0.8, in warm season, and r=0.5 in cold season) with each other in both seasons. The higher values of sodium and chloride concentration in block IV (Na=56.9; Mg/L, Cl=104.1 Mg/L) could be because of the anthropogenic salt from the road during the winter season.

5.2.2 Hydrogeochemical facies

The concentration of major cations (Ca, Mg, Na) and anions (HCO_3^-, SO_4^{2-}, Cl^-) of the groundwater are plotted in a Piper diagram (Piper 1944) using AquaChem 5.1 (Schlumberger water services, Waterloo, Canada) to determine the water type

(Fig. 5.3). The groundwater of study area and nearby areas, soil water, and river Saale are dominated by alkaline earth metals (Ca, Mg). Hydrogen bicarbonate dominates in soil water, groundwater (in plots BIIIA02 and BIIIA13 of block III) and groundwater in Muschelkalk geologic unit. Chloride and SO_4^{2-} dominate in all other groundwater wells in the experimental field and groundwaters in Upper and Middle Buntsandstein. Three water types are found in the study area and nearby study area: Ca-Mg-HCO_3, Ca-Mg-SO_4, and Ca-Mg-Cl. Ca-Mg-HCO_3 is dominant in groundwater with Muschelkalk geologic unit and plots BIIIA02 and BIIIA13 of Block III of the experimental field. The rest of the plots in the experimental field and groundwater in the upper, lower and middle Buntsandstein are dominated by Ca-Mg-SO_4 and Ca-Mg-Cl water types.

Piper diagrams can also be used to identify mixing of waters. According to a study by Morris et al. (1983) when water from two different sources mix in any proportion, the mixture will be plotted on a straight line between the two end members. From our piper plot (Fig. 5.3) we can see that the water type in groundwater of BIIIA02 and BIIIA13 lies in between the soil water and groundwater from other plots. This indicates that the groundwater in these plots are from soil water and other groundwater. The water in these plots (**B**) are more closer to soil water (**A**) than groundwater (**C**). These suggests that soil water contributes to most of the groundwater in these plots.

Semilogarithmic Schoeller diagram (Fig. 5.4) were also used to inspect the chemical data from ground waters, soil water and river Saale. The Schoeller diagram obtained indicates that Ca and HCO_3 are dominant both in groundwater and soil water while SO_4^{2-} is dominant only in groundwater. Unlike other cations and anions chloride showed a wide variation over different seasons and among different groundwater, soil water and river water. Higher concentration of chloride is observed in April/2006 and lower values in summer season. The higher chloride concentration in spring is due to higher precipitation in this season.

The presence of the similar types of hydrogeochemical facies in the majority of the plots of the study area and Buntsandstein suggests that groundwater of the study area have similar hydrochemical signature as Upper Buntsandstein and the

groundwater is probably located in Buntsandstein geologic unit. Plots BIIIA02 and BIIIA13 in block III have different water types than others but, similar hydrochemical characteristic as Muschelkalk.

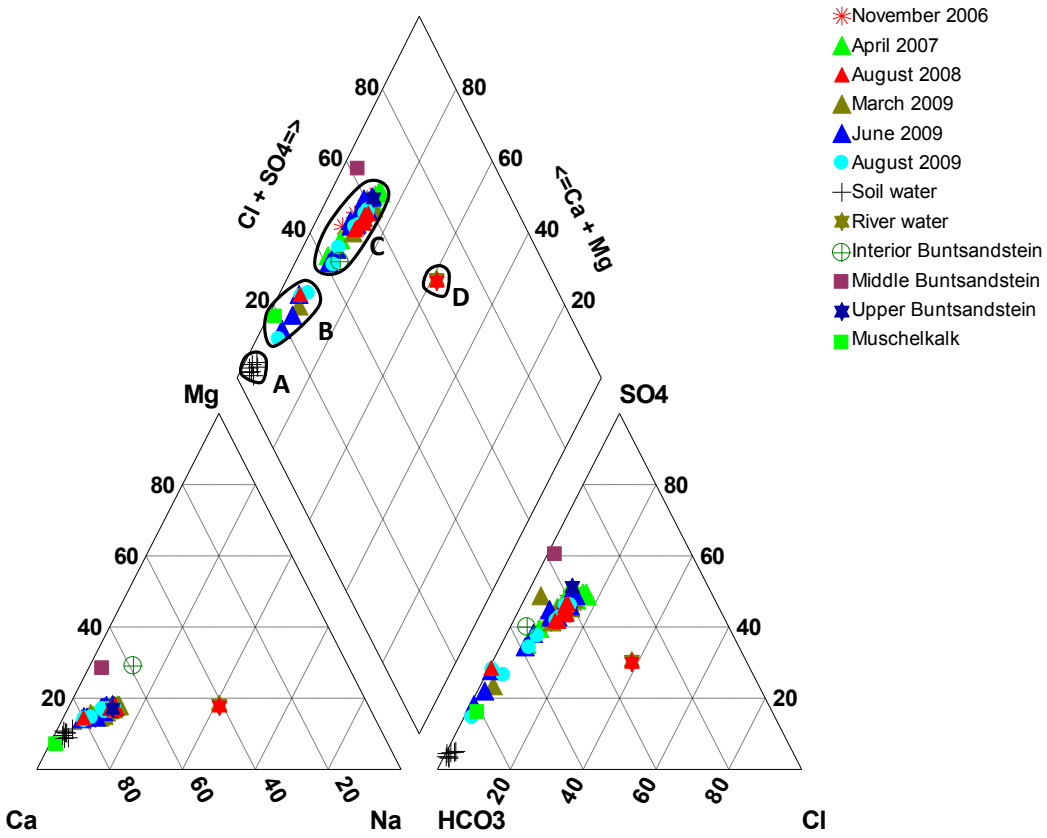

Fig. 5.3 Piper trilinear diagram of water chemistry of the study and nearby area. Hydrochemistry of soilwater **(A)**, groundwater in plots BIIIA02 and BIIIA13 and Muschelkalk **(B)**, groundwater in most plots and Buntsandstein **(C)** and river Saale **(D)**.

5.2.3 Isotopic variation

We also measured the hydrogen and oxygen isotope of the groundwater in our study area. We plotted δ^2H and $\delta^{18}O$ and compared the result with the Global Meteoric Water Line (GMWL) developed by Craig (1961). Global meteoric water line is the relationship between δ^2H and $\delta^{18}O$ in precipitation worldwide. VSMOW (Vienna Standard Mean Ocean Water) is the reference used. According to Craig (1961) the GMWL can be expressed as $\delta^2H = 8\delta^{18}O + 10$.

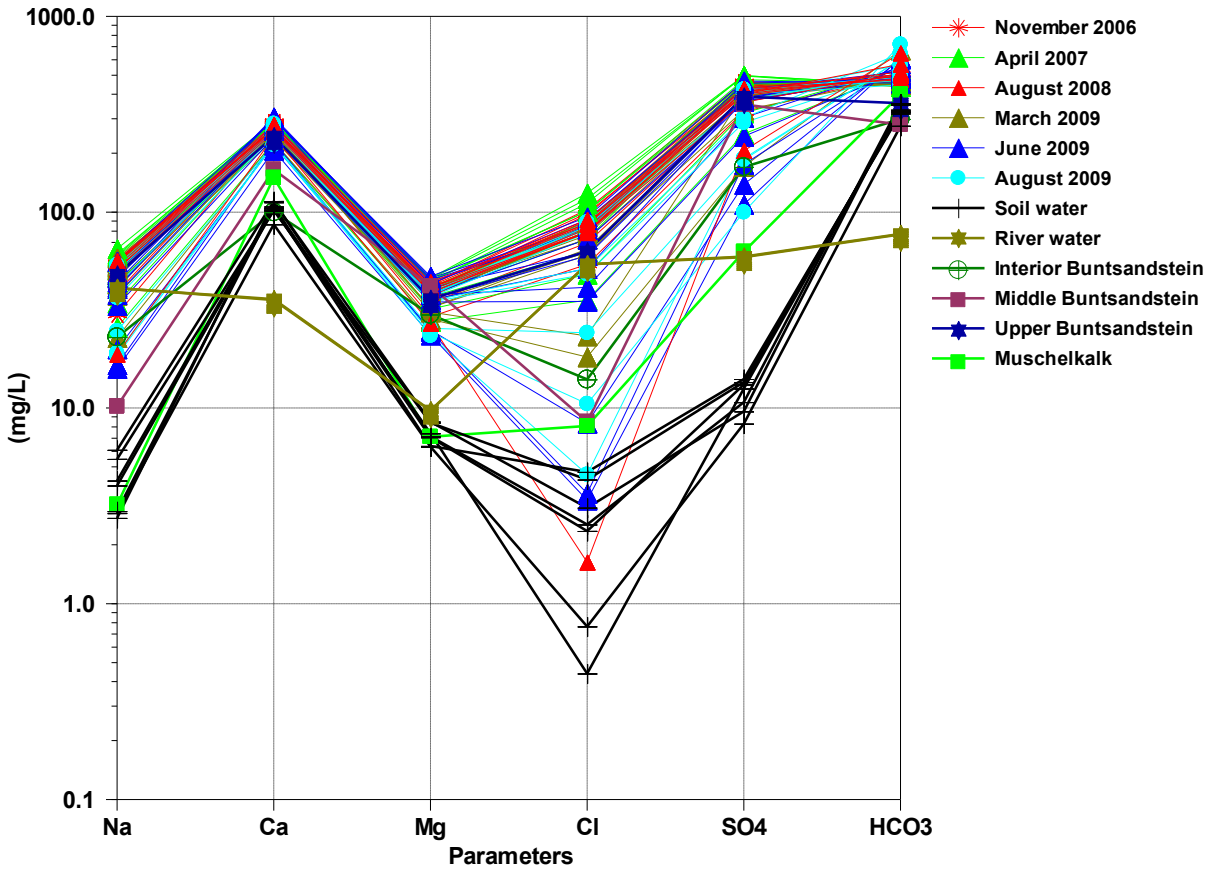

Fig. 5.4 Schoeller diagram of the of the groundwater samples from study area and nearby area, soil water of the study area and river Saale samples

Clark and Fritz (1997) showed that temperature can affect isotope fractionation; the colder the season, the greater the amount of fractionation that occur. In the groundwater of our study area the δ^2H ranges from -63.35 to -53.23 while $\delta^{18}O$ varies from -8.9 to -7.23. We could also see spatial variation in enrichment (Fig. 5.7). Most of the ground waters in wells of block III specially plot BIIIA13 and BIIIA02 are more enriched than groundwater in other plots. This could be because of the calcite mineral in those plots. Calcium precipitates by reacting with water and carbon dioxide to form calcite. According to Clark and Fritz (1997) difference in bond strength for isotope of the same element provide for their difference in rate of reaction. Therefore, the light oxygen isotope in water molecule is taken up by calcium and enrich the heavy oxygen as a result. We also observed that, cold season

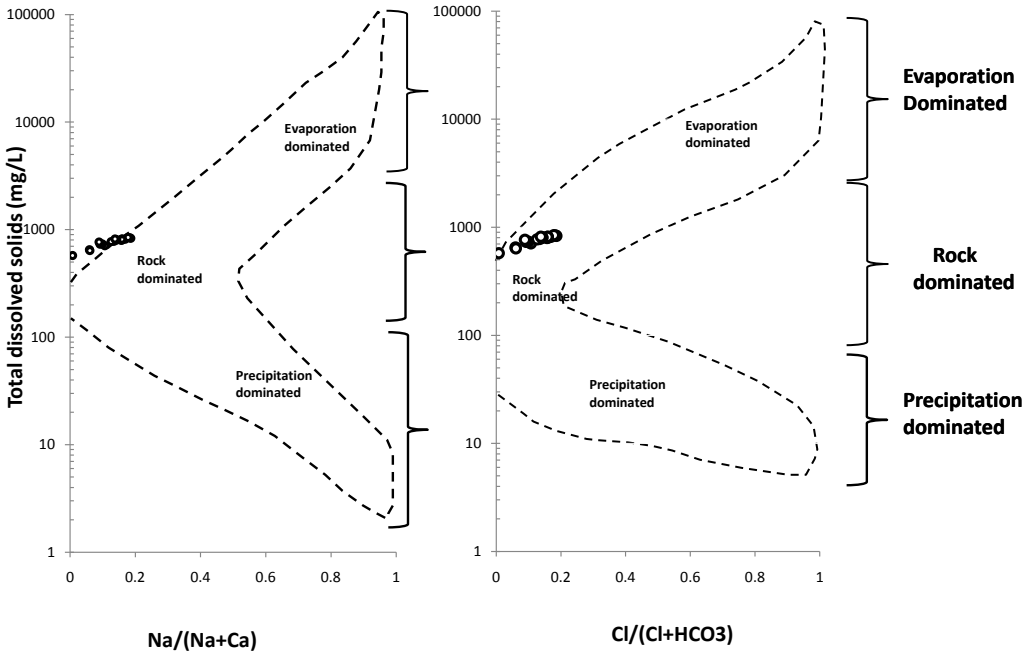

Fig. 5.5 Mechanisms controlling groundwater chemistry (after Gibbs (1970))

(e.g. December) resulted in depletion (Fig. 5.6).

5.2.4 Results of Factor and Cluster analysis

Factor analysis was used to identify the governing underlying processes and hierarchical cluster analysis was used to detect the spatial similarity between the sampling points. The factor analysis results (Tab. 5.4 and Tab. 5.5) indicate that there are five dominant processes which account together for about 90% of the variance of the dataset in both seasons. Therefore these factors were used to explain the background hydrochemical processes without losing significant characteristic of the groundwater composition.

Factor analysis result shows that 53% in cold season and 43% in warm season of the variation of the groundwater hydrochemical data is due to factor 1 consisting of Ba, Ca, Cl^-, EC, HCO_3^-, K, Li, Mg, Na, SO_4^{2-}, and Sr which reveal groundwater-

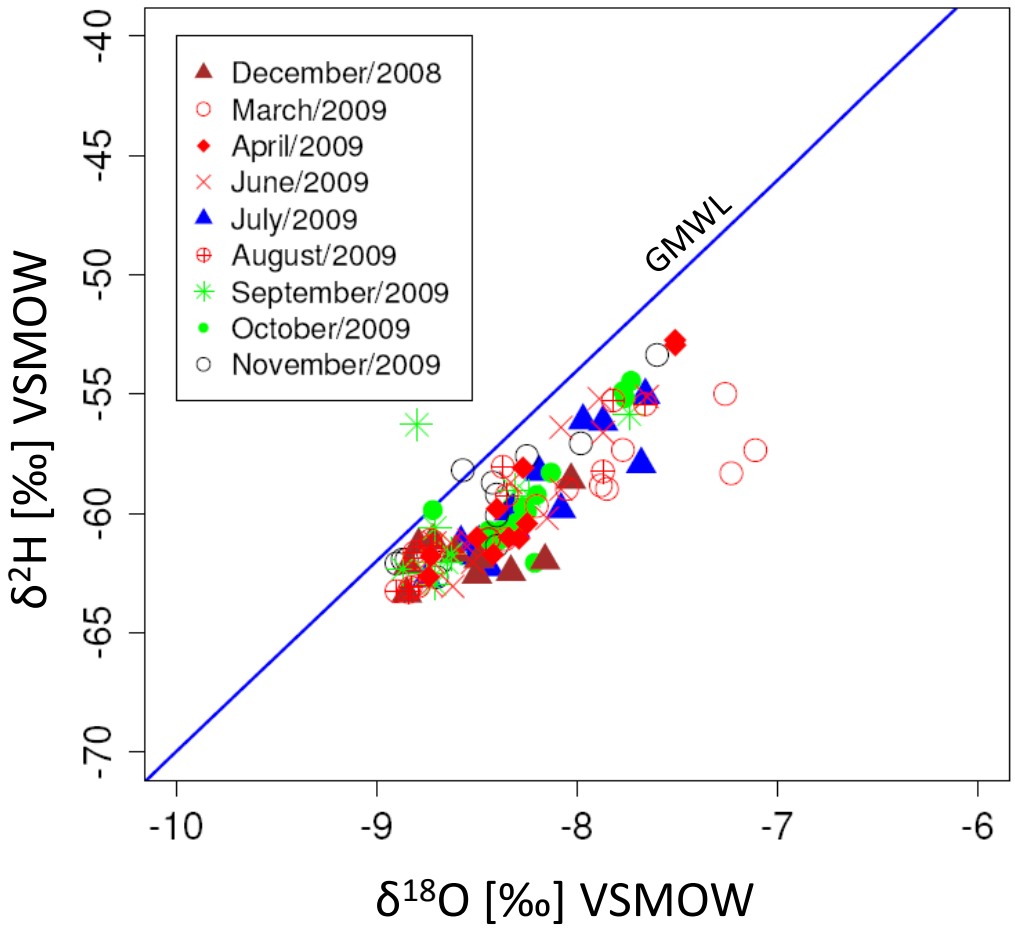

Fig. 5.6 The $\delta^2 O$ and $\delta^{18} H$ composition of groundwater from all wells at different months of the year. The GMWL (global meteoric water line is based on oxygen and hydrogen isotope relationship developed by Craig (1961))

geologic matrix interaction. In addition to that, U and V are also among factor 1 in cold season. Calcium, Cl^-, K, Li, Mg, Na, SO_4^{2-} and Sr have positive factor loading and Ba, HCO_3^-, U, and V have negative factor loadings. A likely precipitates in the groundwater that control over the concentration of most of the cations and anions were interpreted by using PHREEQC program. The result shows that calcite ($CaCO_3$), dolomite ($CaMg(CO_3)_2$, quartz (SiO_2), and siderite ($FeCO_3$) (only in some areas) are likely the reactive minerals and probably responsible for the change in chemical composition of the groundwater. The presence of these minerals were also validated by using x-ray differaction (XRD).

Gibbs diagram which is represented as the total dissolved solids (TDS) as a function of $Na^+/(Na^+ + Ca^{2+})$ and $Cl^-/(Cl^- + HCO_3^-)$ are also widely used to

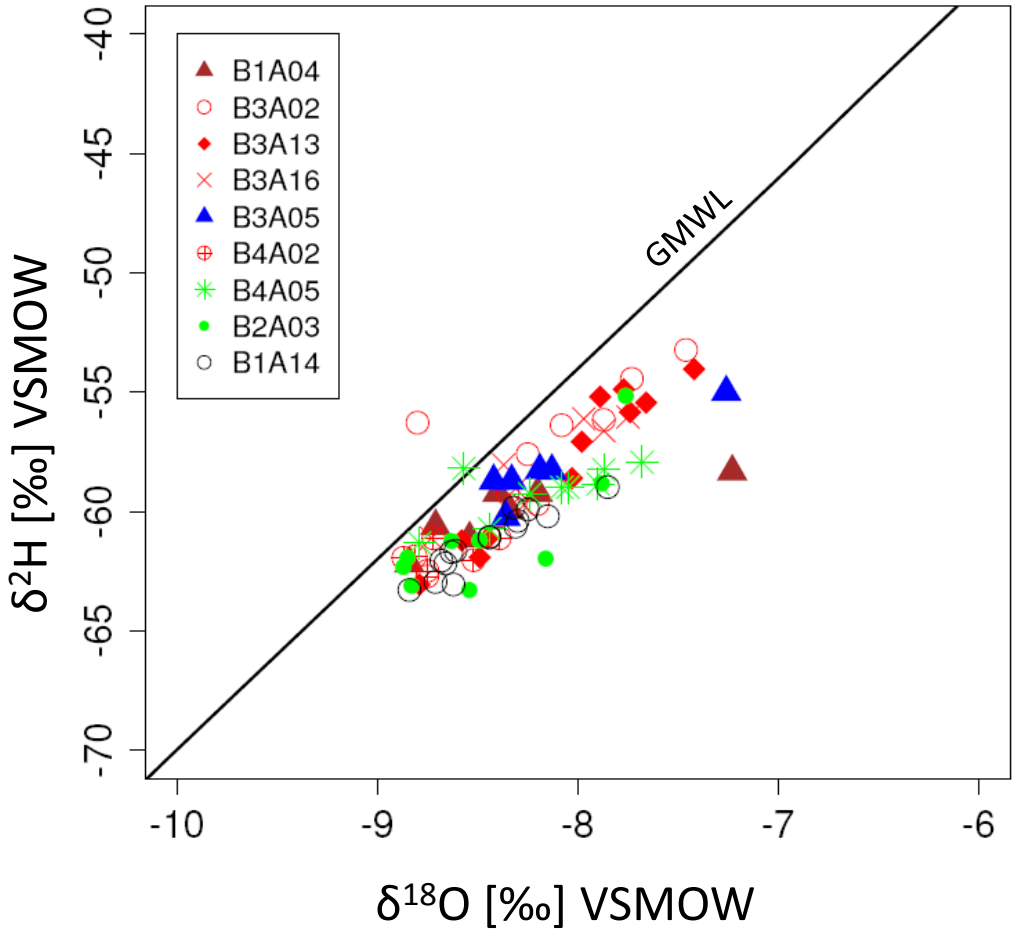

Fig. 5.7 Spatial variation of $\delta^2 O$ and $\delta^{18} H$ composition of groundwater from all wells. The GMWL (global meteoric water line is based on oxygen and hydrogen isotope relationship developed by Craig (1961))

assess whether dissolved chemicals are rock weathering-dominated, precipitation-dominated or evaporation-dominated Gibbs (1970). The hydrochemical data of the study area is drawn in the Gibbs diagram (Fig. 5.5) and it shows that the groundwater of the study area is dominated by the weathering of the geologic material.

A likely control over the concentration of barium in natural water is the solubility of barite ($BaSO_4$), which is a fairly common mineral (Hem (1989)). In the study area Barite is slightly supersaturated with the groundwater. Because of its multiple sources, SO_4^{2-} might limit the concentration of barium. Therefore, for a given solubility constant of barite, as sulphate concentration increases the barium concentration decreases. That would be possible reason why barium is negatively related to sulphate.

Table 5.4 Eigen values of factors and proportion of variances

	Cold season (March-2009, April-2007, November-2006)									
Factors	**1**	**2**	**3**	**4**	**5**	**6**	**7**	**8**	**9**	**(10-28)**
Eigen value	11.90	5.27	3.68	2.44	1.78	1.49	0.69	0.44	0.31	0.00
Proportion	42.52	18.82	13.14	8.71	6.35	5.33	2.47	1.57	1.10	0.00
Cumulative (%)	**42.52**	**61.33**	**74.48**	**83.18**	**89.53**	**94.86**	**97.33**	**98.90**	**100.00**	
	Warm season (June-2009, August-2008, August-2009)									
Factors	**1**	**2**	**3**	**4**	**5**	**6**	**7**	**8**	**9**	**(10-28)**
Eigen value	14.73	4.33	3.22	1.82	1.58	1.06	0.60	0.41	0.26	0.00
Proportion	52.59	15.47	11.50	6.50	5.63	3.78	2.15	1.46	0.93	0.00
Cumulative (%)	**52.59**	**68.06**	**79.56**	**86.06**	**91.69**	**95.47**	**97.62**	**99.07**	**100.00**	

Table 5.5 Extracted and rotated factors for Cold season (March, April, November) and Warm season (June, August), the values in boldface indicate dominant parameters in the extracted factor.

Para.	**F1**	**F2**	**F3**	**F4**	**F5**	**F1**	**F2**	**F3**	**F4**	**F5**
pH	-0.31	-0.10	**0.90**	-0.20	0.13	0.23	0.00	0.16	**0.93**	0.11
EC	**0.95**	-0.18	-0.08	0.22	-0.01	**0.98**	-0.11	-0.05	0.12	-0.07
Eh	0.14	**-0.94**	0.09	0.07	0.06	0.16	-0.34	**-0.89**	-0.06	-0.16
T	0.42	-0.10	-0.17	**0.63**	-0.22	-0.03	**-0.79**	-0.09	0.09	0.28
O_2	0.30	-0.09	**0.81**	-0.26	-0.05	0.08	0.39	0.01	0.10	**-0.87**
B	**0.92**	-0.16	-0.30	0.18	0.00	**0.54**	**-0.70**	-0.28	0.14	0.30
Ba	**-0.85**	0.22	-0.42	0.09	-0.12	**-0.83**	0.06	0.27	0.35	0.01
Ca	**0.95**	-0.30	0.07	0.06	-0.03	**0.83**	0.43	0.13	0.12	-0.27
Co	-0.15	**0.67**	-0.37	**0.59**	-0.07	0.18	-0.35	-0.13	**0.82**	-0.03
Cu	0.18	**-0.66**	-0.45	-0.15	0.06	0.28	0.25	**-0.82**	0.16	0.12
Fe	-0.21	**0.93**	0.13	0.10	0.12	-0.17	-0.09	**0.84**	-0.14	0.37
K	**0.78**	-0.08	**-0.59**	0.10	-0.02	**0.75**	-0.52	-0.33	0.17	0.01
Li	**0.65**	-0.24	**-0.71**	0.05	-0.04	**0.66**	-0.47	-0.48	0.23	-0.08
Mg	**0.95**	-0.04	-0.27	0.16	-0.02	**0.97**	-0.13	-0.13	0.06	-0.10
Mn	0.15	0.10	-0.02	**0.94**	-0.10	0.33	-0.11	0.04	0.03	**-0.81**
Na	**0.95**	-0.17	-0.17	0.17	-0.02	**0.95**	-0.14	-0.16	0.16	-0.04
Ni	0.27	0.10	-0.35	**0.69**	0.15	0.42	**-0.79**	-0.08	0.32	-0.17
S	**0.95**	-0.18	0.06	0.21	0.00	**0.93**	-0.07	0.26	0.01	-0.11
Si	0.39	**-0.78**	0.21	0.22	0.16	0.04	0.11	-0.25	**0.79**	-0.28
Sr	**0.65**	-0.50	-0.46	-0.01	0.10	**0.64**	0.42	-0.15	0.14	-0.57
U	**-0.57**	0.05	0.00	-0.21	**0.71**	0.02	**0.68**	-0.29	0.18	0.36
V	**-0.58**	0.26	0.29	-0.28	**0.58**	-0.02	**0.94**	0.05	0.04	-0.22
Zn	0.35	-0.26	0.01	0.09	**0.82**	-0.16	-0.40	**-0.79**	0.14	0.28
Cl	**0.93**	-0.19	-0.25	0.15	-0.07	**0.95**	-0.18	-0.18	0.14	-0.06
SO_4	**0.95**	-0.16	0.05	0.23	-0.05	**0.95**	0.04	-0.07	0.20	-0.22
NO_3	0.53	-0.46	**-0.61**	-0.17	-0.14	0.02	-0.02	**-0.78**	-0.13	0.19
HCO_3	**-0.93**	0.26	0.02	-0.12	0.08	**-0.79**	-0.08	0.45	-0.24	0.28
DOC	-0.46	0.28	-0.48	**-0.60**	-0.09	-0.44	-0.06	**0.52**	-0.17	0.36

(**SD**=standard deviation, **DOC**=dissolved organic carbon, (F)=Factor)

Cobalt, Eh, Cu, Fe, NO_3^- (to a lesser extent) and Si are the second factor which accounts for 15% variation of the hydrochemical dataset in cold season. Copper, DOC, Eh, Fe, NO_3^- and Zn are the third factor and accounts for 13% of variation in dataset in warm season. Both factors indicates that redox and mainly redox sensitive elements play role for the change in hydrochemical data in cold and warm

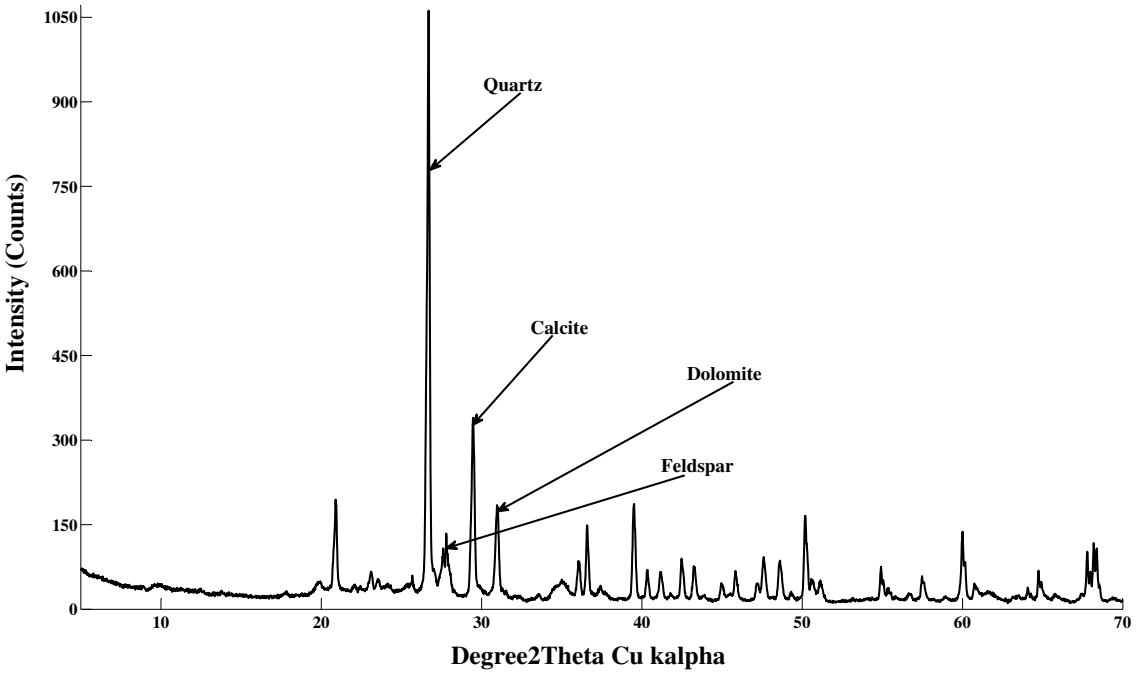

Fig. 5.8 X-ray differaction of the soil samples from the study area

seasons. The redox potential is significantly higher in cold season than in warm season. This could be related to the increase in solubility of the oxygen in cold season, as a result of decrease in temperature. Dissolved organic carbon (DOC) and NO_3^- are also important factors in warm season probably because of the relatively higher temperature which enhances degradation of organic material. The degradation process consumes oxygen and might result in reducing behavior of the groundwater and Fe^{3+} can be reduced as a consequence.

Nitrate, pH and O_2 together accounts for 11.5% variation in cold season and Ni, T, U and V are the second factor which accounts for 18.8% of the variation in warm season. DOC, Mn, T, and Zn in cold season and O_2, Mn^{2+}, pH, and Si in warm season also contributed to the variation but to a lesser extent. The complete list of factors (5 dominating facors) with their loading are shown in Tab. 5.5

Groundwater chemical composition of the study area showed spatial variation in terms of some of the variables. To detect the spatial similarity in chemical composition, cluster analysis were performed on the selected sampling points for two sampling periods. The resulted dendrogram is shown in Fig. 5.9 for April 2006 and

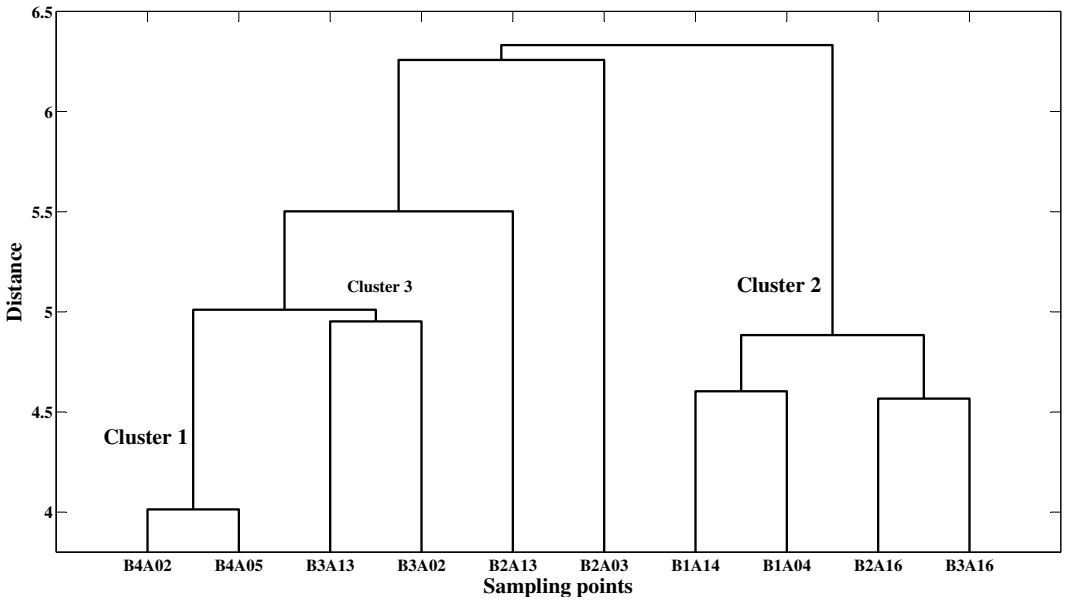

Fig. 5.9 Dendrogram of groundwater sampling wells based on hydrochemical and physical properties, November 2006

Fig. 5.10 for June 2009. Plots BIIIA02 and BIIIA13 of block III showed similarity and Plots BIVA02 and BIVA05 of the block IV also show similarity in both seasons. Plots within block II show no similarity like other blocks. Generally plots in the same block show similarity in both seasons.

According to soil characteristics, the experiment was set up in four blocks containing an equal number of plots to avoid confounding of experimental effects with soil heterogeneity Roscher et al. (2004). Based on groundwater chemical composition, the current study also indicated that plots in the same block generally show similarity. However, plots in different block show differences in chemical composition.

5.2.5 Seasonal Variations

The groundwater of the study area shows seasonal variation with respect to some parameters. In order to evaluate seasonal variation the dataset was divided in to two categories. Then the mean values of the parameters were compared using t-test (Tab. 5.6).

Most of the major cations and anions show no significant variation due to the

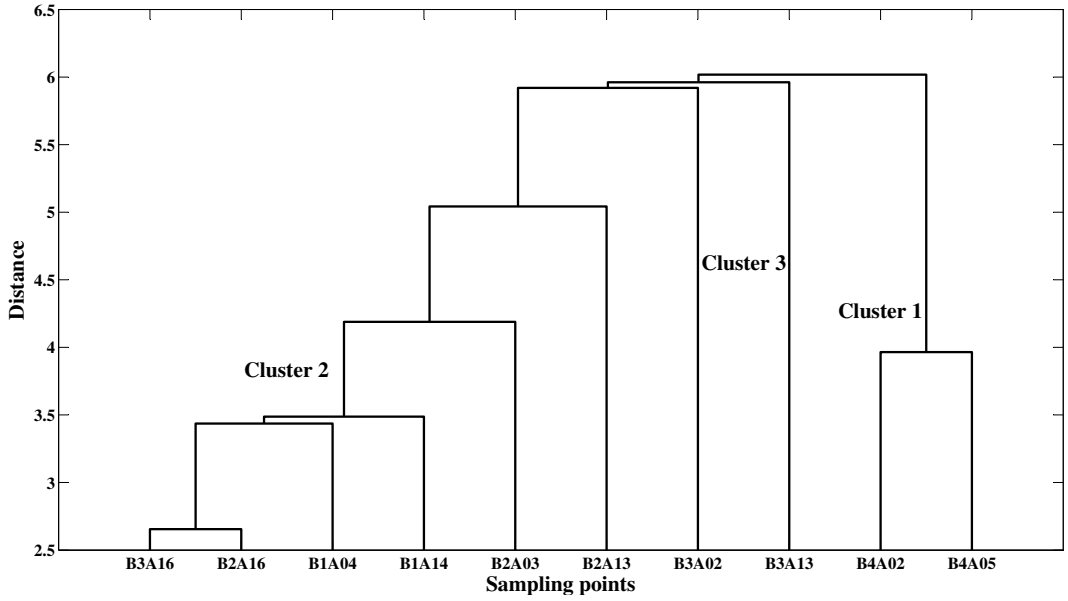

Fig. 5.10 Dendrogram of groundwater sampling wells based on hdrochemical composition and physical properties, August 2009

seasonal change. However, B, Ba, DOC, Eh, Fe^{2+}, HCO_3^-, Mn, Ni, O_2, pH, Si, Sr, T, U, V, Zn show significant difference between the two seasons. Eh and oxygen concentration in the aquifer varied from relatively less oxidizing in warm season (279±132 mV) to more oxidizing in the cold season (423±46 mV). Dissolved organic carbon is higher in cold season (5.87±0.62 mg/L) than in warm season (3.52±0.75 mg/L). Hydrogen bicarbonate also increased in warm season. Barium is higher in warm season than in cold season. Iron also showed seasonal variation, (0.10±0.15 mg/L in cold season;(0.18±0.15 mg/L) in warm season). Nitrate shows spatial variation but its seasonal variation is not significant.

The higher value of the Eh in cold season attributes to increase in solubility of oxygen. That would possibly resulted in Eh and oxygen increase in cold season as the temperature is decreased.

Dissolved organic carbon (DOC) shows seasonal variation; The DOC values during the warm season are elevated compared to cold season. DOC in the soil profile of the experimental field is generally decreasing with increasing depth over the range of depths 10-60 cm. Groundwater fluctuation data also reveal that the groundwater table is shallower in spring and fall. Therefore, there will more DOC in these

Table 5.6 Seasonal variation of measured parameters-significance at 95% confidence interval

Para.	Unit	Cold mean	SD	Warm mean	SD	Comparison t value	P value	Remark
pH	pH	**7.03**	0.06	**7.23**	0.23	-2.60	0.02571	**Significant**
EC	[μS/cm]	**1571.30**	124.25	**1497**	165	1.15	0.26800	**Insignificant**
Eh	[mV]	**423**	46	**279**	132	3.25	0.00765	**Significant**
T	[°C]	**9.74**	0.17	**16.84**	0.91	-24.24	5.9E-10	**Significant**
O_2	[mg/L]	**4.45**	0.71	**3.19**	0.31	5.13	0.00023	**Significant**
B	[μg/L]	**234**	64	**157**	72	2.49	0.02286	**Significant**
Ba	[μg/L]	**83.4**	12.5	**117.1**	20	-4.53	0.00039	**Significant**
Ca	[mg/L]	**267**	12	**268**	24	0.22	0.82570	**Insignificant**
Fe	[mg/L]	**0.10**	0.15	**0.18**	0.15	-1.20	0.04387	**Significant**
K	[mg/L]	**3.60**	1.72	**3.95**	1.84	-0.44	0.66260	**Insignificant**
Li	[μg/L]	**14.20**	5.73	**13.76**	6.64	0.16	0.87570	**Insignificant**
Mg	[mg/L]	**38.8**	4.8	**37.6**	5.9	0.51	0.61370	**Insignificant**
Mn	[μg/L]	**1018**	764	**400**	388	2.28	0.03968	**Significant**
Na	[mg/L]	**48.7**	9.9	**43.7**	11.8	1.03	0.31560	**Insignificant**
Ni	[μg/L]	**4.33**	0.61	**3.27**	1.02	2.82	0.01312	**Significant**
Si	[mg/L]	**4.82**	0.33	**5.28**	0.24	-3.56	0.00253	**Significant**
Sr	[mg/L]	**2.52**	0.90	**1.00**	0.44	4.77	0.00036	**Significant**
U	[μg/L]	**6.16**	0.6	**9.83**	1.18	-8.79	6.8E-07	**Significant**
V	[μg/L]	**5.16**	0.46	**0.99**	0.43	20.93	4.8E-14	**Significant**
Zn	[μg/L]	**44.2**	11.2	**26.7**	13.45	3.15	0.00570	**Significant**
Cl^-	[mg/L]	**81.3**	21.4	**63.5**	27.4	1.63	0.12200	**Insignificant**
SO_4^{2-}	[mg/L]	**410**	67	**352**	100	1.54	0.14280	**Insignificant**
NO_3^-	[mg/L]	**7.72**	6.56	**10.58**	17.83	-0.48	0.64330	**Insignificant**
HCO_3^-	[mg/L]	**478**	36	**531**	60	-2.40	0.02998	**Significant**
DOC	[mg/L]	**5.87**	0.62	**3.52**	0.75	7.40	1.7E-06	**Significant**

(**SD**=standard deviation, **DOC**=dissolved organic carbon)

periods, because of more DOC as we go up to the upper soil. However, according to a study by Steinbeiss et al. (2008) DOC concentration in soil solution of the experimental field showed maximum concentration in summer and early fall and minimum concentration in late winter. The soil is the source of the DOC in the groundwater and the groundwater should follow the pattern in soil. In contrary, this study showed that the DOC concentration in groundwater which we assumed its source is from soil, is higher in winter (cold season) than in warm season.

Hydrogen bicarbonate concentration in warm season was also higher than in cold season. According to Appelo and Postma (1994) CO_2 production is an important

consequence of organic matter oxidation which within the aquifer may induce carbonate mineral dissolution. Therefore, hydrogen bicarbonate increases with increasing dissolution of organic matter in the groundwater. Pearson correlation between HCO_3^- and DOC (r=0.5, season and r=0.8, warm season) suggests that HCO_3^- may partly be the consequence of degradation of organic matter. The higher value in summer values attributes to the increase in activity of the biochemical reaction as temperature increases. It is shown in Anderson (1973) that carbon dioxide production is highly correlated with temperature and showed logarithmic increase with rising soil temperature. According to Harmon (1989) temperature increases CO_2 production as follows:

$$LogPco_2 = -3.3 + 0.08T(^\circ C) \tag{5.1}$$

Therefore, it is expected that the hydrogen bicarbonates are increased.
According to a study by Appelo and Postma (1994) CO_2 pressures are highest when respiration is maximum during summer, and decreases in autumn and winter. Land use and biological productivity are therefore important in determining CO_2 pressure in soils Appelo and Postma (1994). There is more vegetation cover in the experiment field in summer than in winter season. Therefore, there will be diffusion of CO_2 from the soil to the groundwater during summer time and result in production of more hydrogen bicarbonates.

The higher value of Ba in warm season than in cold season could be for the following reason. There is relatively more addition of the sulphate and cations in cold season than in warm season (there is seasonal variation of SO_4^{2-}, Na, Cl^-, Sr at significance level of about 80%). Studies show that for small change of some of these ions result in significant change in Ba concentration. Barite mineral solubility can be increased by factor of 1.5 to 2 for each tenfold increase in ionic strength produced by addition of Na, and Cl^- to the groundwater Dillon and Goldstein (1984). Addition of sulphate other than barite mineral also reduces the Ba concentration as discussed in the previous section. Therefore, these two mechanisms might resulted in reduction of effective concentration of barium from the groundwater.

Seasonal variation of iron is related to presence of electron acceptors (oxygen,

nitrate,...) in the groundwater of the study area. Fe^{2+} is more readily soluble in oxygen and other electron acceptor poor groundwater. In this study the oxygen concentration is higher in cold season than in warm season, hence the Fe^{2+} concentration is higher in warm season. Oxygen concentration is low because of less solubility at higher temperature season and also consumption by microbes for organic material degradation.

According to study by Appelo and Postma (1994) it appears that nitrate reduction by organic matter is a common processes in aquifers. But in this study it is not clear if the nitrate reduction depends on the organic matter degradation. The Pearson coefficient show very weak correlation between the DOC and NO_3^- (r=-0.3 in warm season, r=0 in cold season).

However, there is relatively higher iron concentration in plots BIIIA02, BIIIA13, and BIIIA16 of Block III because of relatively reducing environments. Because the oxidizing environment is varied with the season the concentration of Fe was also varied with the season.

5.2.6 Effect of Saale river

The low dissolved solids and other ions in plots (BIIIA02 and BIIIA13) in block III are suspected that they might be in contact with water from the channel which goes underground from river to the main experimental field. The next chapter will make use of natural chloride as a tracer and PHREEQC hydrogeochemical modeling to study the effect of the channel. We also investigated the effect of the river on plots in block I during mean river flow and higher flow (e.g. during flooding).

Chapter 6

Effect of surface water on the groundwater of the study area [2]

6.1 Introduction

The effect of biodiversity on ecosystem function is complex and requires understanding of all interacting systems, such as hydrology, geology and above ground plant diversity of the study area. In this chapter hydrogeochemical modeling using PHREEQC, time series analysis and chloride (hydrological tracer) were used to investigate the effect external factors (nearby river Saale, precipitation and an underground channel) on the groundwater of a large grassland diversity experiment (Jena experiment).

There are different ways to study the effect of surface water on the groundwater. Constantz (2008), Anderson (2005) used analysis of subsurface temperature pattern to provide information about surface-water/ground-water interaction. McCarthy et al. (1992), Rodgers et al. (2004) used stable isotopes and chemical tracer to identify the source of water. In our study PHREEQC was used to investigate

[2]The content is based on the proceeding: Tessema SG, Mirgorodsky D, Merten D, Hildebrandt A, Attinger S, Büchel G: Effect of river Saale on groundwater hydrochemistry of Jena biodiversity experimental field: A hydrogeochemical modeling approach, Proceedings of 11th International Multidisciplinary Scientific GeoConference SGEM, Albena, Bulgaria, 20-25.06.2011, Vol. II, page 807- 814

the effect of Saale river on the groundwater and also to predict the effect of the river during times of elevated water levels, when the influx from the river increases. With PHREEQC we can investigate the effect of chemical reaction and variation in temperature and other environmental conditions on the chemistry of groundwater. Therefore we can get more reliable and better information than with other methods. Besides PHREEQC, we also used chloride as a tracer to investigate the effect of mixing of channel water with groundwater. Chloride has been widely used in hydrology as a natural tracer (Kirchner et al. 2010, Scanlon 1991, Allison and Hughes 1983). Geochemical reactions do not affect chloride concentration. By comparing the concentration of chloride in river water and groundwater we can gain insight in to how and if there exists mixing of those water bodies. Use of chloride as a hydrological tracer is discussed in detail in *Section 2.4*. Time series analysis was also used to investigate if rainfall at the site and discharge of river Saale are correlated to groundwater head of the study area. The aim of this study is to investigate the effect of river Saale on the groundwater chemistry at representative river stage (mean flow) and also to predict the groundwater chemistry at higher river stages, when the discharge of river Saale increases. The other objective is to study if the water in the channel mixes with the groundwater of the study area. Hydrogeochemical modeling using PHREEQC was used to investigate the effect of the river and chloride ion was used as a conservative to investigate the effect of the channel.

6.1.1 Investigated area

The investigation area is shown in the *Fig. 6.1*, and the detail of geology, hydrology, river Saale, and the design of the experimental field is described in *Chapter 3*. The map of the water table in March-2009 shows that the flow direction is from southwest to northeast direction (*Fig. 3.8*). Groundwater flow gradient in our study area is higher in summer season than in wet season. The investigation was made in March/2009 when the flow gradient is low. Groundwater samples from groundwater wells of biodiversity experiment field and river Saale water sample from two points (upstream and downstream of the study area) were collected in

Fig. 6.1 The estimated projection of the channel, river Saale and groundwater wells in Jena biodiversity experiment. The numbers in the map shows plot number in a given block.

March 2009. Hydraulic head of the groundwater head wells are also recorded since 2006 using data logger. The sampling procedure and analytical methods used for analysis are discussed in *Chapter 4*.

6.1.2 Time series analysis

A time series is defined as any series of data measured at successive times at uniform time interval. Different studies used time series analysis to identify the interrelationship between hydrological events (rainfall, groundwater fluctuation, river discharge) (Lee et al. 2001, Chae et al. 2010, Larocque et al. 1998). Cross correlation and autocorrelation analysis are some of the forms of time series analysis and are used to

interpret hydrological processes. The cross correlation analysis is used to establish a link between the input time series, x_t and the output time series, y_t (Larocque et al. 1998). The correlation function $r_{xy}(k)$, for $k > 0$ is defined as (as outlined by (Larocque et al. 1998)):

$$r_{xy}(k) = \frac{C_{xy}(k)}{\sigma_x \sigma_y} \tag{6.1}$$

$$C_{xy}(k) = \frac{1}{n} \sum_{t=1}^{n-k} (x_t - \bar{x})(y_{t+k} - \bar{y}) \tag{6.2}$$

where $C_{xy}(k)$ is the cross correlogram, and σ_x and σ_y are the standard deviation of the time series. The delay is defined as the lag between $k = 0$ and the maximum $r_{xy}(k)$. If $r_{xy}(k) > 0$ for $k > 0$, then the input influences the output; when $r_{xy}(k) > 0$ for $k < 0$, then the output influences the input.

Autocorrelation refers to the correlation of a time series with its own past and future values. It can be assessed by using autocorrelation function. If an event has a long term influence on the time series, the slope of the autocorrelation function, *r(k)* decreases slowly (Larocque et al. 1998):

$$r(k) = \frac{C(k)}{C(0)} \tag{6.3}$$

$$C(k) = \frac{1}{n} \sum_{t=1}^{n-k} (x_t - \bar{x})(x_{t+k} - \bar{x}) \tag{6.4}$$

where k is the lag time ($k = 0$ to m), n is the length of time series, x is a single event $\bar{x}$ is the mean of the events and m is the cutting point. We used cross-correlation functions to study the relationship between groundwater head, rainfall at the site and Saale river discharge. We assumed the rainfall and river discharge as input and the change in groundwater as an output.

From time series data in Fig. 6.2, we can see that the groundwater heads in all blocks fluctuate in the same pattern. This suggests that they are affected by the same hydrological features in a similar way. We also expanded section of Fig. 6.2 where all the hydrological features are maximum (to easily identify the differences) as shown in Fig. 6.3. From this figure we can see that rainwater is directly or indirectly

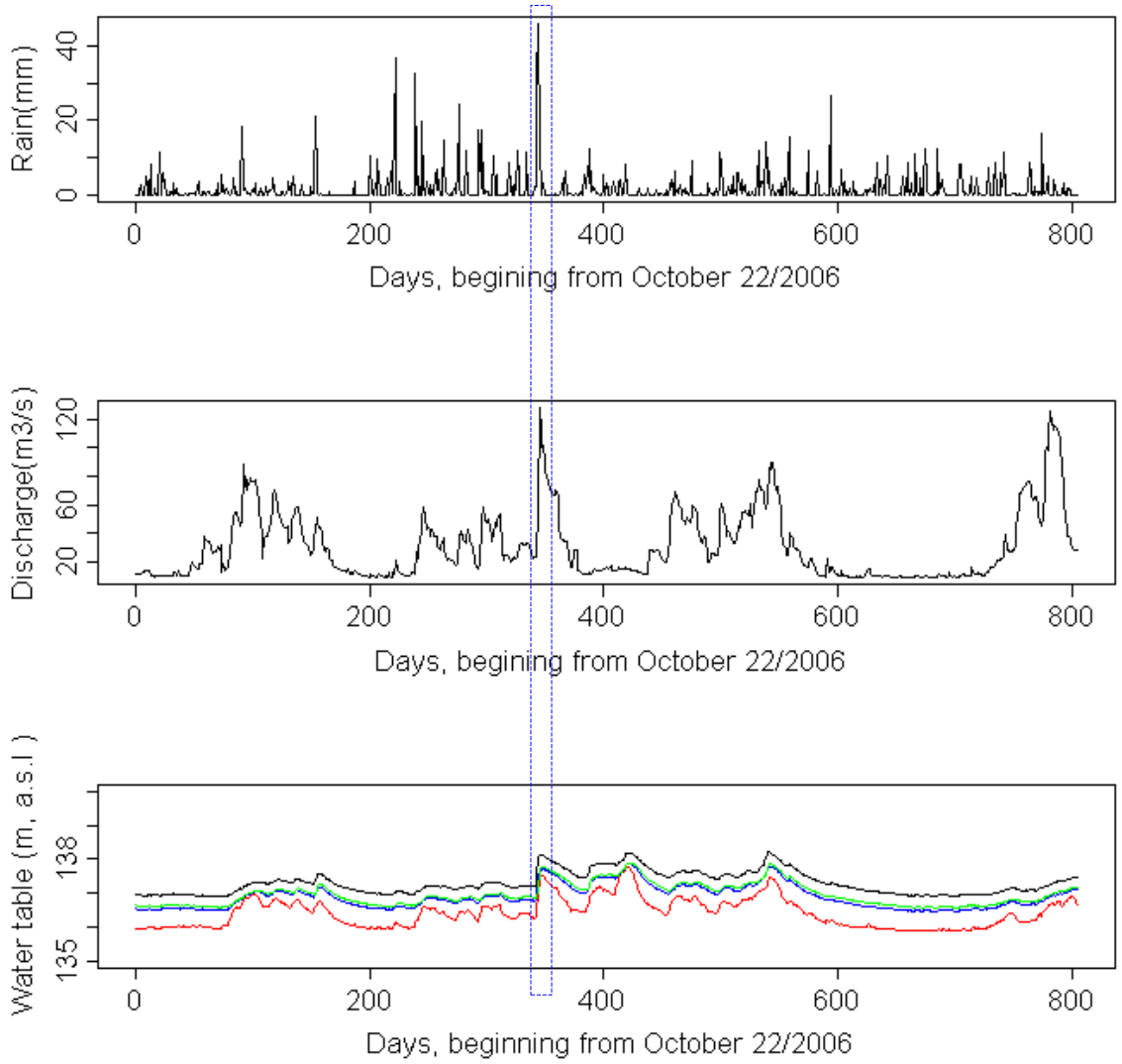

Fig. 6.2 Time series data of precipitation, Saale discharge and groundwater head in block I (red), block II (blue), block III (green) and block IV (black) from October 2006 to December 2008. The rectangular enclosed section is expanded and shown in Fig. 6.3.

the reason for the fluctuation of the river discharge and groundwater heads. The water table fluctuation also shows that the water flow gradient is from block IV to block I. Therefore, we can infer that at mean river flow, the groundwater fluctuation is due to precipitation.

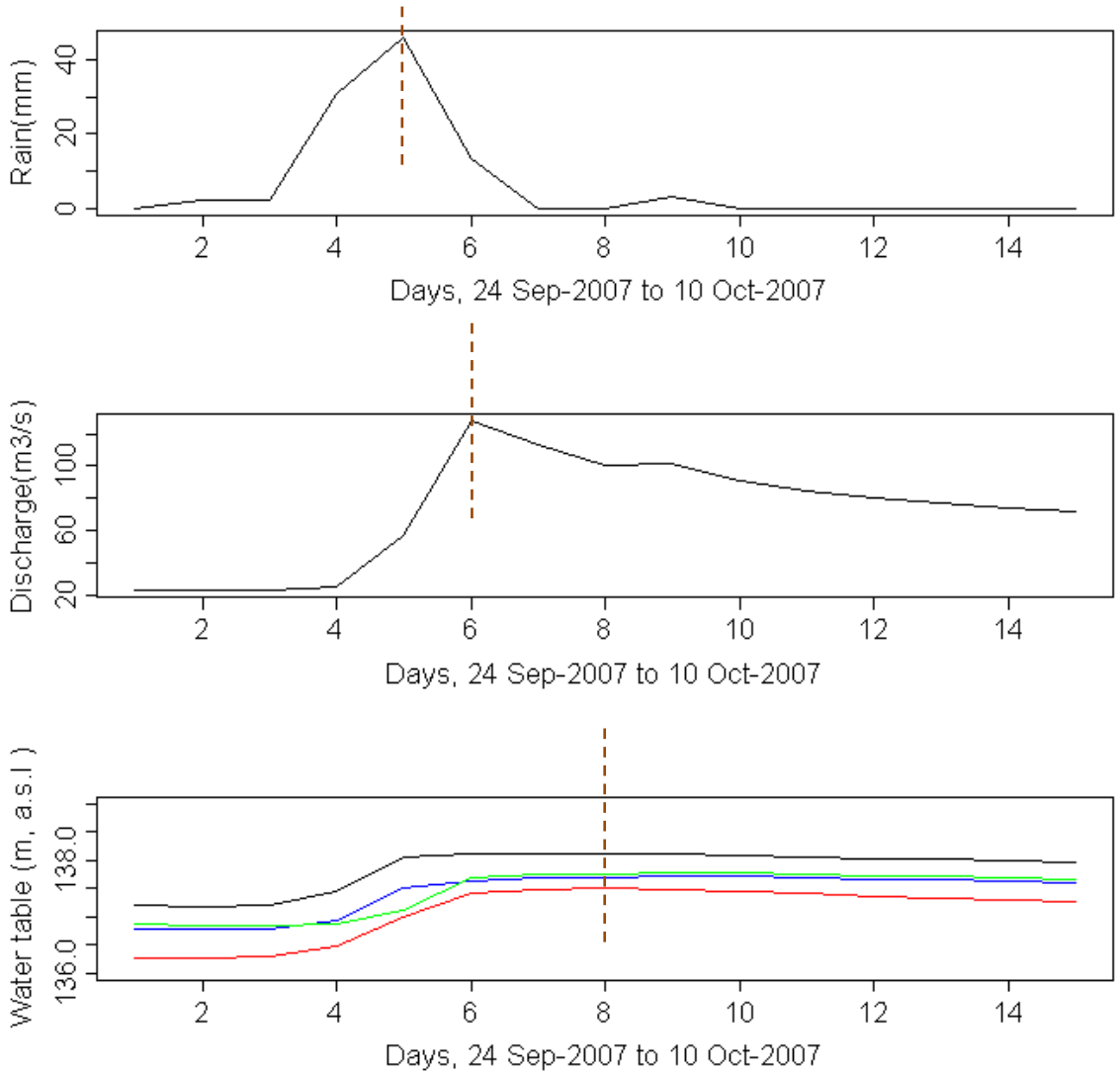

Fig. 6.3 Time series plot of groundwater head, rainfall and river Saale discharge of the rectangular enclosed section in Fig. 6.2. The time series data is from 24 September, 2007 to 10 October, 2007. The dotted line shows the maximum value of the corresponding hydrological event.

6.1.3 Mixing in PHREEQC

For principles and keyterms in hydrogeochemical modeling using PHREEQC, refer *Section 2.3*. We used PHREEQC to calculate the chemical composition after mixing of surface and groundwater or among groundwater by using MIX block in PHREEQC. This can be done by first estimating the mixing factor. We used concentration of chloride (assumed to be conservative) in river water and groundwater

to calculate the mixing proportions.

We assumed that the groundwater at any place in the Jena experiment should be a mixture of upstream groundwater (block IV) and river Saale water. The effect of river was investigated with PHREEQC by varying the presumed proportion of the river versus groundwater in the upstream (block IV). We calculated the mixing proportion in March 2009 by measured chloride concentration in river and groundwater in block IV, and obtained 55/45 (groundwater to river water). We used this proportion in PHREEQC to calculate all other concentrations and to determine other physical and chemical properties. We also predicted the chemical composition at low and high river flow seasons.

6.2 Results and Conclusion

6.2.1 Effect of River

We calculated the composition at proportions 85/15 (i.e. mixing 85 parts of groundwater with 15 parts of river water, the expected mixing during low flow conditions in the river) and 15/85 (groundwater/river, expected during high flow conditions in the river) to represent low and high river discharge season. At higher proportion of the river (15/85) the concentration of Ca, Cl, Mg, Fe, K, Mn, SO_4^{2-} and nitrate changed significantly. At average river flow (85/15) the composition of groundwater in block I concentration did not vary significantly. The compositions of all the three scenarios are indicated in *Table 6.1.* We also investigated the cross-correlation between time varying river discharge and groundwater level. The cross-correlation analysis result between river discharge and groundwater wells in different blocks are shown in Fig.3. The correlation coefficient between the discharge and groundwater wells vary between 0.4 in block IV (far from the river) to 0.6 in block I (near to the river) and this suggest that the correlation is weak. This indicates that there are other factors like rain which result in fluctuation of the groundwater.

Table 6.1 Measured and simulated groundwater composition at different groundwater-river water proportion

Parameters	**Measured**			**Groundwater/River water proportion-Simulated**		
	Block IV	Block I	Upstream Saale	85/15	55/45	15/85
Temp	6.6	6.4	6	6.5	6.3	6.1
pH	7	7.1	7.5	7	7.1	7.2
Units	mg/l	mg/l	mg/l	mg/l	mg/l	mg/l
Alkalinity	461	496.6	77.4	403.9	288.6	135
B	0.26	0.18	0.02	0.22	0.15	0.058
Ba	0.08	0.08	0.07	0.08	0.07	0.07
Ca	261.5	268.8	35.9	227.5	159.9	**69.7**
Cl	88.9	73.1	54.2	83.8	73.4	**59.5**
Fe	0.004	0.132	0.038	0.009	0.019	**0.033**
K	5.2	2.2	4.6	5.1	4.9	**4.7**
Li	0.02	0.009	0.003	0.017	0.012	0.006
Mg	41	36.2	9.7	36.3	27	**14.4**
Mn	0.35	0.46	0.02	0.3	0.2	**0.07**
NO3	14.4	3.3	23.5	15.8	18.5	**22.1**
Na	52	47	40.9	50.4	47.1	42.6
P	0.1	0.061	0.05	0.093	0.078	0.058
Zn	0.026	0.04	0.065	0.032	0.044	0.06
SO4	405	402.8	59.3	316.4	205.1	**56.6**

6.2.2 Effect of the channel

Chloride concentration was measured at the inlet of the channel and at the groundwater wells in block IV and virtually "mixed" in PHREEQC to assess the role of the channel water for affecting groundwater chemistry. The values were then compared with chloride concentration in block III. The chloride concentration in block III is less than both the Cl concentration at the channel inlet and groundwater well in block IV. This suggests that the channel did not have any effect on the groundwater wells in block III. The values of the measurements are shown in *Table 6.2*.

Table 6.2 Chloride concentration in river Saale and groundwater in block III and block IV of the experiment field.

	River Saale sample		**Groundwater concentration**			
	Upstream Saale (Channel inlet)	Downstream Saale	Block IV	Block III	Expected conc. if there is leak	Remark
Chloride (mg/L)	54.2	54.1	88.5	**18.2**	54.2-88.5	No leak
SD	0.1	0.1	0.1	0.1		

(**SD**=standard deviation)

6.2.3 Results from time Series analysis

Autocorrelation of hydrological events

If an event has long-term influence on the time series, the slope of autocorrelation function r(k) decreases slowly (Larocque et al. 1998). The graphs in *Fig. 6.5* shows that groundwater head and discharge have long term influence on the time series. However, precipitation doesn't relate to its history. We can see that the slope of groundwater head as shown in **A** and **B** and discharge, **D** have gradual decreasing slope which indicates the long term influence on the time series. However, most of the precipitation autocorrelation coefficient data are zero or near zero at 95% confidence interval. Therefore daily precipitation data is random at the scale considered. The time series of groundwater head in **A** is steeper (responds to a change quickly) than in **B**. This is because, the unsaturated zone is mainly loamy (higher hydraulic conductivity compared to silty loam) at location where Head1 **(A)** was recorded, and is mainly silty loam at location where Head4 was recorded **(B)**.

Cross correlation between groundwater head and rainfall

The cross-correlation between rainfall as input and groundwater heads as output are shown in Fig. 6.6 (A, B, C and D). The correlation coefficient, $r_{xy}(k) > 0$ for k> 0 for all groundwater heads and rainfall. Therefore, the rain has an influence on the groundwater head. The maximum $r_{xy}(k)$ value varies between 0.35 to 0.5. This indicates that there is correlation but not very strong. We can also see that the

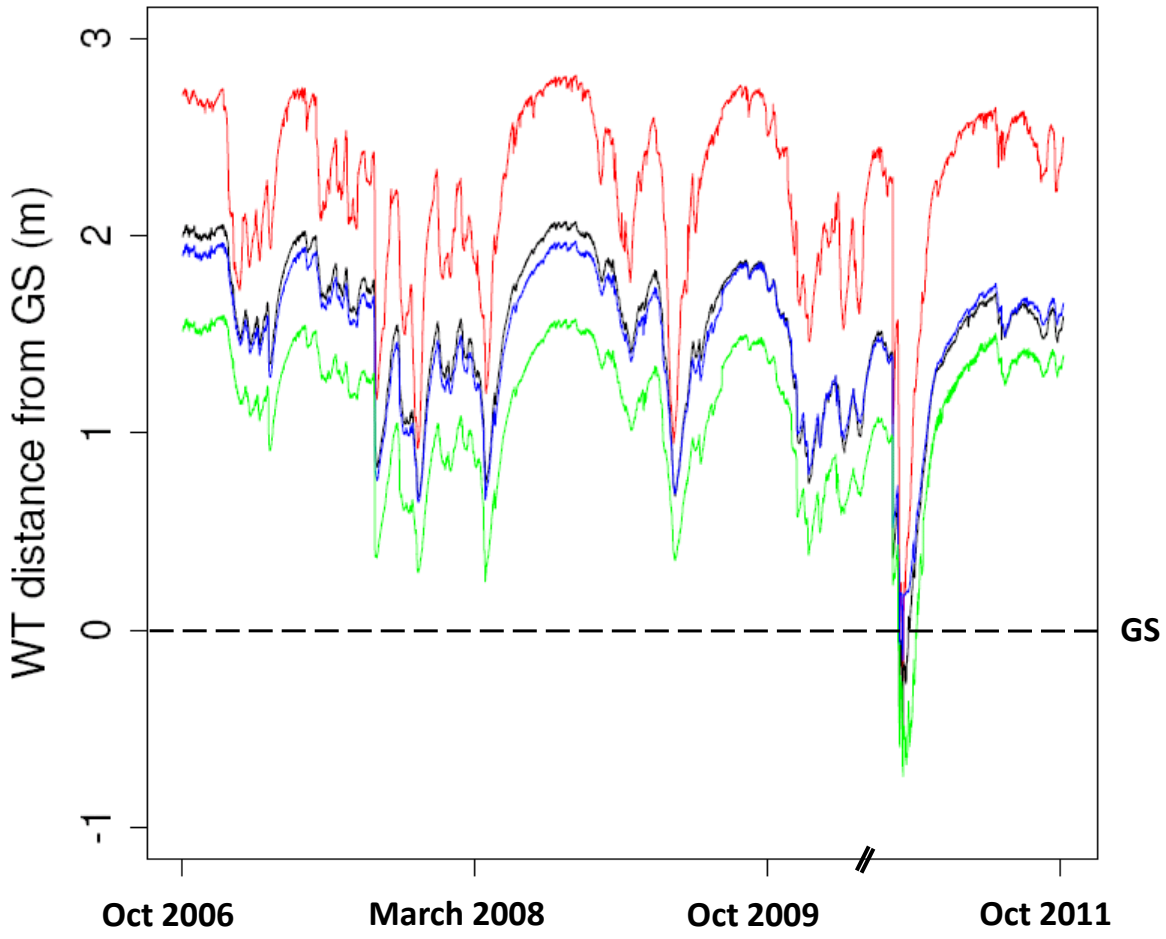

Fig. 6.4 Groundwater head and precipitation over time period 2006-2011

correlation is stronger as we move from block IV to block I. This is because, the soil texture in block I is mainly loamy material as shown in *Fig. 5.2* which has higher conductivity than silty material which is dominant in blocks far from the river. We can also see that the delay time for the all the wells investigated are 3 days or less.

Cross correlation between discharge and groundwater head

We also analyzed the correlation between discharge (as input) and groundwater head (as output) for the time between September 2007 and November 2007. The result shows (Fig. 6.6, E, F, G and H) that $r_{xy}(k) < 0$ for k>0. Therefore, the input

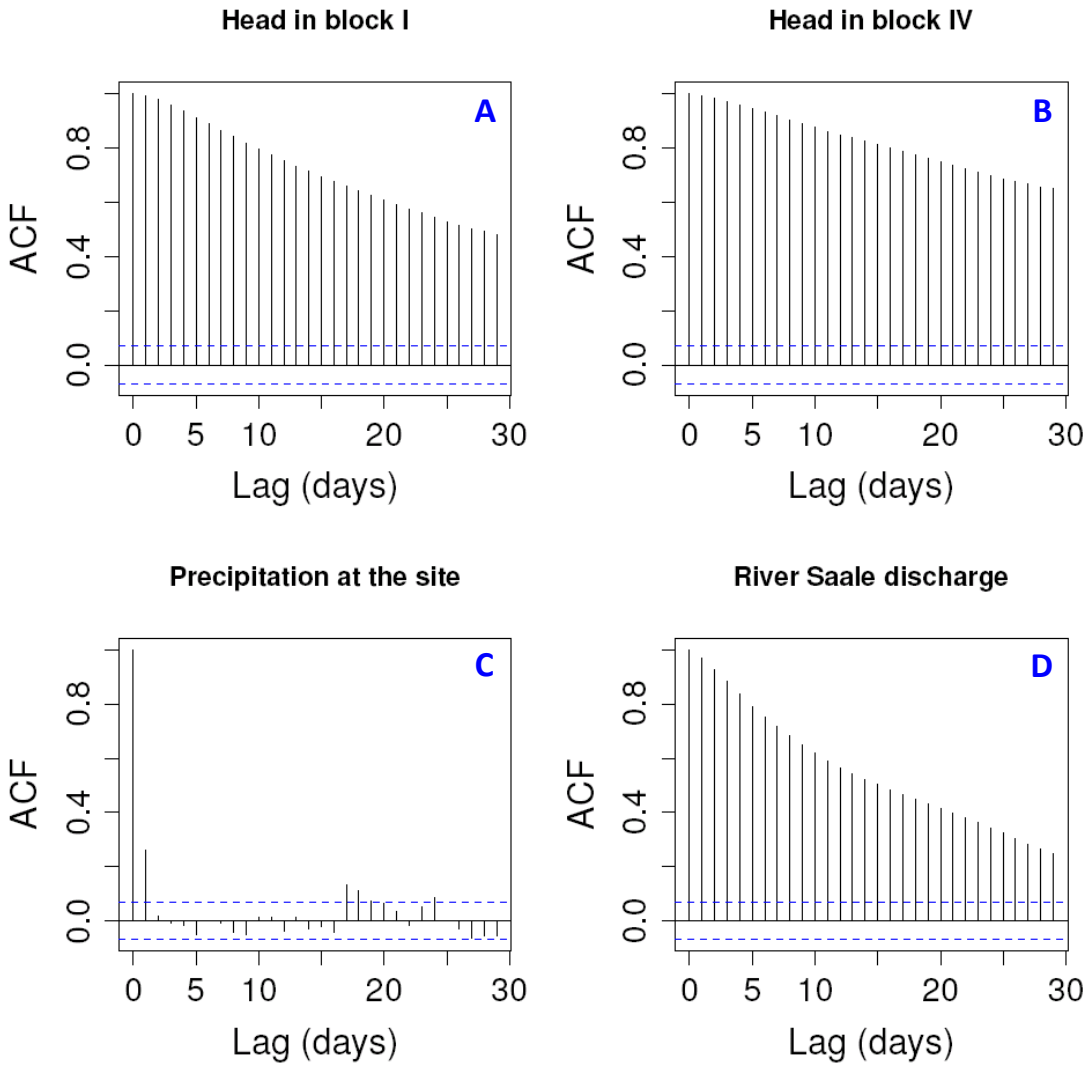

Fig. 6.5 Autocorrelation coefficients (ACF) of groundwater head, rainfall and river Saale discharge. The time series data is from October 2006 to December 2008

(discharge) did not have effect on the output (head). This also supports the result by hydrogeochemical modeling. It is the groundwater which has effect on the river discharge with correlation coefficient of about 0.6.

6.3 Conclusions

The river water generally did not have significant effect on the groundwater of the study area at mean annual river flow. However, some of the elements (Ca, Cl, Mg, Fe, K, Mn, SO_4^{-2} and nitrate) are predicted to be affected when the influx increases

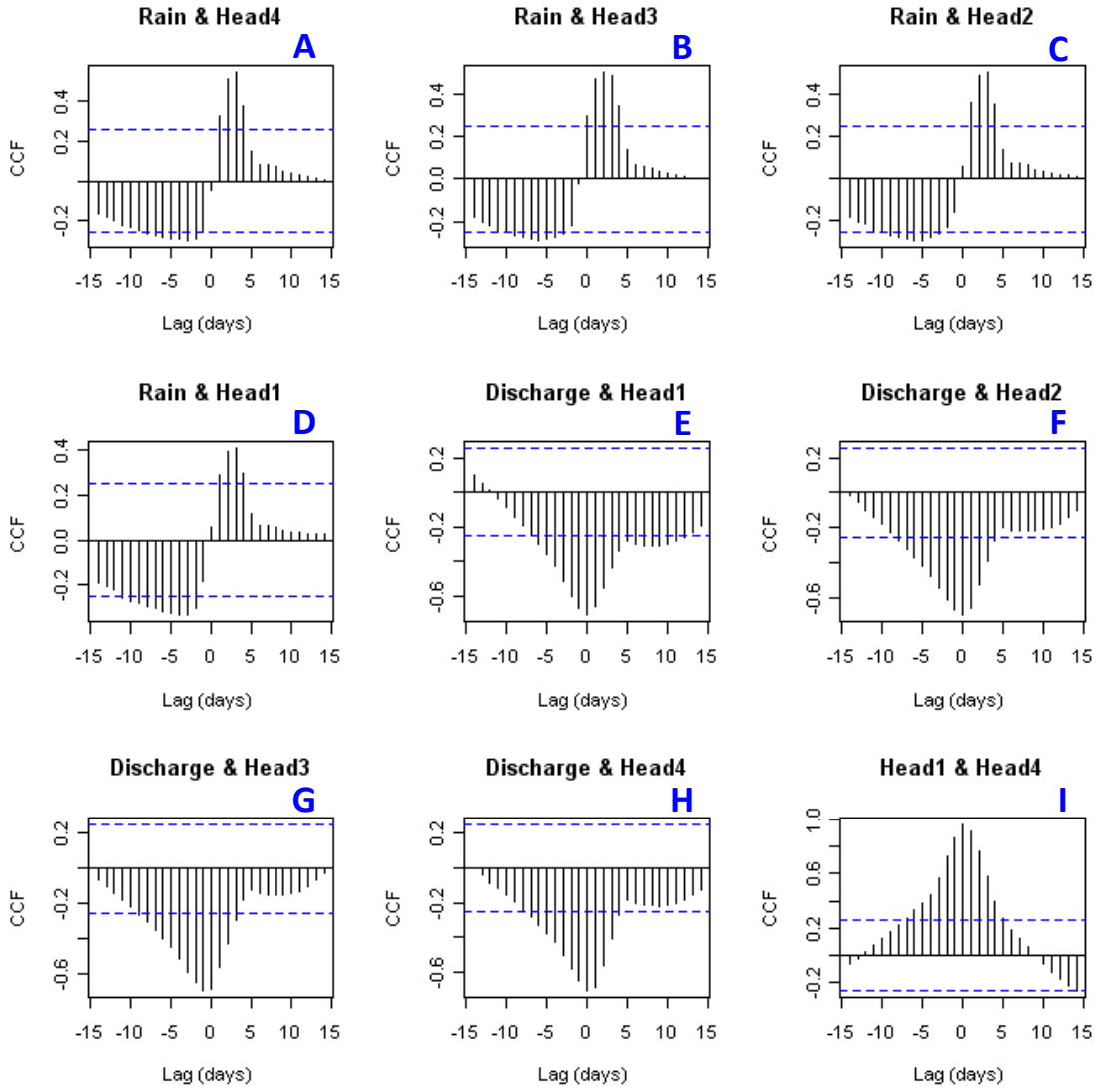

Fig. 6.6 Cross-correlation of time series data of precipitation, groundwater head in Block I, II, III and Block IV and river Saale discharge. The time series data is from September 2007 to November 2007

(for examples during high water levels in the river). The cross-correlation between time series of the rainfall and groundwater head shows that they are correlated but not strong. The correlation of river discharge and groundwater head also shows that the discharge does not influence the groundwater head of the study area for the considered periods of time. The chloride concentration in the channel inlet and in the groundwater shows that the channel which flows toward the experiment field did not affect the groundwater in block III of the study area.

Chapter 7

Effect of biodiversity on shallow groundwater: Using natural chloride as a tracer[3]

7.1 Introduction

Water cycling is important ecosystem process and is affected by ecosystem properties such as leaf area, vegetation height and leaf conductance which may be related to level of biodiversity. Jiang et al. (2007), Hooper and Vitousek (1998) studied how different components of diversity are correlated to soil water content. Jiang et al. (2007) showed that both species diversity and functional group diversity are negatively correlated with soil water content in arid region. However, the authors considered only the water content in the upper 20cm depth of the soil. According to Hooper and Vitousek (1998) the effect of biodiversity on moisture content is seasonal. Both functional group composition and richness did not influence soil moisture content in April. However, the effect was seen in summer and moisture content was affected by the difference in functional group in lower layers of the soil.

[3]The content is based on the paper **to be submitted**: Tessema S.G., Mirgorodsky D., Merten D., Hildebrandt A., Attinger S., Büchel G.: Effect of biodiversity on shallow groundwater: Vertical chloride transport modeling approach

The studies on how different diversity level and functional groups affect water flow in unsaturated zone are less addressed and are also contradicting. Our objective is therefore, to use chloride ion (assumed to be a conservative tracer) transport in the unsaturated zone to understand how biodiversity influences water flow in the unsaturated zone. Our hypothesis is that, higher plant diversity level result in more upward convective flow of water during period of water stress. As a result more chloride ion accumulates near the surface.

Many studies used chloride as a tracer to study the flow of water in the unsaturated zone. According to study by Nakayama et al. (1973), Jacques et al. (2008) chloride accumulated near the surface because of upward water flow. The explanation how chloride can be used as hydrological tracer is given in *Section 2.4*. We measured the chloride concentration in the soil profile at four different depths during period of water stress and compared its accumulation in different diversity level. We also calculated the chloride concentration in the soil profile by solving convective diffusion equation using laplace transforms.

Unsaturated zone hydrology

Pores below the water table are filled with water and are called saturated zone. However, the water between water table and ground surface is filled with water and other gases, is known as unsaturated zone. Water in the unsaturated zone comes from precipitation and ground water (during capillary rise). The different subsurface zones are shown in the Fig. 7.1.

Some of the terms and concepts in unsaturated zone are described below.

Volumetric water content: of a soil is the volume of the contained water divided by the total volume of the soil (Fetter 1994). Mathematically, it is written as:

$$\theta_v = \frac{V_w}{V_\beta} \tag{7.1}$$

where V_w and V_β are volume of water and volume of the total soil respectively. The soil texture significantly affects water content of a soil material (Pachepsky and

Rawls 2004, Walker 1989). The moisture content and total available soil moisture holding capacity for different textures are shown in Fig. 7.2.

Capillary rise: water molecules at water table are subjected to an upward attraction

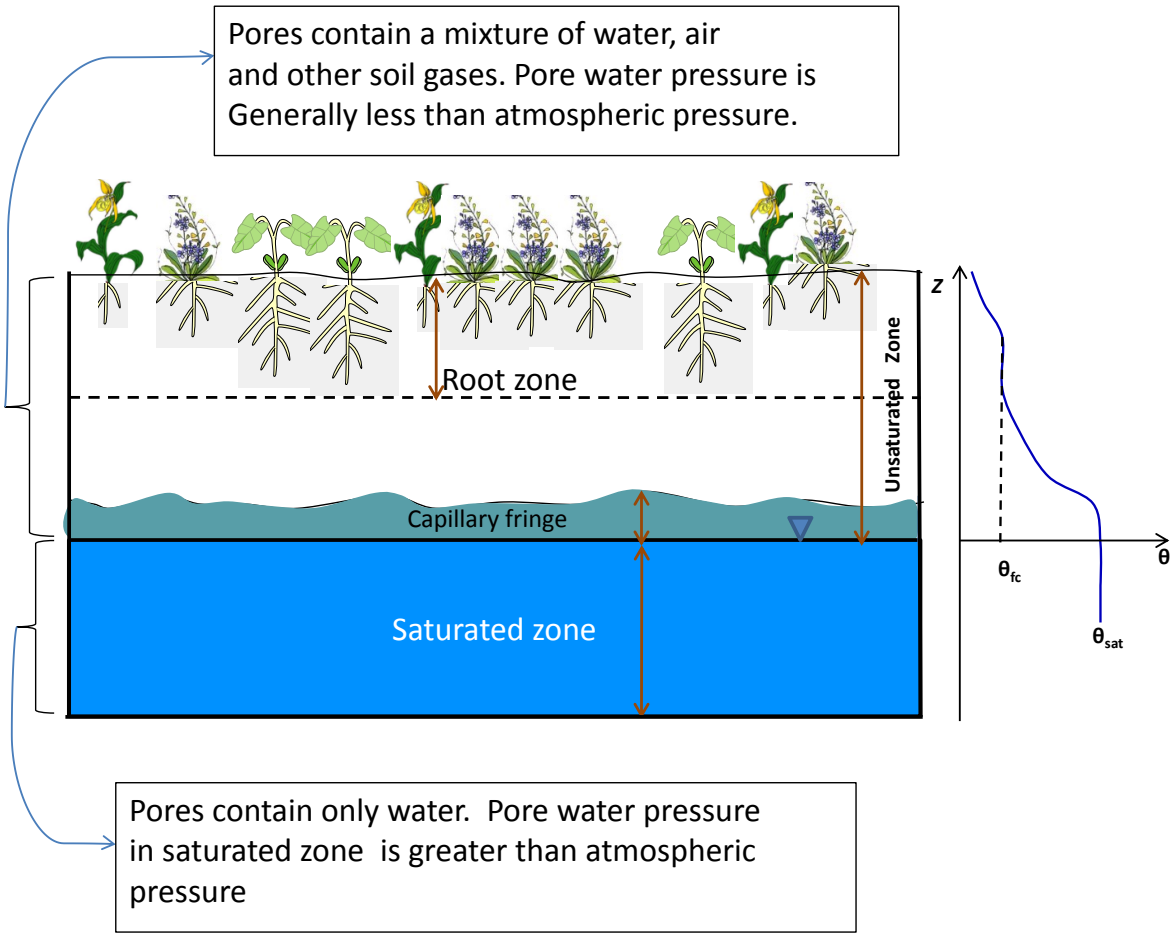

Fig. 7.1 Conceptual diagram of subsurface water zone. Capillary fringe is the saturated zone above water table. The general moisture content profile adapted from Hornberger et al. (1998) is also shown on the right side of the diagram. Θ= moisture content, Θ_{fc}= moisture content at field capacity, Θ_{sat}=moisture content at saturation

due to surface tension of the air-water interface and the molecular attraction of the liquid and solid phases (Fetter 1994). Capillary rise is a function of surface tension of the fluid, density of fluid, acceleration of gravity and radius of capillary tube. Most of these parameters are the same for geologic matrix except the radius of capillary tube. In our study area the soil texture of the upper layer is mainly loamy and clayey materials as shown in the *Fig. 5.2*. We can see from this figure that, soil

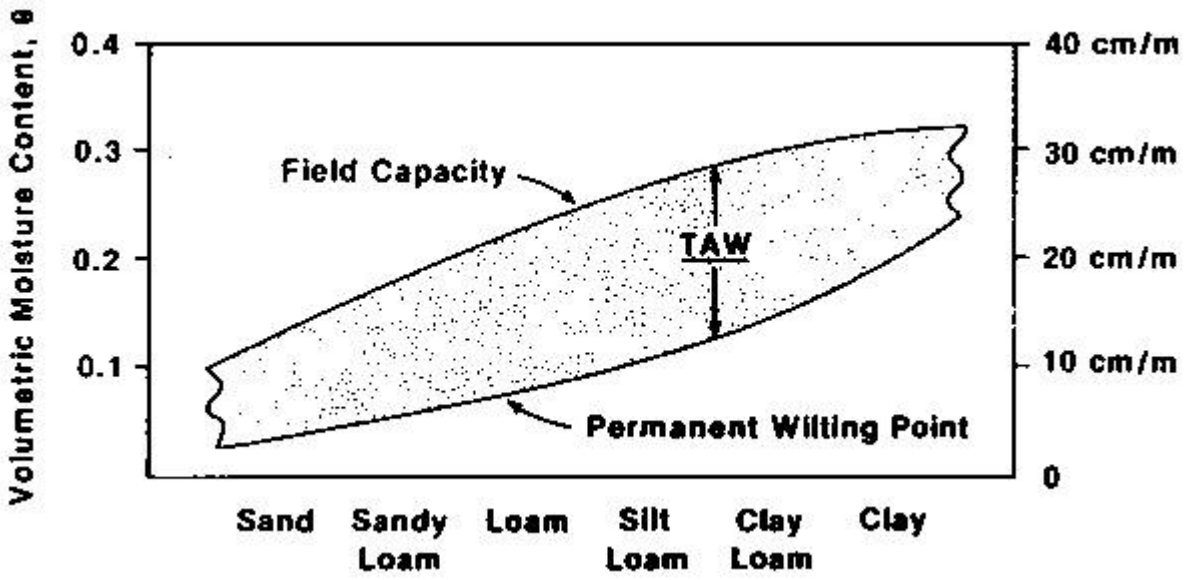

Fig. 7.2 Relationship between soil types and total available soil moisture holding capacity, field capacity and wilting point, taken from (Walker 1989), TAW= Total Available Water. The moisture content diagram is not scaled.

texture in block I is mainly loamy upper and sandy in the lower layer. The texture in block II and III are generally silty loam at the upper 150cm and mixture of gravel and sand at the lower layer. The lower layer of block III is mainly sandy gravel and gravely material. Therefore, we expect differences in capillary rise during water stress in summer time. Height of capillary rise for different types of sediment is shown in *Table 7.1*. The capillary fringe is higher in the fine grained soils than in course grained ones because of greater tension created by the smaller pore created (Fetter 1994).

Table 7.1 Height of capillary rise in sediments, taken from (Fetter 1994).

Sediment	Grain diameter(cm)	Pore Radius(cm)	Capillary rise (cm)
Fine silt	0.0008	0.0002	750
Coarse silt	0.0025	0.0005	300
Very fine sand	0.0075	0.0015	100
Fine sand	0.0150	0.003	50
Medium sand	0.03	0.006	25
Coarse sand	0.05	0.010	15
Very coarse sand	0.2	0.040	4
Fine gravel	0.5	0.1	1.5

The description of the study area and detail of experimental design is found in

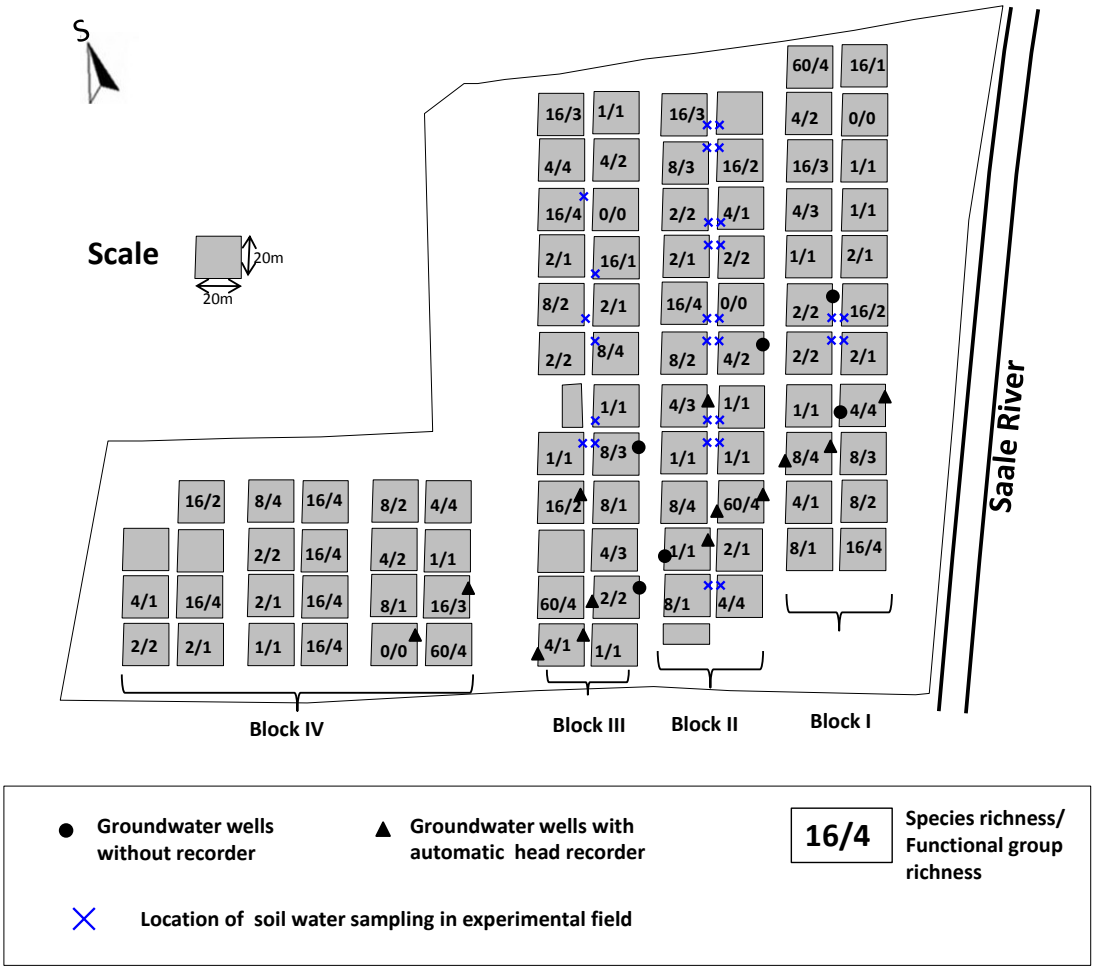

Fig. 7.3 Location of soil water samples in experimental field.

Chapter 3. Soil water sampling was conducted from suction plates of 29 plots (shown in *Fig. 7.3)* during the summer season in 2010. The sampling was conducted in July 6/2010, August 5/2010, August 19/2010, September 2/2010, September 14/2010 and October 12/2010. The samples were taken from 20 cm, and 30 cm depth in block I (from four plots), 10 cm, 20 cm, 30 cm, and 60 cm depth in block II (18 plots), 20 cm, and 30 cm depth in block III (seven plots). The suction plates in block I and III are equipped to measure at depths of only 20 and 30cm. The collected sample was then preserved at a temperature of about 4°C until analysis. Precipitation and other meteorological data (humidity, wind speed, temperature, vapor pressure, density of air, and solar radiation) were collected at the site tower managed by the by Max-Planck Institute for Biogeochemistry/Jena. Leaf area index (LAI), vegetation height

and soil moisture content were used from Jena experiment database management.

7.1.1 Comparison method

From study in *Chapter 5* we found that the ground water chemical composition showed spatial variation in terms of chloride concentration. Generally plots in the same block tends to have similar chloride concentration in the groundwater, except plots BIIIA02 and BIIIA13, which showed a much higher difference in chloride concentration compared to other groundwater in other plots. Therefore, we decided to compare plots with the same chloride composition in the groundwater. Comparing nearby plots (plots in the same block) also has other advantages; it removes the effect of heterogeneity of the soil material and also differences in depth of water table.
We identified the time when the net upward flow takes place as explained in the next sections. We then calculated the chloride accumulation in this periods for plots with different diversity level and compared the results.

7.1.2 Upward flow determination

We used daily precipitation and also calculated daily evapotranspiration from the meteorological data to estimate when net flow in the unsaturated zone is potentially upward. We calculated the net vertical flow (from precipitation and evapotranspiration balance) between April-2010 and December-2010. Penman-Monteith equation as cited in Allen et al. (1998) was used to calculate evapotranspiration from different plots of the experimental field.

$$\lambda E_T = \frac{\left(\Delta\left(R_n - G\right) + \frac{\rho_a C_p (e_s - e_a)}{r_a}\right)}{\left(\Delta + \gamma\left(1 + \frac{r_s}{r_a}\right)\right)} \tag{7.2}$$

Where, γ(Pa/K) is the psychrometric constant, λ(MJ/Kg) is latent heat evaporation, ET(mm/day) evapotranspiration rate, G ($MJ/m^2.day$) is gained heat flux, Δ (KPa/°C) is the slope of saturation vapor pressure versus temperature curve, C_p (MJ/kg.°C) is the specific heat of air, $\rho_a(kg/m^3)$ is the density of air, e_s (KPa) and

e_a (KPa) are saturated vapor pressure and mean ambient vapor pressure. r_a(s/m) and r_s(s/m) are aerodynamic resistance and bulk surface resistance.to determine the rate of potential evapotranspiration from the plots. R_n $(MJ/m^2.day)$ is net radiation. It can be calculated as:

$$R_n = (1 - \alpha)R_i, \tag{7.3}$$

where R_i $[MJ/m^2day]$ is incoming short wave radiation and α is albedo which shows the fraction of incoming radiation reflected. Albedo of a given area depends on the type of vegetation cover (Zerling et al. 2003). Some studies (Hales and Neelin 2004, Tsuji et al. 1998, Mei and Wang 2010) also investigated the relationship between albedo and leaf area index. According to these authors albedo decreases as the LAI increases. We used empirical formula by Tsuji et al. (1998) to estimate plot specific albedo from LAI values. According to this study:

$$Albedo(\alpha) = 0.23 + (LAI - 4) * \frac{2}{60} \tag{7.4}$$

The estimated values of albedo are shown in Table 7.2. G $[MJ/m^2day]$ is the soil heat flux. Because there is loss of heat from the soil during night time, the net daily heat flux is relatively small and can be considered to be zero (Allen et al. 1998).
Bulk surface resistance $r_s[S/m]$: is resistance to flow mainly from stomatal control. According to Kirkham (2005) surface resistance depends on stomatal conductance and LAI. It is calculated as:

$$r_s = \frac{r_{leaf}}{0.5LAI} \tag{7.5}$$

where, r_{leaf} is the stomatal resistance. Stomatal resistance is the resistance to water vapor between leaf and boundary layer (Kirkham 2005). We could not get values for specific species and therefore, we assumed plots do not differ in terms of stomatal resistance. For our study we assumed a value of 100s/m (The value reported for grasses by Allen et al. (1998)). We used measurement of leaf area index for all plots (Table 7.3) and calculated surface resistance for considered plots.
Psychrometric constant (γ): is the constant which relates atmospheric pressure of

a given area with latent heat of vaporization and specific heat of moist air. It is approximated as (Allen et al. 1998):

$$\gamma = \frac{C_p P}{\xi \lambda}, \tag{7.6}$$

where P [KPa] is the atmospheric pressure at the location, $\lambda[Mj/Kg]$ is latent heat of vaporization, ξ is ratio of molecular weight of water vapor to dry air ($\xi = 0.622$), and C_p [MJ/kg°C] is specific heat of moist air.

Aerodynamic resistance r_a [s/m]: is resistance to flow of water vapor. It is function of wind speed and height of vegetation (Allen et al. 1989). The formula to calculate aerodynamic resistance is:

$$r_a = \frac{\ln\left(\frac{Z_m - d}{Z_{om}}\right) \ln\left(\frac{Z_h - d}{Z_{oh}}\right)}{k^2 u_2} \tag{7.7}$$

Where Z_m is the height of wind measurement, r_a aerodynamic resistance, Z_h height of humidity measure (m), d=zero place displacement height (m), Z_{om} and Z_{oh} are roughness length governing momentum transfer and heat vapor transfer (m), k is von Karman's constant (0.4) and u_2 is wind speed at height Z (m/s). d, Z_{om} and Z_{oh} are determined as:

$$d = \frac{2H_c}{3}, Z_o m = 0.123 H_c, Z_o h = 0.1 Z_o m \tag{7.8}$$

where H_c is the plant height. u is the wind speed at 2m. The wind speed measured at other heights can be adjusted by the following formula:

$$u = u_h \frac{4.87}{ln(67.8z - 5.42)} \tag{7.9}$$

where u is wind speed at 2m, while u_h is the wind speed at other heights from the ground surfaces. The average heights of vegetation for all plots are estimated from data published by Weigelt et al. (2009). The wind speed measuring sensor by meteorological station at our study site is located at 4m above the ground surface while the humidity is at 2m above ground surface. We therefore scaled the wind

speed to 2m height by using Equation 7.9.

Latent heat of vaporization (λ): is the heat required for the phase change from liquid water to vapor. It is calculated as:

$$\lambda = 2.501 - (2.361 * 10^{-3})T_{mean} \tag{7.10}$$

where, $\lambda[MJ/Kg]$ is latent heat of vaporization and T_{mean} is the mean air temperature.

Slope of saturation vapor pressure curve (δ) is calculated as:

$$\delta = \frac{2504exp(\frac{17.27T}{T+237.2})}{(T+237.3)^2} \tag{7.11}$$

where, δ $[KPa/^{\circ}C]$ is slope of saturation vapor pressure curve and T $[^{\circ}C]$ is air temperature. Other meteorological parameters (temperature, saturated vapor pressure, actual vapor pressure, humidity, wind speed at 4m, solar radiation) were directly recorded every 10 minutes by climate station at the study area.

Precipitation and Evapotranspiration

Climate data were taken from weather station located in the middle block of the experimental field (at 0684356, 5647697 UTM). The daily precipitation was also determined from available weather station data (every 10 minutes) from April-December 2010. We used Penman-Monteith equation to calculate the daily evapotranspiration. The daily evapotranspiration, precipitation and their difference for plots B1A16 and B2A01 are shown in *Fig. 7.4*. We can determine the period of water deficit (i.e. ET>rainfall). This is a period, when water flow within the soil could be directed upward. From the *Figure 7.4* and *Figure 7.5* we can see that the net upward flow is likely to occur from beginning of June to beginning of August 2010. Therefore, we expect the upward chloride transport or accumulation of chloride at the near surface during this period.

Table 7.2 Estimated parameters to be used in Penman-Monteith equation. LAI was use to calculate the albedo and surface resistance. Stomatal resistance of 185s/m were used to estimate surface resistance.

Block	Plot	LAI (m^2/m^2)	Albedo (α)	Surface resistance (r_s)[sm^{-1}]
B1	A05	1.68	0.15	220.24
B1	A06	1.81	0.16	204.42
B1	A16	1.09	0.13	339.45
B1	A17	1.19	0.14	310.92
B2	A01	2.86	0.19	129.37
B2	A04	1.35	0.14	274.07
B2	A05	1.16	0.14	318.97
B2	A06	1.9	0.16	194.74
B2	A06	1.9	0.16	194.74
B2	A08	2.42	0.18	152.89
B2	A09	1.92	0.16	192.71
B2	A10	1.67	0.15	221.56
B2	A12	1.6	0.15	231.25
B2	A15	2.04	0.16	181.37
B2	A17	2.01	0.16	184.08
B2	A18	2.33	0.17	158.80
B2	A19	1.52	0.15	243.42
B2	A19	1.52	0.15	243.42
B2	A20	1.15	0.14	321.74
B2	A21	3.59	0.22	103.06
B2	A22	3.6	0.22	102.78
B3	A05	2.27	0.17	163.00
B3	A06	1.49	0.15	248.32
B3	A17	0.65	0.12	569.23

7.1.3 Transport modeling

The upward movement of water in the soil profile causes transport of chloride ion via advection. We assumed chloride ion to be inert, and therefore, it travels in the soil at about an average rate equal to the upward seepage velocity of the water. We used the average of net flux of water over time period considered and mean moisture content of the upper 60cm depth to determine the seepage velocity. The other mechanism of solute (chloride) transport is by diffusion due to concentration gradient. Hu and Wang (2003) reviewed the diffusion coefficients of various ions at different volumetric water content. The diffusion coefficient of chloride in most of the soil texture at volumetric water content of 20 to 40% lies between 10^{-6} and 10^{-5} cm^2/s. According to Rowell et al. (1967), cited in White and Broadley (2001) the

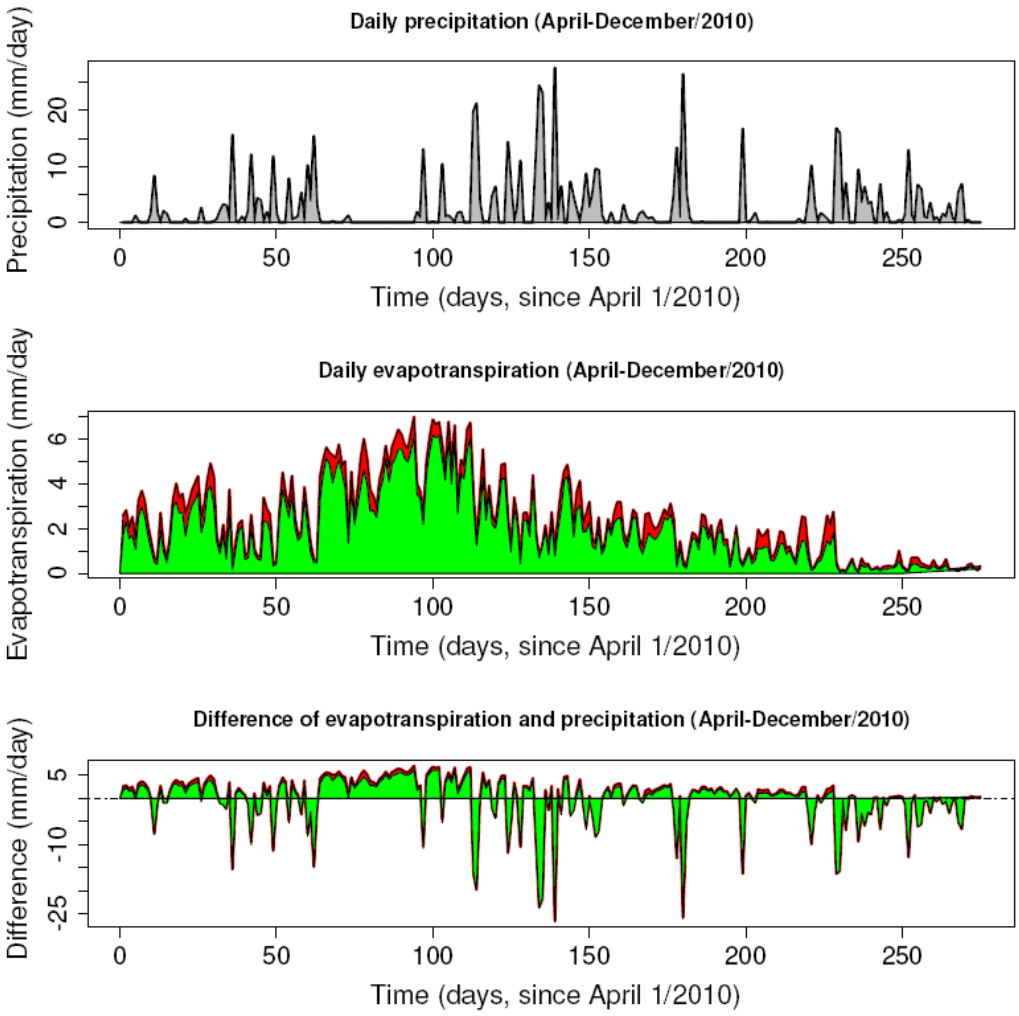

Fig. 7.4 Evapotranspiration, precipitation and net water balance from April 2010 to December 2010. The daily evapotranspiration is for Plot B2A01 with all functional group in it (red) and B1A16 a plot with grasses and short herbs (green)

typical diffusion coefficient of chloride in moist soil is $2 - 9 \times 10^{-6} cm^2/s$. For our case we assumed a value of $9 \times 10^{-6} cm^2/s$.

One-dimensional diffusion convection transport of solute transport in unsaturated zone is mathematically formulated as:

$$\frac{\partial c(z,t)}{\partial t} = \frac{D}{R}\frac{\partial^2 c(z,t)}{\partial z^2} - \frac{v}{R}\frac{\partial c(z,t)}{\partial z} - \frac{\lambda}{R}c(z,t) \tag{7.12}$$

where, c =concentration of chloride ion, [M/L3], D is dispersion coefficient [L2/T], V pore water velocity [L/T], R is retardation factor, λ first order decay coefficient, Z is vertical space coordinate [L] and t is the time [T]. For our problem we assumed, no

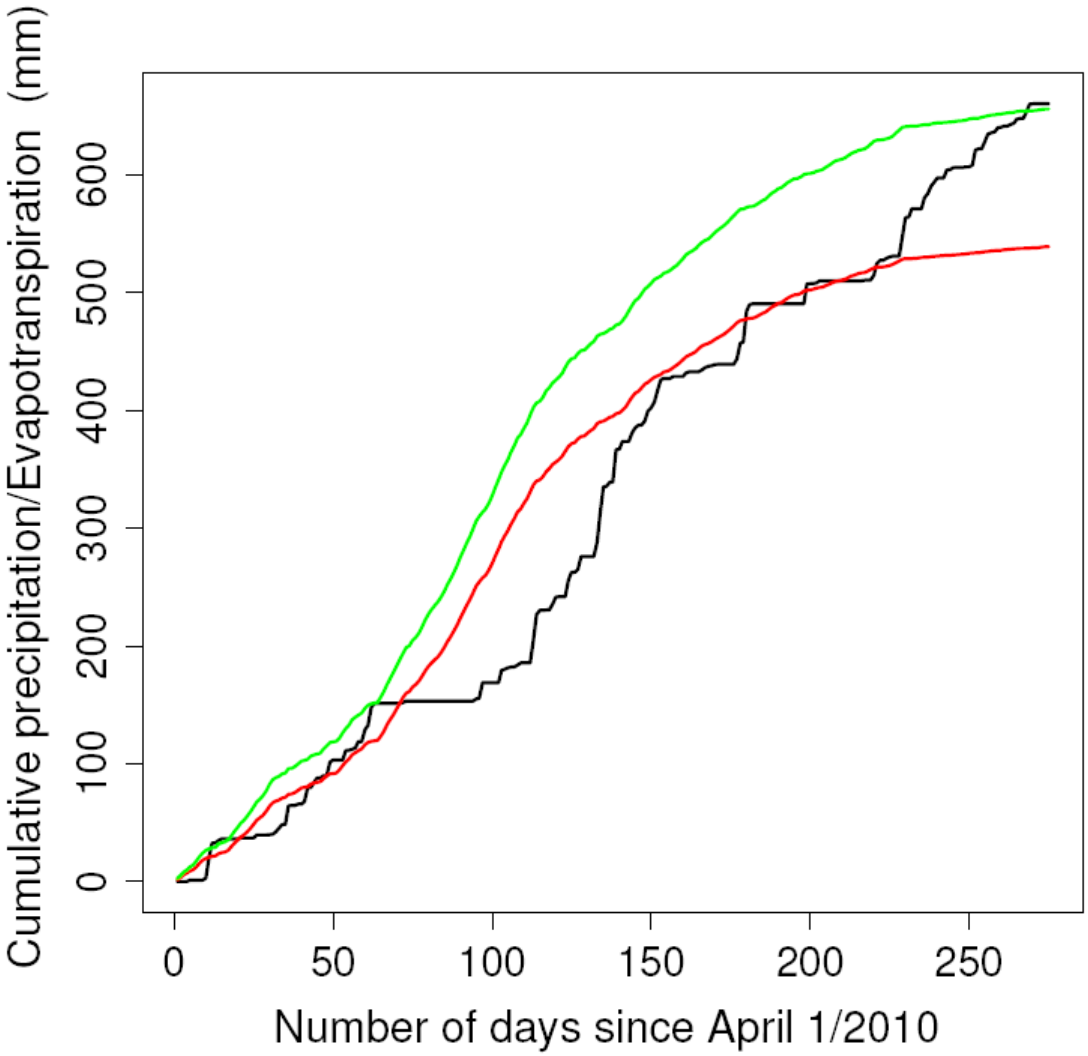

Fig. 7.5 Cumulative evapotranspiration and precipitation from April 2010 to December 2010 for Plot B2A01 with all functional group in it (green) and B1A16 a plot with grasses and short herbs (red)

chemical reaction (chloride ion is assumed to be conservative), upward flow, V=-v and water content to be constant in the profile.

The simplified equation after the assumption is:

$$\frac{\partial}{\partial t}c\left(z,t\right) = \left(D\right)\frac{\partial^2}{\partial z^2}c\left(z,t\right) + v\frac{\partial}{\partial z}c\left(z,t\right) \tag{7.13}$$

We estimated the chloride profile in the unsaturated zone by solving the equation analytically, by first converting the partial differential equation (PDE) in to ordinary differential equation using Laplace Transform.

7.2 Results and discussion

7.2.1 Net flow direction

The result from precipitation and evapotranspiration balance suggests that the time from beginning of June- to beginning of August-2010, the net flow is upward most of the time as shown in Fig. 7.4. Therefore, we assumed this period as a time of water stress and calculated chloride transport in the unsaturated zone to investigate the upward flow of water for different aboveground plant diversity level. There was some precipitation at the end of identified stress time. But we assumed that it does not have significant effect on our result. Fig. 7.6 shows that the change in chloride

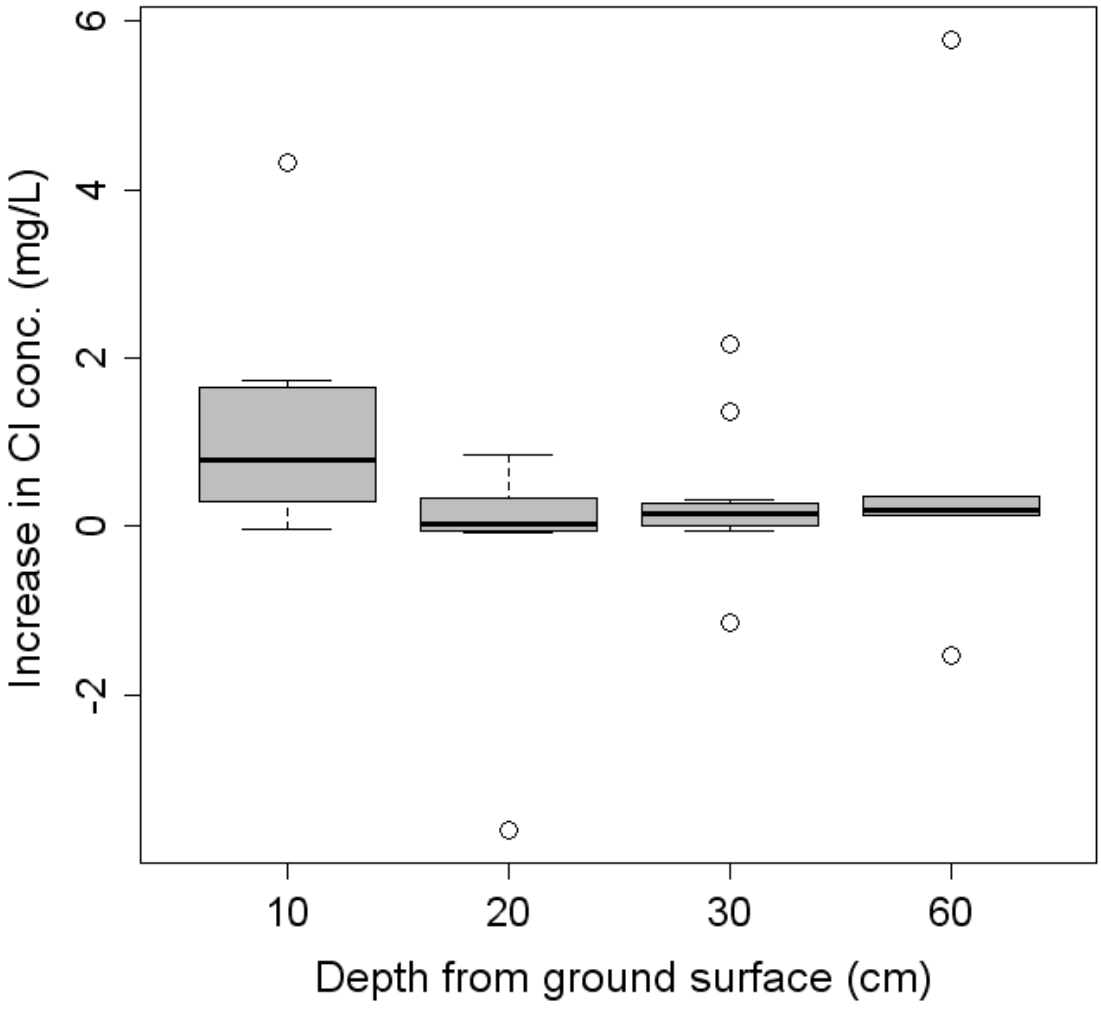

Fig. 7.6 The increase in chloride concentration in different depth during the water stress time

concentration at different depth. The accumulation is higher at the top 10cm than other depths. This could be because of other processes (such as evaporation and root zone water uptake) resulted in additional increase in the concentration of chloride as we come closer to the surface. The other reason is that, because the diffusion coefficient of chloride is so small the accumulated chloride in the upper surface due to advection will not be transported faster to lower layer.

We also calculated net flux for plots we considered for comparison. The difference in the rate of evapotranspiration attribute to the difference in surface and aerodynamic resistance to water and heat flow. The aerodynamic resistance is a function of plant height and wind speed while while the surface resistance can be calculated from leaf area index and stomatal resistance of the plant. The average heights of the plants and LAI measurement in 2005-2008 from Weigelt et al. (2009), all in August were used for resistance calculation.

Then the calculated net fluxes were used to compute the chloride concentration in the soil profile. The results of calculated chloride concentration profile from different plots are shown in Fig. 7.7.

We can also see that diversity is related positively with heights of plants and also leaf area index (Fig. 7.8. From Equation 7.5 we discussed that surface resistance to flow of heat and water vapor is inversely proportional to LAI. This leads to increase in LAI results in reduction of surface resistance. The rate of evapotranspiration is therefore, increase with increase of diversity. The results of evapotranspiration for some of the plots are shown in Fig. 7.4. To summarize, more diverse plots have taller heights and higher LAI than less diverse plots, which result in less aerodynamic and surface resistance and therefore, higher evapotranspiration.

7.2.2 Biodiversity and water flow

We could not see significant relationship between species richness and groundwater upward flow ($r=0.26$, $P=0.1168$). But, it has positive correlation with functional richness at significant level $P<0.1$ ($r=0.27$, $P=0.0997$). However, we could see that plots with all the four functional groups and plots, generally with mixture of tall

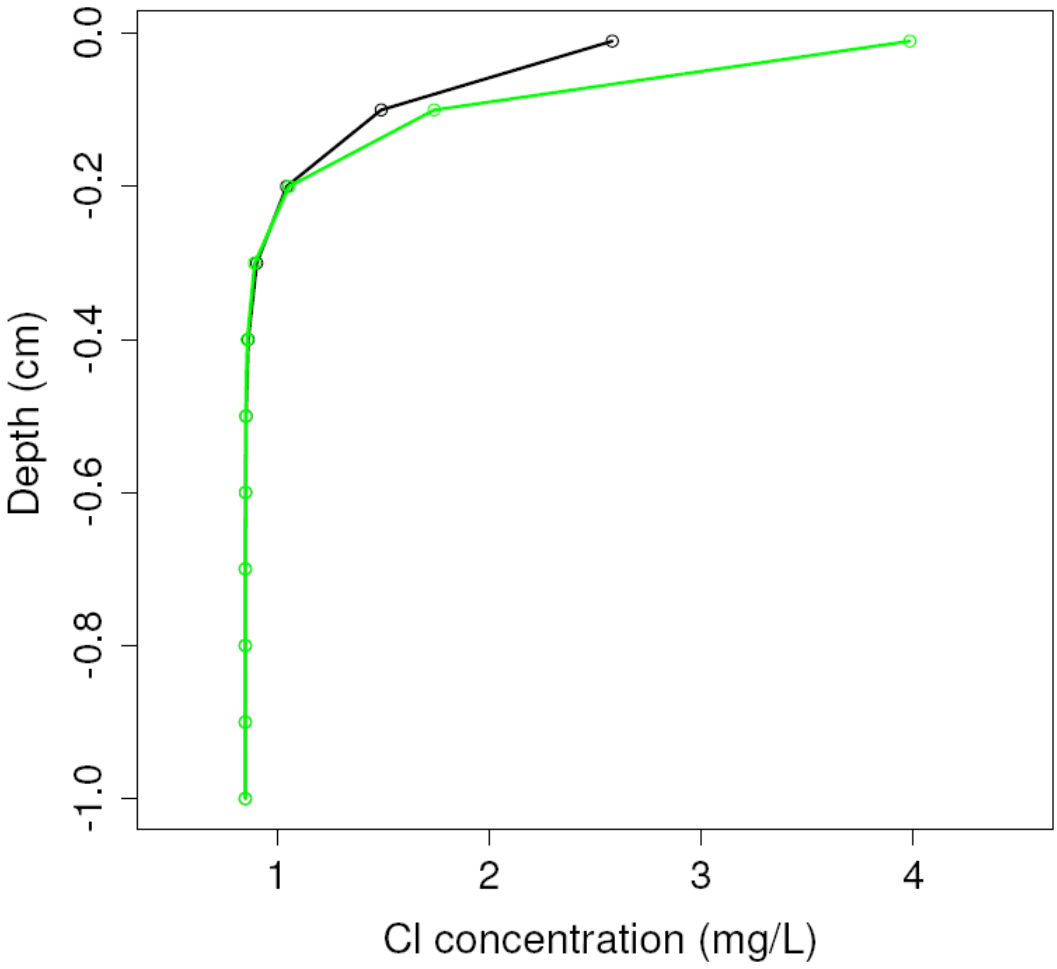

Fig. 7.7 Chloride profile in the unsaturated zone determined analytically. The result presented is for plot B2A01 (green) and B1A16 (black).

herbs and legumes resulted in relatively higher accumulation of chloride in the upper layer, which implies that there was more upward flow of groundwater during water stress. We also observed that plots with functional group of only grass resulted in no accumulation of chloride at the near surface. This shows that there is no significant upward flow of water in these plots. We could also observed in this study that the chloride accumulation was also in 60cm depth which shows that increase in concentration was not because of only root zone transpiration but also due to upward groundwater flow during water stress.

A two three way ANOVA was used to study if leaf area index, species richness and functional group richness and their interaction has significant effect on the

Table 7.3 Chloride accumulation, species richness and types of functional groups and mean height of vegetation of month August for years 2005-2008 (data for mean height of vegetation of each year is taken from Weigelt et al. (2009)).

Plot	Depth (cm)	Cl_i	Cl_f	ΔCl	$LAI_{av.}$	LAI_{2010}	Diversity	FG type	Mean.veg height (m)
B1A05	30	0.32	0.50	0.18	1.68	1.52	2	L	0.56
B1A06	30	0.25	0.20	-0.05	1.81	2.92	16	T	0.23
B1A16	30	0.42	0.47	0.05	1.09	0.8	2	GS	0.14
B1A17	30	1.67	0.54	-1.14	1.19	0.39	2	GT	0.26
B2A01	10	0.75	5.08	4.33	2.86	0.74	4	GLST	0.21
B2A01	20	0.28	1.13	0.85	2.86	0.74	4	GLST	0.21
B2A04	60	1.78	0.23	-1.54	1.35	0.84	1	T	0.20
B2A05	60	0.35	0.57	0.22	1.16	1.19	1	T	0.22
B2A06	10	0.30	1.41	1.11	1.9	3.18	4	LS	0.2
B2A06	20	0.33	0.36	0.03	1.9	3.18	4	LS	0.2
B2A06	30	0.19	0.34	0.15	1.9	3.18	4	LS	0.2
B2A08	20	0.25	0.31	0.06	2.42	1.99	2	LT	0.15
B2A08	30	0.21	1.58	1.37	2.42	1.99	2	LT	0.15
B2A09	10	0.32	0.29	-0.04	1.92	3.44	4	S	0.09
B2A09	20	0.40	0.36	-0.04	1.92	3.44	4	S	0.09
B2A09	30	0.18	0.33	0.15	1.92	3.44	4	S	0.09
B2A10	60	0.31	6.10	5.79	1.67	2.09	16	GS	0.22
B2A12	10	0.35	0.81	0.46	1.6	3.51	8	T	0.25
B2A12	20	0.20	0.15	-0.05	1.6	3.51	8	T	0.25
B2A12	30	0.21	0.20	-0.01	1.6	3.51	8	T	0.25
B2A15	60	0.25	0.38	0.13	2.04	2.83	1	L	0.29
B2A17	10	0.30	1.88	1.57	2.01	2.55	8	LS	0.14
B2A17	20	0.34	0.93	0.60	2.01	2.55	8	LS	0.14
B2A17	30	0.35	0.58	0.23	2.01	2.55	8	LS	0.14
B2A18	10	0.32	0.72	0.40	2.33	1.23	16	GLST	0.17
B2A18	20	0.29	0.38	0.09	2.33	1.23	16	GLST	0.17
B2A19	10	0.32	2.04	1.73	1.52	3.82	2	S	0.2
B2A19	20	0.27	1.05	0.78	1.52	3.82	2	S	0.2
B2A19	30	0.38	0.50	0.12	1.52	3.82	2	S	0.2
B2A20	10	0.23	0.42	0.19	1.15	3.7	2	LS	0.09
B2A20	20	0.44	0.37	-0.07	1.15	3.7	2	LS	0.09
B2A21	60	0.20	0.56	0.36	3.59	1.39	8	LST	0.23
B2A22	60	0.34	0.52	0.18	3.60	0.51	16	LST	0.43
B3A05	20	0.28	0.33	0.05	2.27	1.15	8	LST	0.37
B3A06	20	0.27	0.21	-0.06	1.49	2.31	1	G	0.22
B3A06	30	0.27	0.58	0.31	1.49	2.31	1	G	0.22
B3A17	20	4.29	0.68	-3.61	0.65	3.21	1	S	0.06
B3A17	30	1.96	4.12	2.16	0.65	3.21	1	S	0.06

increase in chloride concentration during the considered water stress time. The result (7.4) shows that, LAI is responsible for the increase in chloride concentration

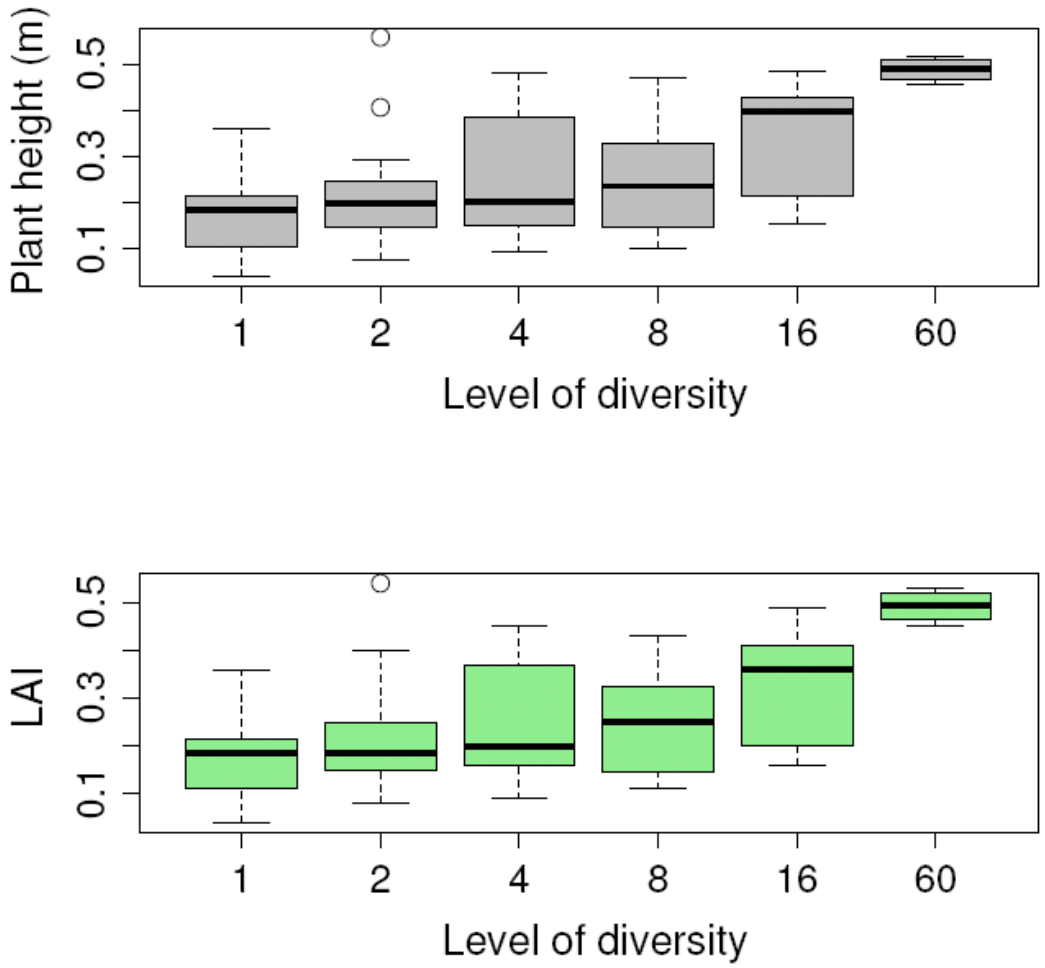

Fig. 7.8 Plant height and LAI against diversity level, data shown in Table 7.3.

Table 7.4 Analysis of variance of effect of species richness, functional group richness, and leaf area index (LAI) on the increase in chloride concentration.

Source of variation	**Df**	**Sum Sq**	**Mean Sq**	**F value**	**Pr(>F)**
LAI	1	6.123	6.1227	3.7899	**0.06098**
Species richness	1	1.738	1.7384	1.076	0.307878
FG-richness	1	1.304	1.3045	0.8075	0.37603
LAI:Species richness	1	13.325	13.3245	8.2477	**0.00742**
LAI:FG richness	1	4.693	4.6927	2.9047	0.098658
Species richness:FG richness	1	1.203	1.203	0.7447	0.395018
LAI:Species richness:FG richness	1	0.317	0.3167	0.1961	0.661103
Residuals	30	48.466	1.6155		
Total	37	77.169	30.318		

(P=0.06098). The interaction of LAI and species richness also is the source of variation (P=0.00742). However the species richness and functional group richness did not have significant effect on the increase in concentration.

Chloride accumulation in plots with mixture of grasses and short herbs (e.g. B3A06) were compared with plots made of mixture of legumes and tall herbs (e.g. B2A12). The result shows that plots with mixture of grasses and short herbs had little or below detection limit chloride accumulation. This suggests that there is only limited or no upward flow of water from the groundwater. This could be because of shallowness of roots of grasses and short herbs. Studies [unpublished report] shows that tall herbs have tap-rooted and have relatively deep root structure. Grasses have a significantly shallower distribution of root lengths than tall herbs and legumes. We infer from this that, plots with different root depth are capable of stress resistance as they can take water from groundwater. We also compared plot B2A18 (plots with all functional groups present) and B2A07 (plot with no plant species) at 20cm depth. The result showed that there is more accumulation of chloride near the surface in B2A18 than in the B2A07. Therefore, the more diverse (functional group richness) the plots are the more flow of water from the groundwater during water stress.

Our result shows that chloride accumulation was positively related to leaf area index (LAI). However, the correlation is weak, and significant at $P< 0.1$; ($r=0.28$, $P=0.086$). LAI is positively related to species richness according to study by and also Fig. 7.8. Legumes and tall herbs also have relatively higher leaf area index and might result in higher transpiration which creates more driving force to take up water from the groundwater. From analysis of variance we have seen that the variation of the chloride accumulation is due to the variation in leaf area index. From the ANOVA table we can see that the probability that the LAI is the source of variation is 0.96 at 95% confidence interval.

We also compared moisture content-diversity-chloride accumulation relationships for six plots (B1A05, B1A16, B1A17, B2A01, B2A12, and B2A19) which are nearly in same geologic matrix and soil types. All of them are in block I and II where the upper soil is loamy and lower layer is sandy material. Therefore, we do not expect significant difference in capillary rise because of difference in soil texture. We compared plots B1A16 with diversity level of 2 and functional groups, grass and short herbs and B1A17 plot which has also diversity level of 2 and functional groups

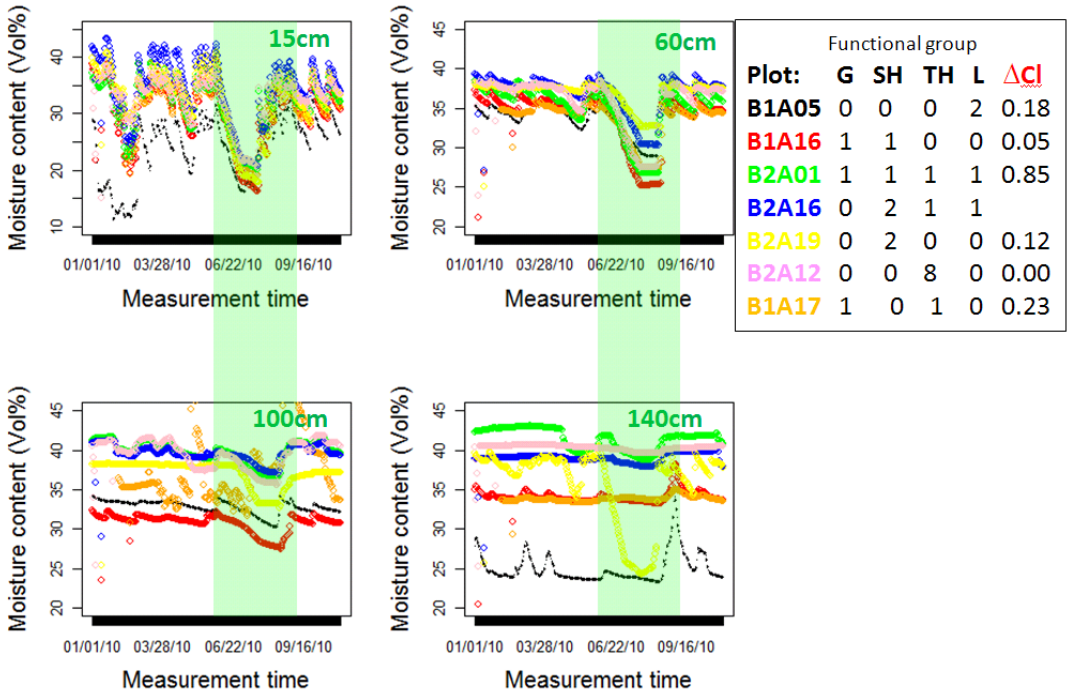

Fig. 7.9 Moisture content, chloride accumulation and functional group and species richness

grass and tall herbs as indicated in Fig. 7.9. We could see that B1A17 has more moisture content than B1A16 in all depths. Therefore the functional group tall herbs has the capacity to takeup water from the groundwater during water stress. Tall herbs are functional groups with medium or tall canopy height and vegetative and flowering plants (Roscher et al. 2004). That could be a reason why they resulted in upward groundwater flow and chloride accumulation as a result.

Therefore, the water movement in unsaturated zone seems affected by the type of functional group or mixture of functional group the plot contain instead of species richness. Mixtures with deep rooted and less deep rooted can complement each other and might uptake more water from the groundwater during water stress. Legumes and tall herbs are deep rooted and mixtures of these functional group may result in flow of more water to the upper surface and more chloride as a result.

We also solved the chloride transport in unsaturated zone analytically. The chlo-

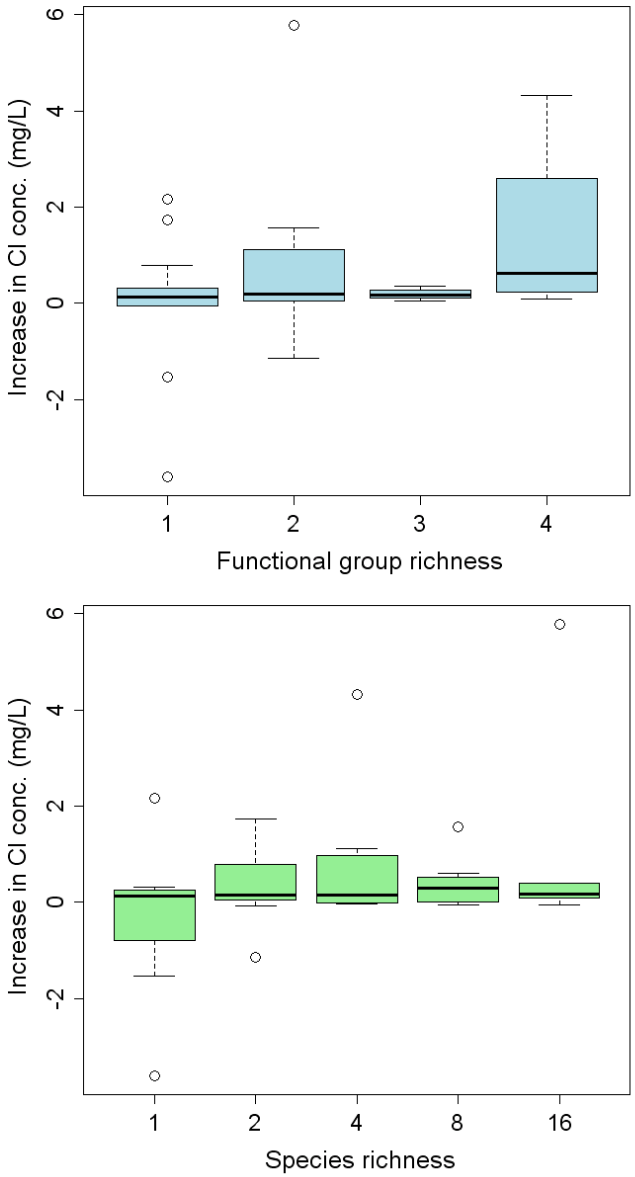

Fig. 7.10 Chloride increase as a function of species richness and functional group richness

ride concentration measured in July at different depths were used as initial condition and the measurement at the beginning of August was used as the final concentration in the analytical method. The initial and final concentration of chloride represents the beginning and end of water stress time. The result of diffusion-convection equation generally shows that, the higher the plant diversity is the more accumulation of chloride is expected at shallow layers (Fig. 7.7). The concentration is generally higher in the top 20cm.

7.2.3 Conclusion

From our result we conclude that, species richness does not have clear relationship with water flow in unsaturated zone or moisture content. It is the type of functional group or mixture of functional group which controls the water flow or the moisture content of the soil.

Plots with mixture of shallow and deep roots functional groups resulted in better moisture distribution in the unsaturated zone.
More diverse plots have higher LAI and vegetation height than less diverse plots. The higher LAI and taller vegetation heights reduced surface resistance and aerodynamic resistance to flow of water vapor which in turn increased the rate of evapotranspiration. Plots with higher rate of evapotranspiration accumulated more chloride near the surface of the earth, because of more pull up of water from the saturated zone.

Chapter 8

General discussion and Conclusions

8.1 General discussion

The effect of biodiversity on the subsurface water flow was studied, by first characterizing the study area and then investigating the effect of hydrological features (channel and river Saale) on the main experimental area of the field. To compare different diversity level in terms of subsurface water flow, we first identified which of the plots have similar background in terms of soil texture, groundwater physical and chemical property, and groundwater levels. From the results of hydrochemical characterization (Chapter 5) we found that plots in block III (BIIIA02 and BIIIA13) have relatively different chemical composition and different lower layer soil texture than other plots. The lower layer texture in these plots are generally gravelly and gravelly sand. The other plots have sandy lower layer in the range of 2 to 3 meter below ground surface. In gravely and gravely sand texture both horizontal and vertically velocity of water is fast ((Langmuir 1977) and water holding capacity is low. The low dissolved solid composition (as studied in Chapter 5) in this section (block III) of the experimental area attributes to the soil texture property.

We also used chloride as a tracer and hydrogeochemical modeling to understand

if the river and channel have significant effect on the study area and we could not see significant effect from both river and the channel at mean river flow. Hence at mean river flow, both the river and the channel did not contribute to the difference in physical and chemical property of the subsurface water.

To investigate the effect of level of diversity on ecosystem process, we compared plots in the same block or plots near the each other, that have the same background property. Similarity of plots in terms of chemical and physical property were analyzed by using cluster analysis and the result is shown in (Figures 5.9 and 5.10) and their texture property is shown in Fig. 5.2. Spatial variation of hydrochemical chemical composition was made and the result shows that plots generally with in the same block except block III have the same physical and chemical property. We also specifically compared chloride ion and we could not see we could not see significant difference among most plots except plots in Block III. The chloride concentration in these plots (BIIIA02 and BIIIA13) are very low compared to the other plots.

To avoid effect of soil heterogeneity the experiment was set up in 4 blocks (Roscher et al. 2004). Our result also shows that most plots in the same block have the same chemical and physical property but block III show variability among plots both in groundwater chemical composition (Chapter 5). This could be likely because of the difference in soil texture which result in difference in soil hydraulic property (Cosby et al. 1984, Hornberger et al. 1998, Younger 2008, van Genuchten 1980). According to Langmuir (1977) if the groundwater flow velocities are higher, it usually result in groundwater that has relatively low dissolved solids because of the short rock contact time.

From hydrochemical characterization of the groundwater we interpreted that groundwater-geologic matrix interaction is the main factor which controls the composition of the groundwater. The water types are also identified and are mainly Ca-Mg-HCO_3, Ca-Mg-SO_4, and Ca-Mg-Cl. We also investigated the water types in geologic units near the study area. Ca-Mg-HCO_3 is dominant in groundwater with Muschelkalk geologic unit groundwater in the upper, lower and middle Buntsandstein are dominated by Ca-Mg-SO_4 and Ca-Mg-Cl water types. This suggests that our groundwater is hosted in buntsandstein/mushelkalk geologic units.

The channel and river Saale also did not show significant effect on the study area at the mean river flow. However,when the flow in the river increase (e.g. during flooding) it will result in change in concentration and value of some physical and chemical properties (Ca, Cl, Fe, K, Mg, Mn, NO_3 and SO_4). NO_3, K and Fe concentrations in plots near to the river predicted to be increased significantly. Therefore, if there is frequent flooding, then the addition of nitrate through river influx is high. According to study by Oelmann et al. (2007) the net nitrogen of the experimental field of the same area was calculated based on total deposition,fixation, mowing and leaching from soil. However, the addition of nitrogen by river influx (during flooding) is higher and affects the heterogeneity of the soil in terms of nitrate content. Therefore, this component of nitrogen should be considered for study after flooding times. This component of nitrogen will result in higher nitrogen content in plots near the river (Block I) than other plots of the experimental field. From the chloride investigation in the channel and groundwater wells suspected to be affected by the channel, we found out that they do not mix. Therefore, the channel not will not affect the study area at all flow rates of the river.

Diversity effect on chloride transport

We used chloride transport in the unsaturated zone to study the effect of biodiversity on the subsurface water flow. Our hypothesis was that, there will be more transport of chloride (as a result of upward flow of water) near the earth's surface in plots with higher diversity level. However, from our result, the diversity level did not show significant correlation with chloride increase during water stress. One of the explanation for this is that, there was some rainfall at the end of assumed water stress period. The rainfall might reversed the flow direction and leached the chloride accumulated. It is rather the type of functional group or mixture of functional group which determined the increase of chloride in the upper layer during water stress. Plots with a mixture of grasses and tall herbs resulted in relatively higher chloride concentration in the upper surface. We could also see correlation between functional group richness and chloride transport. This could be likely because of

the species complementarity effect (Hooper et al. 2005) as discusses in *Section 2.1.* Functional groups with tap-root system (e.g. tall herbs) can take water from deeper soil (Jiang et al. 2007). The more functional group type we have the better vertical root distribution we have in the plot, which result in more flow of water and chloride transport as a result. Our results are consistent with findings of Jiang et al. (2007). According to this author the difference in plant functional trait better explains diversity effect on water flow than species richness.

LAI effect on chloride transport

We could also see that LAI was one of the factor for the increase in chloride concentration. According to Spehn et al. (2000) LAI increased significantly with logarithms of plant species number, with the number of functional group and with the presence of legumes during growth period. LAI increase also increase the rate of evapotranspiration by reducing the surface resistance. Hence, there will be more pull up of water and chloride as a result. In our study the increase in chloride concentration showed positive correlation with increase in LAI. Therefore, the increase in chloride and species richness were expected to have positive correlation. However, we could not see significant correlation.

In our study the composition of functional group was important in determining the moisture content or water transport in the subsurface. In our study the mixture containing total herbs and grasses resulted in more accumulation of chloride in the upper part. This shows that there was more upward flow of water in these plots. Therefore, we can infer that, plots with traits of shallow and deep root mixture take up more water from shallow groundwater during water stress.

Moisture content-chloride transport-diversity

Most of the moisture content variation during water stress are on the top 60cm. There is no much change in moisture content of the soil below 100cm as it gets water from the nearby saturated zone. From Fig. 7.9 we can see that the moisture

content in 100 and 140cm is generally constant except for plot B1A17. The moisture variation is mainly in the upper 60cm depth, and we could not see any clear relationship with diversity level.

The result from autocorrelation coefficient (Fig.6.5) shows that, because of the heterogeneity of the soil (unsaturated zone) the response of groundwater head for both river discharge and rainfall was quick in wells near to the river than groundwater wells far from the river. Therefore it is difficult to compare the groundwater heads in relation to the aboveground biodiversity. We could not also compare the moisture content of different depth of plots with different diversity level as they have no the same background system.

Comments on the experimental design

Some aspect of the experimental design also contributed for the uncertainties of our results. One of the design aspect is the location of groundwater wells in the plots. The wells are located at the corner and edge of the plots. Therefore, the possibility that the we measure the property other than the plot area is high. It would better represent the plot if the wells are in the middle of the plots.

One of the suggestion for ongoing research in Jena experiment is, before comparing biodiversity and ecosystem processes, it is important to make sure that the background property of the plots are the same with respect to the variable compared. In this study we found that, plots specially in block III (BIIIA02 and BIIIA13) should not be compared to other block plots if the variables to be compared are element cycling, water cycles and any other variables influenced by these two.

8.2 Conclusions

The groundwater of the study area was characterized in terms of hydrochemical composition, spatial and seasonal variation of its physical and chemical properties.

The main source of heterogeneity of the hydrochemical pattern is due to EC, Na, K, Li, Ca, Mg, Cl^-, Sr, SO_4^{2-}, HCO_3^- and Ba. This attributes to the groundwater-geologic matrix interaction. The main source of variation of these elements were due to solubility changes in reactive precipitates such as, calcite ($CaCO_3$), dolomite ($CaMg(CO_3)_2$, quartz (SiO_2), and siderite ($FeCO_3$) in some locations. Spatial variation of hydrochemical composition analysis result shows that the sampled plots in block III (BIIIA02, BIIIA13) have relatively different chemical composition than other plots. They generally have the same composition as groundwater in Muschelkalk geologic unit while the other plots show similarity with Upper Buntsandstein.

The result of time series analysis, hydrogeochemical modeling using PHREEQC and natural chloride (used a tracer) shows that the river Saale at mean flow and the channel from the river to the main experimental field did not have effect on the groundwater of the study area.

The upward chloride transport during water stress, could not show us clear correlation between the aboveground diversity and water flow in the unsaturated zone. However, we could see the correlation between chloride transport and LAI. The increase in LAI resulted in increase in chloride concentration. The LAI increase resulted in higher rate of evapotranspiration, which in turn increased chloride concentration in the upper surface.

8.3 Problems and limitations

One of our hypothesis is to determine chloride transport during water stress. However, it was difficult to get continuous period of time with water stress. For our study the period we considered was not fully period of water stress. There was some precipitation with in the considered periods, specially during the end of the period.

It is also important that the geologic matrix and soil texture should be as similar as possible to compare the water transport with respect to aboveground biodiversity. But, in our study area we could see heterogeneity in the soil texture which affect the water transport. So, we tried to compare plots which did not have so much

difference in soil texture.

The other problem is, roots of most of the grass types in the study area are not deep. In addition, the groundwater table is low during water stress which makes the accessibility to be difficult.

8.4 Outlook

In terms the investigation of biodiversity on subsurface process, I think it would be better to consider change in the size of the plots. The plot size can be reduced and then we might have all kind of diversity level in the same block , which then reduces the difference in soil texture heterogeneity, affected by the river in the same way and also the plots can be easily manipulated and controlled.

The distribution of the groundwater wells are not throughout the experiment field; it is only along two parallel transect as shown in Fig. 5.1. It is therefore, important to have groundwater wells throughout the experiment field to better represent and characterize the experiment field in terms of groundwater flow. It is also difficult to extrapolate the water table for plots outside the transect lines.

Bibliography

Aigner, T. and Bachmann, G. H.: 1992, Sequence-stratigraphic framework of the German Triassic, *Sedimentary Geology* **80**, 115–135.

Allen, R. G., Jensen, M. E., Wright, J. L. and Burman, R. D.: 1989, Operational estimates of reference evapotranspiration, *Agronomy Journal* **81**, 650–662.

Allen, R. G., Pereira, L. S., Raes, D. and Smith, M.: 1998, Crop evapotranspiration-guidelines for computing crop water requirements, *FAO Irrigation and Drainage Paper* (56).

Allison, G. and Hughes, M.: 1983, The use of natural tracers as indicators of soil-water movement in a temperate semi-arid region, *Journal of Hydrology* **60**, 157–173.

Alther, G. A.: 1979, A simplified statistical sequence applied to routine water quality analysis: A case history, *Ground water* **17**, 556–561.

Anderson, J.: 1973, Carbon dioxide evolution from two temperate, deciduous woodland soils, *Journal of Applied Ecology* **10**, 361–378.

Anderson, M. P.: 2005, Heat as a ground water tracer, *Groundwater* **43**, 951–968.

Appelo, C. and Postma, D.: 1994, *Geochemistry, groundwater and pollution*, A.A. Balkema, Rotterdam, pp 536.

Babar, M.: 2005, *Hydrogeomorphology: Fundamentals, Applications and Techniques*, New India Publishing, New Delhi, pp 272.

Bachmann, G. H.: 1998, The Germanic Triassic: General, *Hallesches Jahrb. Geowiss.* **6**, 19–22.

Barnes, C. and Allison, G.: 1988, Tracing of water movemenet in the unsaturated zone using stable isotopes of hydrogen and oxygen, *Journal of Hydrology* **100**, 143–176.

Bethke, C. M.: 2008, *Geochemical and biogeochemical reaction modeling*, Cambridge University Press, New York, pp 543.

Bohn, H., McNeal, B. and O'Connor, G.: 1979, *Soil chemistry*, John Wiley & Sons, New York, pp 307.

Bolt, G. H. and Bruggenwert, M.: 1978, *Soil chemistry*, Elsevier Scientific Publishing Company, Amsterdam, pp 281.

Bongartz, K., Steele, T. D., Baborowski, M. and Lindenschmidt, K.-E.: 2007, Monitoring, assessment and modelling using water quality data in the Saale river basin, Germany, *Environmental Monitoring Assessement* **135**, 227–240.

Bruelheide, H. and Udelhoven, P.: 2005, Correspondence of the fine-scale spatial variation in soil chemistry and the herb layer vegetation in beech forests, *Forest Ecology and Management* **210**, 205–223.

Bruno, J. F., Stachowicz, J. J. and Bertness, M. D.: 2003, Inclusion of facilitation into ecological theory, *TRENDS in Ecology and Evolution* **18**, 119–125.

Cardinale, B. J., Srivastava, D. S., Duffy, J. E., Wright, J. P., Downing, A. L., Sankaran, M. and Jouseau, C.: 2006, Effects of biodiversity on the functioning of trophic groups and ecosystems, *Nature* **443**, 992–989.

Chae, G.-T., Yun, S.-T., Kim, D.-S., Kim, K.-H. and Joo, Y.: 2010, Time series analysis of three years of groundwater level data (Seoul, South Korea) to characterize urban groundwater recharge, *Quarterly Journal of Engineering Geology and Hydrogeology* **43**, 117–127.

Chapelle, F. H.: 2000, The significance of microbial processes in hydrogeology and geochemistry, *Hydrogeology Journal* **8**, 41–46.

Chen, K., Jiao, J. J., Huang, J. and Huang, R.: 2007, Multivariate statistical evaluation of trace elements in groundwater in a coastal area in Shenzhen, China, *Environmental Pollution* **147**, 771–780.

Clark, I. D. and Fritz, P.: 1997, *Environmental isotopes in hydrogeology*, Lewis Publishers, New York, pp 328.

Constantz, J.: 2008, Heat as a tracer to determine streambed water exchanges, *Water Resources Research* **44**, 1–20.

Cook, P. G. and Herczeg, A. L.: 2000, *Environmental tracers in subsurface hydrology*, Kluwer Academic Publishers, Boston, pp 529.

Cosby, B., Hornberger, G., Clapp, R. and Ginn, T.: 1984, A statistical exploration of the relationshipos of soil moisture characteristics to the physical properties of soils, *Water Resources Research* **20**, 682–690.

Craig, H.: 1961, Isotopic variations in meteoric waters, *Science* **133**, 1702–1703.

Davis, J.: 1986, *Statistics and data analysis in geology*, John Wiley & Sons, New York, pp 646.

Dillon, W. R. and Goldstein, M.: 1984, *Multivariate analysis: Methods and application*, John Wiley & Sons, New York, pp 587.

Fetter, C.: 1994, *Applied hydrogeology*, Prentice Hall, New Jersy, pp 691.

Fisher, R. F., Binkley, D. and Pritchett, W. L.: 2000, *Ecology and management of forest soils*, John Wiley and Sons, New york, pp 489.

Fornara, D. and Tilman, D.: 2009, Ecological mechanisms associated with the positive diversity-productivity relationship in an N-limited grassland, *Ecology* **90**, 408–418.

Gaston, K. J. and Spicer, J. I.: 2006, *Biodiversity: An introduction*, Blackwell publishing, Oxford, pp 191.

Gaupp, R., Voigt, T. and Lützner, H.: 1998, Stratigraphy and sedimentological evolution of lower and middle Triassic deposits in the SE part of German Triassic basin, *Hallesches Jahrb. Geowiss.* **6**, 99–120.

Gibbs, R.: 1970, Mechanisms controlling world water chemistry, *Science* **170**, 1088–1090.

Gimmi, T. and Waber, H.: 2004, Modeling of tracer profiles in pore water of argillaceous rocks in the benken borehole: Stable water isotopes, chloride and chlorine isotopes, *Technical report 04-05* **6**, 99–120.

Hagdorn, H., Horn, M. and Simon, T.: 1998, Muschelkalk, *Hallesches Jahrb. Geowiss.* **6**, 35–44.

Hales, K. and Neelin, J. D.: 2004, Sensitivity of tropical land climate to leaf area index: Role of surface conductance versus albedo, *American Meteorological Society* **17**, 1459–1473.

He, B. B.: 2009, *Two-dimensional x-ray diffraction*, John Wiley & Sons, New Jersy, pp 426.

Hem, J. D.: 1989, *Study and interpretation of the chemical characteristics of natural water*, U.S. Geological Survey, Water-Supply, Washington D.C., pp 263.

Hooper, D., Chapin-III, F., Ewel, J., Hector, A., Inchausti, P., Lavorel, S., Lawton, J., Lodge, D., Loreau, M., Naeem, S., Schmid, B., Setala, H., Symstad, A., Vandermeer, J. and Wardle, D.: 2005, Effects of biodiversity on ecosystem functioning: A consensus of current knowledge, *Ecological Monographs* **75**, 3–35.

Hooper, D. U. and Vitousek, P. M.: 1998, Effect of plant composition and diversity on nutrient cycling, *Ecological Monographs* **68**, 121–149.

Hornberger, G. M., Raffensperger, J. P., Wiberg, P. L. and Eshleman, K. N.: 1998, *Elements of physical hydrology*, The Johns Hopkins University Press, Baltimore, pp 307.

Houghton, J., Ding, Y., Griggs, D., Noguer, M., van der Linden, P. and Xiaosu, V.: 2001, *Climate Change 2001: The Scientific Basis*, Cambridge University Press, Cambridge, UK, pp 83.

http://ec.europa.eu/environment/soil: 2010, Soil biodiversity: Functions, threats and tools for policy makers-technical report-2010-049. Accessed: 30/09/2011.
URL: *http://ec.europa.eu/environment/soil*

http://www.cbd.int/climate/intro.shtml: 2010, Convention on biological diversity: Climate change and biodiversity. Accessed: 30/09/2011.
URL: *http://www.cbd.int/climate/intro.shtml*

http://www.cbd.int/doc/legal: 1992, Convention on biological diversity. Accessed: 30/08/2011.
URL: *http://www.cbd.int/doc/legal/cbd-en.pdf*

http://www.iaea.org: 2011, Environmental isotopes in the hydrological cycle : Principles and applications. Accessed: 04/11/2011.
URL: *http://www.iaea.org*

Hu, Q. and Wang, J. S.: 2003, Aqueous-phase diffusion in unsaturated geologic media: A review, *Critical Reviews in Environmental Science and Technology* **33**, 275–297.

Jacques, D., Simunek, J., Mallants, D. and van Genuchten, M.: 2008, Modeling coupled hydrologic and chemical processes: Long-term uranium transport following phosphorus fertilization, *Vadose Zone Journal* **7**, 698–711.

Jiang, X. L., Zhang, W. G. and Wang, G.: 2007, Effects of different components of diversity on productivity in artificial plant communities, *Ecological Research* **22**, 629–634.

Kaiser, H.: 1958, The varimax criterion for anhe varimax criterion for analytic rotation in factor analysis, *Psychometmka* **23**, 187–200.

Kaiser, H.: 1959, Computer program for varimax rotation in factor analysis, *Educational and Phycological Measurement* **19**, 413–420.

Kirchner, J. W., Tetzlaff, D. and Soulsby, C.: 2010, Comparing chloride and water isotopes as hydrological tracers in two scottish catchments, *Hydrological Processes* **24**, 1631–1645.

Kirkham, M. B.: 2005, *Principles of soil and plant water relations*, Elsevier academic press, Amsterdam, pp 500.

Kluge, G. and Müller-Westermeier, G.: 2000, *Das Klima ausgewählter Orte der Bundesrepublik Deutschland*, Berichte des Deutschen Wetterdienstes, Jena, pp 213.

Kottek, M., Grieser, J., Beck, C., Rudolf, B. and Rubel, F.: 2006, World map of the Köppen-Geiger climate classification updated, *Meteorologische Zeitschrift* **15**, 259–263.

Kreutziger, Y.: 2006, *Rückkopplungseffekte Verschieden Diverser Grünlandökosysteme Auf Die Komponenten Des Bodenwasserhaushalts An Einem Auestandort Der Saale*, Dissertation, Friedrich-Schiller-Universität Jena, Jena, pp 173.

Langmuir, D.: 1977, *Aqueous environmental geochemistry*, Prentice Hall, New Jersy, pp 600.

Larocque, M., Mangin, A., Razack, M. and Banton, O.: 1998, Contribution of correlation and spectral analyses to the regional study of a large karst aquifer (Charente, France), *Journal of Hydrology* **205**, 217–231.

Larose, D. T.: 2005, *Discovering knowledge in data: an introduction to data mining*, John Wiley & Sons, New Jersy, pp 222.

Lee, J.-Y., Cheon, J.-Y., Lee, K.-K., Lee, S.-Y., and Lee, M.-H.: 2001, Statistical evaluation of geochemical parameter distribution in a ground water system

contaminated with petroleum hydrocarbons, *Joornal of Environmental Quality* **30**, 1548–1563.

Marquard, E., Weigelt, A., Roscher, C., Gubsch, M., Lipowsky, A. and Schmid, B.: 2009, Positive biodiversity-productivity relationship due to increased plant density, *Journal of Ecology* **97**, 696–704.

McCarthy, K. A., McFarland, W. D., Wilkinson, J. M. and White, L. D.: 1992, The dynamic relationship between ground water and the Columbia river: using deuterium and oxygen- 18 as tracers, *Journal of Hydrology* **135**, 1–12.

McGrady-Steed, J., Harris, P. M. and Morin, P. J.: 1997, Biodiversity regulates ecosystem predictability, *Nature* **390**, 162–165.

McLaren, J. R.: 2006, Effects of plant functional groups on vegetation dynamics and ecosystem properties, *Arctic* **59**(449-452).

Mei, R. and Wang, G.: 2010, Rain follows logging in the Amazon? results from CAM3-CLM3, *Climate Dynamics* **34**, 983–996.

Merkel, B., Planer-Friedrich, B. and Nordstrom, D. K.: 2005, *A practical guide to modeling of natural and contaminated aquatic systems*, Springer, Heidelberg, pp 200.

Merten, D. and Büchel, G.: 2004, Determination of rare earth elements in acid mine drainage by inductively coupled plasma mass spectrometry, *Microchimica Acta* **148**, 163–170.

Merten, D., Geletneky, J., Bergmann, H., Haferburg, G., Kothe, E. and Büchel, G.: 2005, Rare earth element patterns: A tool for understanding processes in remediation of acid mine drainage, *Chemie der Erde Geochemistry* **65**, 97–114.

Miller, G. T. and Spoolman, S.: 2009, *Environmental science*, Brooks Cole, Belmont, pp 452.

Mirgorodsky, D.: 2007, *Untersuchung der Grundwasserschwankungen hinsichtlich hydrologischer, hydrogeologischer und vegetationsspezifischer Einflüsse*

auf dem Biodiversitätstestfield (Jena-Experiment), Diplomarbeit, Friedrich-Schiller-Universität Jena, Jena, pp 143.

Momen, B., Eichler, L., Boylen, C. and Zehr, J.: 1996, Application of multivariate statistics in detecting temporal and spatial patterns of water chemistry in lake George, New York, *Ecological modelling* **91**, 183–192.

Morris, M. D., Berk, J. A., Krulik, J. W. and Eckstein, Y.: 1983, A computer program for a trilinear diagram plot and analysis of water mixing systems, *Ground Water* **21**, 67–74.

Nakayama, F., Jackson, R., Kimball, B. and Reginato, R.: 1973, Diurnal soil-water evaporation: Chloride movement and accumulation near the soil surface, *Soil Science Society America Journal* **37**, 509–513.

Neufeldt, H., Resck, D. V. and Ayarza, M. A.: 2002, Texture and land-use effects on soil organic matter in Cerrado Oxisols, Central Brazil, *Geoderma* **107**, 151–164.

Oelmann, Y., Wilcke, W., Temperton, V., Buchmann, N., Roscher, C., Schumacher, J. and Schulze, E.: 2007, Soil and plant nitrogenpools as related to plant diversity in an experimental grassland, *Soil Science Society of America Journal* **71**, 720–729.

Olmez, I., Beal, J. W. and Villaume, J. F.: 1994, A new approach to understanding multiple-source groundwater contamination: factor analysis and chemical mass balances, *Water Research* **28**, 1095–1101.

Pachepsky, Y. and Rawls, W. J.: 2004, *Development of pedotransfer functions in soil hydrology*, Elsevier, Amsterdam, pp 512.

Palmborg, C., Scherer-Lorenzen, M., Jumpponen, A., Carlsson, G., Huss-Danell, K. and Högberg, P.: 2005, Inorganic soil nitrogen under grassland plant communities of different species composition and diversity, *Oikos* **110**, 271–282.

Pankhurst, D. and Appelo, C.: 2009, User's guide to phreeqc (version 2-a computer program for speciation, batch-reaction, one-dimensional transport, and inverse

geochemical calculations, *U.S. Geological Survey and Water Resources Investigations Report* pp. 99–4259.

Pimm, S. L., Russell, G. J., Gittleman, J. L. and Brooks, T. M.: 1995, The future of biodiversity, *Science* **269**, 347–350.

Piper, A.: 1944, A graphic procedure in geochemical interpretation of water analysis, *Trans American Geophysical Union* **25**, 914–928.

Purvis, A. and Hector, A.: 2000, Getting the measure of biodiversity, *Nature* **405**, 212–219.

R-Team: 2009, R: A language and environment for statstical computing. r foundation for statistical computing, vienna. isbn 3-900051-07-0. url http://www.r-project.org.

Rodgers, P., Malcolm, C. S., Gibbins, C. and Dunn, S.: 2004, Groundwater-surface-water interactions in a braided river: A tracer-based assessment, *Hydrological Processes* **18**, 1315–1332.

Roscher, C., Schumacher, J., Baade, J., Wilcke, W., Gleixner, G., Weisser, W., Schmid, B. and Schulze, E.: 2004, The role of biodiversity for element cycling and trophic interactions: an experimental approach in a grassland community, *Basic and Applied Ecology* **5**, 107–121.

Rowell, D., Martin, M. and Nye, P.: 1967, The measurement and mechanism of ion diffusion in soils. iii. the effect of moisture content and soil-solution concentration on the self-diffusion of ions in soils, *Journal of Soil Science* **18**, 204–222.

Scanlon, B. R.: 1991, Evaluation of moisture flux from chloride data in desert soils, *Journal of Hydrology* **128**, 137–156.

Schaetzl, R. J. and Anderson, S.: 2005, *Soils: genesis and geomorphology*, Cambridge University Press, Cambridge, pp 817.

Seidel, G.: 2003, *Geologie von Thüringen*, E. Schweizerbart'sche Verlagsbuchhandlung, Stuttgart, pp 601.

Shahid, N., Thompson, L. J., Lawler, S. P., Lawton, J. H. and Woodfin, R. M.: 1994, Declining biodiversity can alter the performance of ecosystems, *Nature* **368**, 734–737.

Sharif, M., Davis, R., Steele, K., Kim, B., Hays, P., Kresse, T. and Fazio, J.: 2008, Distribution and variability of redox zones controlling spatial variability of arsenic in the Mississippi river valley alluvial aquifer, Southeastern Arkansas, *Journal of Contaminant Hydrology* **99**, 49–67.

Simpson, E.: 1949, Measurment of diversity, *Nature* **163**, 688.

Smith, E. B.: 2004, *Basic chemical thermodynamics*, Imperial College Press, London, pp 166.

Spehn, E. M., Joshi, J., Schmid, B., Diemer, M. and Körner, C.: 2000, Aboveground resource use increases with plant species richness in experimental grassland ecosystems, *Functional Ecology* **14**, 326–337.

Steinbeiss, S.: 2006, *Einfluss der Biodiversität von Pflanzen auf die Speicherung von Kohlenstoff in Böden und auf den Austrag von gelöstem organischem Kohlenstoff*, Dissertation, Friedrich-Schiller-Universität Jena, Jena.

Steinbeiss, S., Temperton, V. and Gleixner, G.: 2008, Mechanisms of short-term soil carbon storage in experimental grasslands, *Soil Biology and Biochemistry* **40**, 2634–2642.

Stumm, W. and Morgan, J.: 1994, *Aquatic chemistry, chemical equilibria and rates in natural waters*, John Wiley & Sons, Inc., New York, pp 1022.

Suk, H. and Lee, K.-K.: 1999, Characterization of groundwater hydrochemical system through multivariate analysis: clustering in to ground water zones, *Groundwater* **37**, 358–366.

Tilman, D. and Downing, J. A.: 1994, Biodiversity and stability in grasslands, *Nature* **367**, 363–365.

Tilman, D., Knops, J., Wedin, D., Reich, P., Ritchie, M. and Siemann, E.: 1997, The influence of functional diversity and composition on ecosystem processes, *Science* **297**, 1300–1302.

Tilman, D. and Wedin, D.: 1991, Dynamics of nitrogen competition between successional grasses, *Ecology* **72**, 1038–1049.

Troeh, F. R. and Thompson, L. M.: 2005, *Soils and soil fertility*, Wiley-Blackwell, USA, pp 489.

Tromans, D.: 1998, Temperature and pressure dependent solubility of oxygen in water: A thermodynamic analysis, *Hydrometallurgy* **48**, 327–342.

Tsuji, G. Y., Hoogenboom, G. and Thornton, P.: 1998, *Understanding options for agricultural production*, Kluwer Academic publishers, Wageningen, pp 403.

van Genuchten, M. T.: 1980, A closed-form equation for predicting the hydraulic conductivity of unsaturated soils, *Soil Science Society America Journal* **44**, 892–898.

Voigt, H.-J., Hannappel, S., Kunkel, R. and Waendland, F.: 2005, Assessment of natural groundwater concentrations of hydrogeological structures in Germany, *GEOLOGIJA* (50), 35–47.

von Alberti, F.: 1834, *Beitrag zu einer Monographie des bunten Sandsteins, Muschelkalks und Keupers und die Verbindung dieser Gebilde zu einer Formation*, Verlag der J. G. COTTA'schen Buchhandung, Stutgart and Tübingen, pp 366.

Walker, W.: 1989, *Guidelines for designing and evaluatin surface irrigation systems*, FAO irrigation and drainage paper, Number 45, Rome.

Weigelt, A., Marquard, E., Temperton, V. M., Roscher, C., Scherber, C., Mwangi, P. N., von Felten, S., Buchmann, N., Schmid, B., Schulze, E.-D. and Weisser, W. W.: 2009, The jena-experiment: 6 years of data from a grassland biodiversity experiment including species-specific plant biomass, species-specific plant cover, community lai and community height, *Ecological Archives* .

White, P. J. and Broadley, M. R.: 2001, Chloride in soils and its uptake and movement within the plant: A review, *Annals of Botany* **88**, 967–988.

Williams, M. L., Walter, L. M., Ku, T. C., Kling, G. W. and Zak, D. R.: 2003, Effects of co2 and nutrient availability on mineral weathering in controlled tree growth experiments, *Global biogeochemical cycles* **17**, 1–12.

Winter, T. C., Harvey, J. W., Franke, O. and Alley, W. M.: 1998, *Ground water and surface water a single resource*, U.S. Geological Survey, Denver, Colorado, pp 79.

Yerima, B. P. K. and Ranst, E. V.: 2005, *Introduction to Soil Science: Soils of the Tropics*, Trafford Publishing, Victoria, BC, Canada, pp 440.

Younger, P. L.: 2008, *Groundwater in the environment: An introduction*, Blackwell publishing, UK, pp 318.

Zedler, J. B., Callaway, J. C. and Sullivan, G.: 2001, Declining biodiversity: Why species matter and how their functions might be restored in Californian Tidal Marshes, *Bioscience* **51**, 143–176.

Zeng, X. and Todd, C.: 2005, Multivariate statistical characterization of water quality in lake Lanier, Georgia, USA, *Journal of Environmental Quality* **34**, 1980–1991.

Zerling, L., Hanisch, C., Junge, F. W. and Müller, A.: 2003, Heavy metals in Saale sediments - changes in the contamination since 1991, *Acta Hydrochimica et Hydrobiologica* **31**, 368–377.

Zoski, K. W. and Jurs, S.: 1996, An objective counterpart to the visual scree test for factor analysis: The standard error scree, *Educational and Psychological Measurement* **56**, 443–451.

Zuur, A. F., Ieno, E. N. and Elphick, C. S.: 2010, A protocol for data exploration to avoid common statistical problems, *Methods in Ecology and Evolution* **1**, 3–14.

Appendix A

Measured data

Table A.1 Groundwater chemical analysis of August-2008

Parameter	Unit	B1A14	B2A03	B2A13	B2A16	B3A02	B3A13	B3A16	B4A02	B4A05
T	[°C]	18.7	20.7	19.8	18.2	19.5	18.9	20.1	19.4	19.0
LF	[μS/cm]	1666	1589	1605	1643	1246	1541	1634	1594	1604
pH		7.02	7.09	7.02	7.06	7.21	7.06	7.06	7.02	6.98
UH	[mV]	120	450	470	250	340	350	130	470	450
O2	[mg/L]	2.5	4.1	3.6	2.9	3.6	3.2	3.0	2.8	2.7
O2	[%]	26	45	39	31	38	34	33	30	28
Al (MS)	[μg/L]	<1	<1	<1	<1	2.8	<1	<1	<1	<1
Al SD	[μg/L]					0.3				
As (MS)	[μg/L]	3.3	0.32	0.34	3.1	2.49	1	2.4	0.4	0.9
As SD	[μg/L]	0.1	0.04	0.05	0.1	0.02	0.1	0.2	0.1	0.1
B (MS)	[μg/L]	339	319	344	298	86	274	262	328	328
B SD	[μg/L]	3	3	3	1	2	2	2	1	2
Ba (MS)	[μg/L]	134	103	112	95	161	105	114.5	109	120.4
Ba SD	[μg/L]	0.5	1	1	1	1	1	0.1	1	0.4
Ca (OES)	[mg/L]	268	262	265	271	243	257	279	270	281
SD Ca	[mg/L]	1	2	2	7	3	2	2	4	5
Cd (MS)	[μg/L]	<0,1	<0,1	<0,1	<0,1	<0,1	<0,1	<0,1	<0,1	<0,1
Cd SD	[μg/L]									
Ce (MS)	[μg/L]	0.021	0.054	0.129	0.076	0.159	0.112	0.035	0.042	0.06
Ce SD	[μg/L]	0.003	0.005	0.004	0.005	0.004	0.003	0.001	0.002	0.003
Co (MS)	[μg/L]	1.79	0.83	1.64	1.76	1.14	1.93	1.56	0.99	1.43
Co SD	[μg/L]	0.01	0.02	0.03	0.04	0.02	0.06	0.03	0.04	0.03
Cr (MS)	[μg/L]	<0,5	<0,5	<0,5	<0,5	<0,5	<0,5	<0,5	<0,5	<0,5
Cr SD	[μg/L]									
Cs (MS)	[μg/L]	<0,05	<0,05	<0,05	<0,05	<0,05	<0,05	<0,05	<0,05	<0,05
Cs SD	[μg/L]									
Cu (MS)	[μg/L]	0.3	0.4	0.7	0.3	0.38	<0,2	<0,2	0.6	0.5

Cu SD	[µg/L]	0.1	0.1	0.1	0.1	0.01			0.1	0.1
Dy (MS)	[µg/L]	<0,01	0.01	0.013	0.014	0.021	0.017	¡ 0,01	¡ 0,01	¡ 0,01
Dy SD	[µg/L]		0.002	0.002	0.002	0.003	0.002			
Er (MS)	[µg/L]	<0,01	<0,01	<0,01	0.01	0.015	0.013	<0,01	<0,01	<0,01
Er SD	[µg/L]				0.003	0.002	0.001			
Eu (MS)	[µg/L]	<0,01	<0,01	<0,01	<0,01	<0,01	<0,01	<0,01	<0,01	<0,01
Eu SD	[µg/L]									
Fe (MS)	[µg/L]	382	4.3	7	493	184	28.2	277	4.8	5.7
Fe SD	[µg/L]	3	0.2	1	3	3	0.4	4	0.2	0.4
Gd (MS)	[µg/L]	<0,01	0.011	0.014	0.015	0.024	0.019	0.011	<0,01	<0,01
Gd SD	[µg/L]		0.002	0.004	0.003	0.003	0.004	0.001		
Ho (MS)	[µg/L]	<0,01	<0,01	<0,01	<0,01	<0,01	<0,01	<0,01	<0,01	<0,01
Ho SD	[µg/L]									
K (OES)	[mg/L]	6.1	6.1	5.45	5.1	0.71	5.2	4.9	5.9	6.7
SD K	[mg/L]	0.1	0.1	0.05	0.1	0.04	0.2	0.1	0.2	0.1
La (MS)	[µg/L]	<0,01	0.025	0.073	0.04	0.06	0.052	0.013	0.016	0.028
La SD	[µg/L]		0.001	0.003	0.002	0.01	0.002	0.001	0.003	0.003
Li (MS)	[µg/L]	19.4	22.9	21.6	16.6	2.5	20	10.4	21.6	19.4
Li SD	[µg/L]	0.1	0.2	0.2	0.1	0.1	0.1	0.1	0.3	0.1
Lu (MS)	[µg/L]	<0,01	<0,01	<0,01	<0,01	<0,01	<0,01	<0,01	<0,01	<0,01
Lu SD	[µg/L]									
Mg (OES)	[mg/L]	41.1	40.1	38.7	41	27	39	41.1	42	44
SD Mg	[mg/L]	0.2	0.3	0.3	1	0.4	0.5	0.3	1	1
Mn (OES)	[mg/L]	1.51	0.98	1.49	1.28	0.96	1.12	1.26	0.449	0.62
SD Mn	[mg/L]	0.01	0.01	0.01	0.04	0.01	0.02	0.02	0.005	0.004
Na (OES)	[mg/L]	56.6	51.7	55	53	18.8	48.6	50.8	55.9	55.7
SD Na	[mg/L]	0.1	0.4	0.3	1	0.1	0.4	0.5	0.6	0.4
Nd (MS)	[µg/L]	<0,01	0.035	0.06	0.05	0.1	0.07	0.025	0.029	0.037
Nd SD	[µg/L]		0.003	0.01	0.01	0.01	0.01	0.001	0.003	0.006
Ni (MS)	[µg/L]	4.3	4.8	4.9	4.7	2.9	4.8	6.1	3.7	3.8
Ni SD	[µg/L]	0.1	0.1	0.1	0.1	0.1	0.1	0.2	0.1	0.1
P (OES)	[mg/L]	0.23	0.06	0.07	0.08	<0,05	0.08	0.29	0.11	0.18
SD P	[mg/L]	0.01	0.01	0.02	0.01		0.04	0.03	0.02	0.02
Pb (MS)	[µg/L]	<0,1	<0,1	<0,1	<0,1	<0,1	<0,1	<0,1	<0,1	<0,1
Pb SD	[µg/L]									
Pr (MS)	[µg/L]	<0,01	<0,01	0.013	0.013	0.018	0.013	<0,01	<0,01	<0,01
Pr SD	[µg/L]			0.001	0.006	0.001	0			
S (OES)	[mg/L]	144	142	146	146	72.6	126	134	140	139
SD S	[mg/L]	2	3	2	1	0.3	1	2	0.6	3
Si (OES)	[mg/L]	5.38	5.47	5.5	5	5.29	5.21	4.72	5.1	5.21
SD Si	[mg/L]	0.003	0.04	0.1	0.1	0.06	0.02	0.03	0.1	0.03
Sm (MS)	[µg/L]	<0,01	<0,01	0.01	0.011	0.02	0.012	<0,01	<0,01	<0,01
Sm SD	[µg/L]			0.004	0.003	0.004	0.005			
Sr (OES)	[mg/L]	3.06	3.12	2.94	2.9	0.99	2.8	2.52	3.26	3.2

SD Sr	[mg/L]	0.03	0.01	0.01	0.1	0.01	0.05	0.03	0.03	0.05
Tb (MS)	[µg/L]	<0,01	<0,01	<0,01	<0,01	<0,01	<0,01	<0,01	<0,01	<0,01
Tb SD	[µg/L]									
Th (MS)	[µg/L]	<0,1	<0,1	<0,1	<0,1	<0,1	<0,1	<0,1	<0,1	<0,1
Th SD	[µg/L]									
Ti (MS)	[µg/L]	<1	<1	<1	<1	<1	<1	<1	<1	<1
Ti SD	[µg/L]									
Tm (MS)	[µg/L]	<0,01	<0,01	<0,01	<0,01	<0,01	<0,01	<0,01	<0,01	<0,01
Tm SD	[µg/L]									
U (MS)	[µg/L]	12.5	9.4	9.24	12.1	11.2	9.51	8.8	9.8	10.65
U SD	[µg/L]	0.1	0.03	0.01	0.1	0.05	0.04	0.1	0.1	0.06
V (MS)	[µg/L]	1.35	0.91	0.91	1.2	1.93	1.07	1.03	0.95	0.99
V SD	[µg/L]	0.02	0.04	0.01	0.4	0.04	0.08	0.05	0.04	0.05
Y (MS)	[µg/L]	0.07	0.1	0.104	0.14	0.18	0.13	0.076	0.065	0.09
Y SD	[µg/L]	0.01	0.01	0.004	0	0.01	0.01	0.004	0.002	0.01
Yb (MS)	[µg/L]	<0,01	<0,01	<0,01	<0,01	0.013	0.01	<0,01	<0,01	<0,01
Yb SD	[µg/L]					0.002	0.002			
Zn (MS)	[µg/L]	9.6	26.7	73	26.3	63	17.4	3.5	73	85.6
Zn SD	[µg/L]	0.1	0.4	1	0.4	1	0.3	0.2	1	0.4
Fluorid	[mg/L]	<0,40	<0,40	<0,40	<0,40	<0,40	<0,40	<0,40	<0,40	<0,40
SD Fluorid	[mg/L]									
Chlorid	[mg/L]	86.2	78.5	82.2	87.9	1.63	78.8	79.3	91.7	87.2
SD Chlorid	[mg/L]	0.4	0.2	0.1	0.1	0.1	0.1	0.1	0.1	0.1
Sulfat	[mg/L]	414	414	427	429	206	364	401	401	394
SD Sulfat	[mg/L]	1	1	1	1	1	1	1	1	1
Nitrat	[mg/L]	3.7	16.1	17.8	1.0	0.13	7.2	1.0	8.9	21.6
SD Nitrat	[mg/L]	0.1	0.1	0.1	0.1	0.01	0.1	0.1	0.1	0.1
NO3 (Fotometer)	[mg/L]	6	18	19	2	1	9	2	10	23
Nitrit (Fotometer)	[mg/L]	0.185	0.116	0.233	<0,02	<0,02	0.234	0.069	0.135	0.141
Phosphat (Fotometer)	[mg/L]	0.54	<0,05	0.07	0.06	0.06	0.06	0.67	0.08	0.37
Ammonium (Fotometer)	[mg/L]	3.78	<0,05	0.127	0.434	0.326	0.138	2.15	<0,05	0.108
HCO3 (Titration)	[mg/L]	520.7	481	474.5	505.1	649.5	509.5	569.4	498.2	498.4
Haerte (berechnet)	[mmol/L]	8.38	8.19	8.20	8.45	7.17	8.02	8.65	8.46	8.82
DOC	[mg/L]	5.1	2.40	0.9	2.1	4.1	0.8	2.8	2.6	2.7
SD DOC	[mg/L]	0.1	0.03	0.2	0.1	0.3	0.2	0.1	0.2	0.1

Table A.2 Groundwater chemical analysis of March-2009

Parameter	Unit	B1A04E	B1A04W	B1A14E	B1A14W	B1A17E	B2A03E	B2A03W	B2A13W	B2A16E	B3A02W	B3A05E	B3A13	B3A16E	B4A02	B4A05
T	[°C]	6.3	6.6	6.5	6.3	6.3	6.6	6.7	7.1	6.6	6.5	6.7	6.6	6.2	6.3	6.8
LF	[μ S/cm]	1504	1545	1640	1616	1614	1663	1653	1615	1531	1250	1421	1444	1588	1600	1626
pH		7.08	7.15	7.04	7.02	7.17	6.97	6.98	6.95	6.96	7.17	7.41	7.06	7.06	7.01	7.06
UH	[mV]	430	390	480	440	470	450	480	440	280	270	400	430	250	380	340
O2	[mg/L]	4.0	5.4	3.7	3.1	8.8	3.1	3.1	2.8	4.7	3.4	8.1	4.0	5.7	5.9	5.9
O2	[]	34	46	31	26	74	26	26	24	40	29	68	33	41	50	50
Al (MS)	[μg/L]	< 1,2	< 1,2	< 1,2	< 1,2	< 1,2	< 1,2	< 1,2	< 1,2	< 1,2	< 1,2	< 1,2	< 1,2	< 1,2	< 1,2	< 1,2
Al SD	[μg/L]															
As (MS)	[μg/L]	< 1	2	< 1	< 1	< 1	<1	< 1	< 1	1.5	< 1	< 1	< 1	1.4	< 1	< 1
As SD	[μg/L]		0.3							0.2				0.3		
B (MS)	[μg/L]	152	113	233	221	185	264	305	272	241	68	21.5	164	176.2	251	266
B SD	[μg/L]	2	1	1	1	3	4	7	4	2	1	0.2	3	0.3	2	1
Ba (MS)	[μg/L]	73.3	68	65.4	101.2	76.7	83	74	83	72.6	129	53	136	108	74.6	80
Ba SD	[μg/L]	0.6	4	0.3	0.8	0.7	1	1	2	0.2	1	1	1	3	0.3	0.3
Ca (OES)	[mg/L]	259	272	264	268	281	269	257	255	247	229	257	235.5	271	261	262
SD Ca	[mg/L]	3	1	2	2	2	2	1	0.1	1	1	2	0.3	6	4	1
Cd (MS)	[μg/L]	< 0,1	< 0,1	0.13	0.149	< 0,1	0.123	0.21	0.2	< 0,1	< 0,1	< 0,1	< 0,1	< 0,1	< 0,1	< 0,1
Cd SD	[μg/L]			0.03	0.004		0.003	0.04	0.01							
Co (MS)	[μg/L]	0.451	2.09	0.56	0.26	0.16	0.629	0.336	0.71	1.52	1.64	0.49	0.56	1.63	0.462	0.65
Co SD	[μg/L]	0.002	0.06	0.05	0.03	0.02	0.002	0.003	0.02	0.09	0.05	0.02	0.01	0.01	0.002	0.04
Cr (MS)	[μg/L]	< 0,2	< 0,2	< 0,2	< 0,2	0.21	< 0,2	< 0,2	< 0,2	< 0,2	< 0,2	< 0,2	< 0,2	0.6	< 0,2	< 0,2
Cr SD	[μg/L]					0.01								0.1		
Cs (MS)	[μg/L]	< 0,2	< 0,2	< 0,2	< 0,2	< 0,2	< 0,2	< 0,2	< 0,2	< 0,2	< 0,2	< 0,2	< 0,2	< 0,2	< 0,2	< 0,2
Cs SD	[μg/L]															
Cu (MS)	[μg/L]	1.1	0.62	0.8	1	0.78	1.01	1.2	1	0.6	0.38	1.7	1.3	0.54	0.79	1

Cu SD	[μg/L]	0.1	0.02	0.1	0.1	0.01	0.04	0.1	0.1	0.1	0.01	0.1	0.1	0.02	0.02	0.1
Fe (MS)	[μg/L]	3.6	391	0.7	< 0,6	< 0,6	1.9	1	< 0,6	465.6	398.9	1.9	< 0,6	839	2.1	4.8
Fe SD	[μg/L]	0.2	4	0.2			0.5	0.2		2.3	0.8	0.1		6	0.5	0.2
K (OES)	[mg/L]	1	1.01	3.6	3.2	2.1	4.67	5.69	5.2	4.6	0.65	0.27	3.05	3.07	5.34	5.1
SD K	[mg/L]	0.1	0.06	0.1	0.1	0.1	0.03	0.03	0.1	0.1	0.04	0.06	0.03	0.05	0.06	0.1
Li (MS)	[μg/L]	5	5.35	14.2	11.8	9.1	16.3	22.9	20.4	13.7	4.6	1.85	11.5	9.4	19.8	19.9
Li SD	[μg/L]	0.1	0.04	0.1	0.2	0.1	0.1	0.4	0.2	0.1	0.2	0.02	0.2	0.2	0.1	0.2
Mg (OES)	[mg/L]	32.5	32.5	39	38.9	38	41	41.3	40.7	38.3	28.4	30.9	34.63	40.3	41	41
SD Mg	[mg/L]	0.4	0.4	0.1	0.1	1	0.5	0.2	0.3	0.4	0.1	0.4	0.05	0.4	0.2	1
Mn (MS)	[μg/L]	129.6	743	652	782	1.01	2373	666	1388	1249	548	70.6	464.5	1278	313	395
Mn SD	[μg/L]	0.1	3	1	5	0.04	10	9	4	13	2	0.3	0.6	3	3	2
Na (OES)	[mg/L]	43	40.8	53	50.4	48	54	58.2	55.2	48	22.84	37.6	42.8	46.3	51.2	52.7
SD Na	[mg/L]	0.3	0.5	0.2	0.3	1	1	0.3	0.2	1	0.04	0.5	0.3	0.2	0.6	0.5
Ni (MS)	[μg/L]	3.7	3.1	3.658	4.1	2.11	4.17	3.8	4.5	3.4	3.5	2.6	3.5	5.8	3.3	3.52
Ni SD	[μg/L]	0.2	0.1	0.002	0.2	0.01	0.02	0.1	0.2	0.2	0.3	0.2	0.3	0.2	0.2	0.05
P (OES)	[mg/L]	0.082	¡ 0,04	0.05	0.05	¡ 0,04	0.097	0.065	¡ 0,04	0.34	0.06	¡ 0,04	0.07	0.22	0.11	0.08
SD P	[mg/L]	0.003		0.01	0.02		0.006	0.005		0.01	0.01		0.03	0.02	0.02	0.01
Pb (MS)	[μg/L]	< 0,1	< 0,1	< 0,1	< 0,1	< 0,1	< 0,1	< 0,1	< 0,1	< 0,1	< 0,1	< 0,1	< 0,1	< 0,1	< 0,1	< 0,1
Pb SD	[μg/L]															
S (OES)	[mg/L]	131	132	148.4	141	144	156	152	148.9	133	59.3	137	116	130	140	140
SD S	[mg/L]	1	1	0.4	1	5	1	1	0.4	1	0.2	1	1	1	2	1
Si (OES)	[mg/L]	4.91	4.54	4.83	4.77	4.7	5.15	5.18	4.97	4.6	4.38	3.42	4.36	4.28	4.9	4.71
SD Si	[mg/L]	0.03	0.06	0.01	0.01	0.1	0.05	0.05	0.01	0.1	0.04	0.05	0.03	0.04	0.02	0.04
Sr (MS)	[μg/L]	1538	1691	2766	2576	2335	3061	3312	3175	2707	1434	1299	2199	2634	3203	3291
Sr SD	[μg/L]	3	20	17	7	24	15	14	35	9	11	16	4	17	21	23
Ti (MS)	[μg/L]	< 1	< 1	< 1	< 1	< 1	< 1	< 1	< 1	1.1	< 1	< 1	< 1	< 1	< 1	< 1
Ti SD	[μg/L]									0.2						
U (MS)	[μg/L]	8.2	10.7	10.3	9.8	9.7	8.4	8.1	8.27	8.7	11.8	9.2	7.8	8.1	8.2	8.73

U SD	[µg/L]	0.1	0.1	0.1	0.1	0.1	0.1	0.1	0.02	0.1	0.1	0.1	0.1	0.1	0.1	0.01
V (MS)	[µg/L]	< 0,5	< 0,5	< 0,5	< 0,5	< 0,5	¡ 0,5	< 0,5	< 0,5	< 0,5	< 0,5	< 0,5	< 0,5	< 0,5	< 0,5	< 0,5
V SD	[µg/L]															
Y (MS)	[µg/L]	0.05	0.07	0.08	0.101	0.06	0.07	0.081	0.09	0.09	0.13	0.06	0.09	0.08	¡ 0,05	0.07
Y SD	[µg/L]	0.01	0.01	0.01	0.004	0.002	0.01	0.005	0.01	0.01	0.01	0.01	0.01	0.01		0.01
Yb (MS)	[µg/L]	< 0,05	< 0,05	< 0,05	< 0,05	< 0,05	< 0,05	< 0,05	< 0,05	< 0,05	< 0,05	< 0,05	< 0,05	< 0,05	< 0,05	< 0,05
Yb SD	[µg/L]															
Zn (MS)	[µg/L]	41.2	38.9	42.1	42.8	37.6	40	43	44.2	35	31.6	39.6	55.1	38	8.4	43.2
Zn SD	[µg/L]	0.5	0.5	0.1	0.3	0.6	1	0.6	0.9	1	0.8	0.1	0.6	2	0.1	0.2
F (IC)	[mg/L]	< 0,4	< 0,4	< 0,4	< 0,4	< 0,4	< 0,4	< 0,4	< 0,4	< 0,4	< 0,15	< 0,4	< 0,4	< 0,4	< 0,4	< 0,4
SD F	[mg/L]															
Cl (IC)	[mg/L]	64.8	60.4	85.1	76.3	79.1	88	89.4	81.7	80	18.2	23.3	62.4	72.7	88.5	89.3
SD Cl	[mg/L]	0.1	0.1	0.1	0.1	0.1	0.1	0.1	0.1	0.1	0.1	0.1	0.1	0.2	0.1	0.1
SO_4 (IC)	[mg/L]	382	384	431	407	410	447	437	429	381	171	400	332	386	399	411
SD SO_4	[mg/L]	1	1	1	1	1	1	1	1	1	1	1	1	1	1	1
NO_3 (IC)	[mg/L]	3.2	0.5	6.4	5.1	1.1	7.7	19.6	11.5	0.78	0.29	< 0,4	5.4	0.76	12.8	16
SD NO_3	[mg/L]	0.1	0.04	0.1	0.1	0.1	0.1	0.2	0.1	0.02	0.02		0.1	0.07	0.1	0.1
Nitrit (FM)	[mg/L]	0.058	< 0,02	0.207	0.021	¡ 0,02	0.114	0.061	0.095	0.103	< 0,02	< 0,02	0.073	0.113	0.055	0.06
PO_4 (FM)	[mg/L]	0.19	0.06	0.13	0.07	< 0,05	0.34	0.11	0.05	0.82	< 0,05	< 0,05	0.11	0.57	0.27	0.20
Ammonium (FM)	[mg/L]	0.218	0.253	0.195	0.07	< 0,05	0.539	0.059	0.08	1.223	0.29	< 0,05	0.079	0.739	< 0,05	< 0,05
HCO3 (Titration)	[mg/L]	477.7	528.0	470.1	507.2	500.2	463.1	447.3	462.9	466.4	672.2	491.1	486.1	527.3	455.2	467.5
Härte (berechnet)	[mmol/L]	7.80	8.12	8.19	8.29	8.57	8.40	8.11	8.04	7.74	6.88	7.68	7.30	8.42	8.20	8.22
	[°dH]	43.7	45.6	45.9	46.5	48.1	47.1	45.5	45.1	43.4	38.6	43.1	40.9	47.2	46.0	46.1
DOC	[mg/L]	4	3.1	3.1	3.7	3.7	3.2	3.3	4	4.5	4.9	6.1	4.7	4.2	4.3	4.33
SD DOC	[mg/L]	0.1	0.1	0.1	0.2	0.1	0.1	0.1	0.1	0.1	0.1	0.1	0.2	0.2	0.4	0.01

Table A.3 Groundwater chemical analysis of June-2009

Parameter	Unit	B3A16E	B2A16E	B1A04E	B1A14E	B1A14W	B2A03E	B2A03W	B2A13E	B3A02E	B3A02W	B3A13E	B3A13W	B4A02	B4A05
T	[°C]	12.8	12.9	14.4	14.1	14.2	13.7	13.5	13.1	13.9	13.4	12.9	13.8	13.3	13.9
LF	[μS/cm]	1455	1637	1463	1583	1448	1621	1527	1671	1079	1025	1075	1488	1602	1381
pH		7.17	7.10	7.27	7.20	7.13	7.08	7.05	7.04	7.20	7.15	7.18	7.07	7.02	7.11
UH	[mV]	70	50	120	300	460	390	270	440	290	260	280	480	450	450
O2	[mg/L]	4.7	3.6	3.7	3.8	3.6	3.5	3.0	3.6	3.5	3.8	3.5	4.2	3.4	3.3
O2	[%]	41	33	37	36	36	35	29	35	34	37	34	41	32	32
Al (MS)	[μg/L]	6	4	6.4	7	8	8	6	6	12	5	11	12	18	17.4
Al SD	[μg/L]	1	2	0.1	1	1	2	4	2	3	2	3	2	3	0.2
As (MS)	[μg/L]	1	1.5	4.2	0.9	<0,8	<0,8	<0,8	<0,8	1.7	1.6	1.0	<0,8	<0,8	<0,8
As SD	[μg/L]	0.4	0.4	0.4	0.3					0.5	0.5	0.3			
B (OES)	[mg/L]	0.158	0.25	0.137	0.259	0.181	0.24	0.256	0.344	0.025	0.053	0.068	0.295	0.283	0.195
SD B	[mg/L]	0.003	0.01	0.002	0.006	0.002	0.01	0.004	0.003	0.005	0.004	0.002	0.006	0.003	0.006
Ba (MS)	[μg/L]	117.4	90.3	129	74.8	64	94	69.7	101	89	96	121.9	144	82.5	109
Ba SD	[μg/L]	0.2	0.2	2	0.1	1	1	0.2	2	1	1	0.2	1	0.5	1
Ca (OES)	[mg/L]	265	301	303	300	267	306	285	297	228	207	220	261	277	241
SD Ca	[mg/L]	6	16	3	2	10	4	7	4	2	6	2	3	2	3
Ca (AAS)	[mg/L]	230	268	255	263	244	272	247	271	203	189	196	246	261	231
Cd (MS)	[μg/L]	<0,2	<0,2	<0,2	<0,2	<0,2	<0,2	<0,2	<0,2	<0,2	<0,2	<0,2	<0,2	<0,2	<0,2
Cd SD	[μg/L]														
Co (MS)	[μg/L]	<1	<1	<1	<1	<1	1.5	<1	1.00	<1	<1	<1	<1	<1	<1
Co SD	[μg/L]						0.1		0.01						
Cr (MS)	[μg/L]	<0,4	<0,4	<0,4	0.74	<0,4	<0,4	0.8	<0,4	<0,4	<0,4	<0,4	<0,4	<0,4	<0,4
Cr SD	[μg/L]				0.03			0.1							
Cs (MS)	[μg/L]	<0,1	<0,1	<0,1	<0,1	<0,1	<0,1	<0,1	<0,1	<0,1	<0,1	<0,1	<0,1	<0,1	<0,1
Cs SD	[μg/L]														
Cu (MS)	[μg/L]	<0,4	<0,4	<0,4	0.64	0.7	0.43	0.5	0.79	<0,4	<0,4	<0,4	0.91	0.68	0.7

Cu SD	[µg/L]				0.04	0.1	0.04	0.1	0.03				0.02	0.04	0.1
Fe (MS)	[µg/L]	784	435	146.3	25	27	40	19	13	321	402	278	19	38	49
Fe SD	[µg/L]	5	7	0.4	1	1	2	1	1	6	6	2	1	1	1
K (OES)	[mg/L]	1.5	4.7	1.2	3.53	3.23	4.5	4.76	6.2	0.37	0.68	0.8	3.95	6.0	1.99
SD K	[mg/L]	0.3	0.1	0.2	0.03	0.05	0.1	0.03	0.2	0.06	0.01	0.05	0.04	0.2	0.05
Li (MS)	[µg/L]	5.88	14.98	4.66	14.0	11.83	16.3	16.2	22.6	1.89	3.90	5.74	15.9	21.3	9.0
Li SD	[µg/L]	0.03	0.02	0.02	0.2	0.04	0.2	0.1	0.1	0.05	0.04	0.04	0.2	0.3	0.2
Mg (OES)	[mg/L]	37.9	46	35.7	44	36	45	41	47	24.6	23.56	25.0	38	43.0	34.8
SD Mg	[mg/L]	0.5	1	0.1	1	1	1	1	1	0.2	0.05	0.4	1	0.2	0.5
Mn (MS)	[µg/L]	859	1281	402	1270	886	2887	2709	1183	637	340	737	1069	415	350
Mn SD	[µg/L]	5	5	1	5	6	21	5	9	3	1	6	5	7	1
Na (OES)	[mg/L]	38	47.8	40.6	48.8	41.6	46	44	55.9	16.6	15.9	20.0	46.5	56	33.3
SD Na	[mg/L]	1	0.5	0.3	0.4	0.3	1	1	0.3	0.3	0.2	0.1	0.6	1	0.1
Ni (MS)	[µg/L]	2.9	2.2	1.6	2.3	3.6	3.3	5.6	4.3	2.2	1.1	1.9	4.5	3.3	2.2
Ni SD	[µg/L]	0.3	0.4	0.3	0.5	0.3	0.2	0.7	0.5	0.3	0.4	0.1	0.7	0.5	0.5
P (OES)	[mg/L]	0.16	0.22	0.237	0.09	<0,05	0.07	0.17	<0,05	<0,05	<0,05	<0,05	<0,05	<0,05	<0,05
SD P	[mg/L]	0.01	0.02	0.004	0.01		0.01	0.02							
S (OES)	[mg/L]	106	151	136	144.4	120	155	130	162	60.1	36.4	47	126	147	86
SD S	[mg/L]	2	2	1	0.5	2	3	2	1	0.6	0.3	1	2	3	1
Si (OES)	[mg/L]	4.7	5.0	5.32	5.7	5.0	5.5	5.5	5.5	5.1	4.67	4.92	4.8	5.02	4.93
SD Si	[mg/L]	0.1	0.1	0.03	0.1	0.1	0.1	0.1	0.1	0.1	0.01	0.05	0.1	0.03	0.05
Sr (MS)	[µg/L]	2159	3097	1657	2871	2439	3297	2946	3628	865	1226	1238	2765	3543	2395
Sr SD	[µg/L]	9	16	14	11	2	8	19	21	5	7	8	17	15	11
Ti (MS)	[µg/L]	1.1	1.0	1.7	0.9	0.81	0.9	1.3	1.0	0.7	0.8	0.7	0.7	1	1.2
Ti SD	[µg/L]	0.1	0.3	0.3	0.2	0.03	0.1	0.3	0.1	0.1	0.2	0.3	0.1	0.3	0.1
U (MS)	[µg/L]	6.9	9.8	10.82	9.9	10.0	9.24	8.58	8.9	9.0	9.37	8.0	8.2	9.1	10.6
U SD	[µg/L]	0.1	0.1	0.00	0.2	0.1	0.02	0.03	0.2	0.1	0.03	0.2	0.1	0.1	0.2
V (MS)	[µg/L]	<0,2	0.50	2.16	<0,2	<0,2	<0,2	<0,2	<0,2	0.59	0.2	0.2	<0,2	<0,2	<0,2

V SD	[μg/L]		0.01	0.03						0.02	0.1	0.1			
Zn (MS)	[μg/L]	25.2	7.8	8.7	18.4	13.3	13.6	15.8	11.83	28.0	10.3	49.1	55.0	14.2	35.6
Zn SD	[μg/L]	0.2	0.2	0.4	0.4	0.1	0.1	0.2	0.03	0.6	0.1	0.8	0.3	0.1	0.9
F (IC)	[mg/L]	<0,40	<0,40	<0,40	<0,40	<0,40	<0,40	<0,40	<0,40	<0,15	0.18	0.19	<0,40	<0,40	<0,40
SD F	[mg/L]										0.01	0.01			
Cl (IC)	[mg/L]	41.3	84.3	51.5	81.6	59.8	81.5	62.5	94.4	3.66	3.38	8.36	72.8	91.7	35
SD Cl	[mg/L]	0.2	0.1	0.5	0.1	0.1	0.1	0.1	0.1	0.02	0.01	0.02	0.1	0.1	0.1
Sulfat (IC)	[mg/L]	304.1	421.4	384.2	423.4	366	454	377.9	467.0	175.3	109.6	138.4	368.2	428.5	243.8
SD Sulfat	[mg/L]	0.1	0.2	0.2	0.3	0.3	1	0.1	0.3	0.1	0.1	0.1	0.2	0.1	0.2
NO_3 (IC)	[mg/L]	0.81	1.1	1.7	5.2	4	5.4	7.1	14.2	0.21	0.17	0.3	4.8	10.8	97.3
SD NO_3	[mg/L]	0.09	0.1	0.1	0.1	0.1	2.7	0.1	0.1	0.02	0.03	0.02	0.1	0.1	0.1
NO_3 (FM)	[mg/L]						4.9								
Nitrit (FM)	[mg/L]	0.029	0.032	0.056	0.158	0.023	0.088	0.130	0.109	<0,02	<0,02	<0,02	0.139	0.074	0.107
Phosphat (FM)	[mg/L]	0.42	0.55	0.65	0.27	0.08	0.22	0.39	0.12	0.07	0.15	0.1	0.07	0.13	0.1
Ammonium (FM)	[mg/L]	1.347	1.958	1.188	0.337	0.051	0.42	1.943	0.226	0.101	0.211	0.189	0.122	0.084	0.272
HCO_3 (Titration)	[mg/L]	549.8	521.7	507.9	489.8	501.6	480.5	531.2	455.9	571.0	616.2	604.5	497.1	479.7	526.7
Härte (berechnet) (berechnet)	[mmol/L]	7.30	8.58	7.83	8.37	7.57	8.64	7.85	8.70	6.08	5.68	5.92	7.70	8.28	7.20
	[dH]	40.9	48.1	43.9	47.0	42.4	48.4	44.0	48.8	34.1	31.9	33.2	43.2	46.4	40.4
DOC	[mg/L]	5.59	5.4		3.4	3.6	3.8	9.9	4.11	4.8	5.2	4.54	4.0	3.7	4.03
SD DOC	[mg/L]	0.06	0.1		0.2	0.1	0.1	0.3	0.03	0.2	0.3	0.03	0.2	0.04	0.02

Table A.4 Groundwater chemical analysis of August-2009

Para.	Unit	B1A14E	B2A13E	B2A13W	B2A16	B3A02E	B3A02W	B3A13E	B3A13W	B3A16E	B4A02	B4A05
T	[°C]	20.2	18.6	18.7	19.3	19.5	19.3	18.2	18.6	18.8	17.5	18.4
LF	[μS/cm]	1585	1606	1539	1635	1125	1175	1212	1527	1507	1580	1432
pH		8.57	8.95	6.73	7.25	7.19	7.09	7.02	7.08	7.32	7.00	7.10
UH	[mV]	210	210	210	210	220	50	85	250	210	470	430
O2	[mg/L]	3.3	2.2	2.5	2.0	2.8	1.6	2.6	2.5	1.7	2.7	3.2
O2	[%]	35	23	26	21	29	16	25	26	17	28	34
Al (MS)	[μg/L]	< 0,3	7.7	0.6	1.44	1.32	2.1	4.8	9.1	5.8	1.2	0.7
Al SD	[μg/L]		0.6	0.1	0.02	0.04	0.2	0.3	0.1	0.1	0.1	0.1
As (MS)	[μg/L]	< 0,9	1.2	< 0,9	1.33	2	4.6	< 0,9	2.9	1.5	< 0,9	< 0,9
As SD	[μg/L]		0.1		0.04	0.3	0.1		0.5	0.1		
B (MS)	[μg/L]	306	364.8	330	289	69.9	127	150	311	217	298	231
B SD	[μg/L]	3	0.4	3	1	0.5	1	1	4	3	3	1
Ba (MS)	[μg/L]	94.5	181	122.9	109.1	107.6	204.2	168.2	152.6	144.7	87.7	96.4
Ba SD	[μg/L]	0.7	3	0.6	0.5	0.2	0.5	0.2	0.7	0.7	0.9	0.9
Ca (AAS)	[mg/L]	275	261	259	283	223	221	223	257	259	265	246
SD Ca	[mg/L]	1	3	1	2	2	2	1	1	4	1	1
Cd (MS)	[μg/L]	< 0,05	< 0,05	< 0,05	< 0,05	< 0,05	< 0,05	< 0,05	< 0,05	< 0,05	0.09	0.06
Cd SD	[μg/L]										0.02	0.01
Co (MS)	[μg/L]	1.13	12.5	1.70	0.66	1.36	0.56	0.714	1.89	0.888	0.71	0.8
Co SD	[μg/L]	0.02	0.2	0.02	0.02	0.06	0.04	0.005	0.01	0.002	0.01	0.01
Cr (MS)	[μg/L]	< 0,2	< 0,2	< 0,2	< 0,2	< 0,2	< 0,2	< 0,2	< 0,2	< 0,2	< 0,2	< 0,2
Cr SD	[μg/L]											
Cs (MS)	[μg/L]	< 0,15	< 0,15	< 0,15	< 0,15	< 0,15	< 0,15	< 0,15	< 0,15	< 0,15	< 0,15	< 0,15
Cs SD	[μg/L]											
Cu (MS)	[μg/L]	0.11	0.21	0.18	< 0,1	< 0,1	< 0,1	< 0,1	0.23	< 0,1	0.86	0.74
Cu SD	[μg/L]	0.01	0.02	0.03					0.05		0.01	0.02
Fe (OES)	[mg/L]	0.032	0.247	0.017	0.239	0.58	0.387	0.198	1.07	0.2234	<0,004	<0,004
SD Fe	[mg/L]	0.005	0.005	0.004	0.005	0.01	0.006	0.001	0.02	0.0005		
K (OES)	[mg/L]	4.8	7.14	5.99	5.5	0.34	2.0	2.1	4.7	3.56	5.7	2.88
SD K	[mg/L]	0.2	0.03	0.06	0.1	0.05	0.1	0.1	0.5	0.04	0.1	0.04
Li (MS)	[μg/L]	17.3	23.3	22.4	15.4	2.66	6.1	7.9	18.5	7.4	21.0	12.6
Li SD	[μg/L]	0.1	0.2	0.2	0.2	0.02	0.1	0.1	0.02	0.1	0.1	0.1
Mg (AAS)	[mg/L]	38.3	39.0	37.6	40.8	23.4	24.3	25.5	36.8	35.2	38.7	34.7
Mn (OES)	[mg/L]	1.16	6.2	2.32	1.37	0.792	0.78	0.876	1.85	1.40	0.43	0.58
SD Mn	[mg/L]	0.01	0.1	0.04	0.02	0.004	0.01	0.004	0.04	0.02	0.01	0.01
Na (OES)	[mg/L]	53	53.8	51.6	50	19.07	18.5	24.7	49	42.4	52	36.6
SD Na	[mg/L]	1	0.2	0.6	1	0.02	0.2	0.1	1	0.6	1	0.4
Ni (MS)	[μg/L]	3.0	6.3	3.7	2.37	2.75	2.3	2.40	3.90	3.42	3.0	3.1

Ni SD	[μg/L]	0.2	0.2	0.1	0.04	0.05	0.1	0.01	0.02	0.02	0.1	0.1
P (OES)	[mg/L]	0.08	0.15	< 0,04	0.363	0.04	0.60	0.17	0.09	0.89	0.076	0.07
SD P	[mg/L]	0.02	0.02		0.006	0.01	0.03	0.01	0.02	0.01	0.006	0.02
Pb (MS)	[μg/L]	0.081	0.081	0.07	0.090	0.050	0.081	0.053	0.134	0.087	< 0,05	< 0,05
Pb SD	[μg/L]	0.001	0.005	0.01	0.005	0.002	0.005	0.002	0.003	0.001		
S (OES)	[mg/L]	144	140	136	203.2	65.6	60	75.0	128	259	144	98
SD S	[mg/L]	1	1	1	0.6	0.5	1	0.4	2	11	2	1
Si (OES)	[mg/L]	5.70	5.8	5.83	5.4	5.54	6.05	5.48	5.67	5.15	5.2	5.3
SD Si	[mg/L]	0.01	0.1	0.04	0.1	0.01	0.06	0.02	0.03	0.01	0.1	0.1
Sr (OES)	[mg/L]	3.04	3.35	3.21	3.05	0.945	1.42	1.53	2.92	2.30	3.3	2.64
SD Sr	[mg/L]	0.03	0.02	0.01	0.05	0.003	0.02	0.01	0.01	0.01	0.1	0.01
Ti (MS)	[μg/L]	1.1	0.8	0.8	1.14	0.5	1.4	0.93	0.9	1.8	0.53	0.6
Ti SD	[μg/L]	0.1	0.1	0.2	0.04	0.1	0.2	0.03	0.1	0.1	0.02	0.1
U (MS)	[μg/L]	11.32	9.32	8.5	9.76	11.24	11.49	8.34	9.29	7.18	9.40	11.42
U SD	[μg/L]	0.03	0.04	0.1	0.04	0.04	0.01	0.09	0.05	0.07	0.07	0.07
V (MS)	[μg/L]	0.5	0.6	< 0,5	0.61	1.1	1.0	0.6	1.8	0.6	< 0,5	< 0,5
V SD	[μg/L]	0.1	0.1		0.04	0.1	0.1	0.1	0.2	0.1		
Zn (MS)	[μg/L]	23.7	48.9	35.7	13.4	27.0	12.8	14.0	45.5	26.6	20.0	31.2
Zn SD	[μg/L]	0.1	0.6	0.3	0.3	0.4	0.2	0.1	0.4	0.4	0.3	0.8
F(IC)	[mg/L]	< 0,40	< 0,40	< 0,40	< 0,40	< 0,40	< 0,40	< 0,40	< 0,40	< 0,40	< 0,40	< 0,40
SD F	[mg/L]											
Cl (IC)	[mg/L]	82.0	88.9	84.8	82.1	4.57	10.5	24.2	78.3	51.6	86.5	48.3
SD Cl	[mg/L]	0.1	0.1	0.1	0.1	0.01	0.1	0.8	0.1	0.1	0.1	0.1
SO_4 (IC)	[mg/L]	424	418	401	400	188	100	185	375	303	406	287
SD SO_4	[mg/L]	1	1	1	1	1	1	1	1	1	1	1
NO_3 (IC)	[mg/L]	6.1	9.4	20.5	0.4	<0,15	0.5	1.2	8.3	0.9	11.0	
SD NO_3	[mg/L]	0.1	0.1	0.1	0.1		0.1	0.1	0.1	0.1	0.1	
NO_3 (FM)	[mg/L]											70
NO_2 (FM)	[mg/L]	0.100	0.166	0.107	< 0,02	< 0,02	< 0,02	0.364	0.193	< 0,02	0.089	0.207
PO_4 (FM)	[mg/L]	0.19	0.31	0.08	1.02	0.05	1.63	0.38	0.14	2.32	0.10	0.12
Ammonium (ISE)	[mg/L]	0.32	2.14	0.07	3.50	0.19	5.49	0.98	0.63	7.35	0.06	0.27
HCO_3	[mg/L]	489.0	476.0	446.3	564.1	601.9	718.7	605.2	502.3	646.8	472.3	522.6
Härte	[mmol/L]	8.44	8.12	8.01	8.74	6.53	6.51	6.61	7.93	7.91	8.20	7.57
	[°dH]	47.3	45.5	44.9	49.0	36.6	36.5	37.1	44.5	44.4	46.0	42.4
DOC	[mg/L]	3.9	2.5	2.9	2.6	3.5	5.1	4.3	3.1	4.8	2.6	3.0
SD DOC	[mg/L]	0.2	0.1	0.1	0.2	0.2	0.2	0.4	0.3	0.1	0.5	0.1

Table A.5 Groundwater chemical analysis of May-2010

Parameter	Unit	B1A04W	B1A04E	B1A14W	B1A14E	B2A03E	B2A13W	B3A02W	B3A02E	B3A05E	B3A13W	B3A13E	B3A16E	B4A02	B4A05
T	[°C]	10.9	10.9	10.9	10.8	11.2	11.2	11.4	11.4	10.9	11.3	11.4	11.1	10.6	10.5
LF	[μS/cm]	1423	1453	1253	1510	1616	1592	986	1019	1509	1210	1014	973	1448	1354
pH		7.17	7.23	7.21	7.18	7.19	7.17	7.21	7.23	7.32	7.11	7.21	7.32	7.1	7.21
UH	[mV]	240	60	320	210	10	140	190	130	90	390	140	20	160	450
O2	[mg/L]	5.3	5.4	4	3.6	3.1	3.4	2.6	2.7	5.8	3.5	2.8	4.7	2.3	3.2
O2	[%]	49	51	36	33	28	32	24	26	54	32	26	44	22	28
Al (MS)	[μg/L]	6.7	6.3	5.34	5.4	9.9	12	3.1	4.3095	5.737	8.7	172	16.6	7.4	12.69
Al SD	[μg/L]	0.2	0.2	0.01	0.2	0.1	0.1	0.1	0.0007	0.008	0.5	1	0.6	0.2	0.06
As (MS)	[μg/L]	<1	1.621	<1	1.3	2.3	3.8	1.9	1.8	<1	<1	1.79	1.66	<1	<1
As SD	[μg/L]		0.006		0.3	0.4	0.4	0.2	0.4			0.01	0.03		
B (MS)	[μg/L]	150	119.7	132.65	198	275.3	248	56.1	29.6	54	187.5	50.54	274	209	157.8
B SD	[μg/L]	2	0.3	0.07	3	0.9	1	0.2	0.2	1	0	0.05	2	3	0.8
Ba (MS)	[μg/L]	60.2	86.6	65	80.6	250.4	141	144	63	46.53	98	139	170.6	99	98.59
Ba SD	[μg/L]	0.6	0.9	1	0.5	0.5	0.8	3	1	0.09	2	1	0.3	1	0.02
Ca (OES)	[mg/L]	256	270	234	256	263	256	187.1	201.8	290	204	195	171	239	231.0
SD Ca	[mg/L]	4	7	1	7	7	6	0.2	0.8	1	1	1	2	1	0.7
Cd (MS)	[μg/L]	< 0,2	< 0,2	< 0,2	< 0,2	< 0,2	< 0,2	< 0,2	< 0,2	< 0,2	< 0,2	< 0,2	< 0,2	< 0,2	< 0,2
Cd SD	[μg/L]														
Co (MS)	[μg/L]	0.83	1.14	¡ 0,25	1.71	0.96	9.8	0.88	1.08	0.7895	0.368	1.105	1.36	2.41	0.72
Co SD	[μg/L]	0.01	0.04		0.03	0.07	0.2	0.03	0.04	0.0007	0.005	0.007	0.01	0.1	0.03
Cr (MS)	[μg/L]	0.24	0.37	< 0,2	< 0,2	< 0,2	< 0,2	< 0,2	< 0,2	< 0,2	< 0,2	0.43	< 0,2	1	< 0,2
Cr SD	[μg/L]	0.04	0.003									0.07		0.04	
Cs (MS)	[μg/L]	0.14	< 0,1	< 0,1	< 0,1	< 0,1	< 0,1	< 0,1	< 0,1	< 0,1	< 0,1	< 0,1	< 0,1	< 0,1	< 0,1
Cs SD	[μg/L]	0.02													
Cu (MS)	[μg/L]	0.63	0.31	0.8	0.36	1.008	0.51	0.29	0.3	0.42	1.47	0.93	0.608	0.5235	1.75
Cu SD	[μg/L]	0.04	0.01	0.04	0.02	0.007	0.05	0.02	0.03	0.02	0.08	0.004	0.004	0.0007	0.02

Fe (MS)	[μg/L]	1195.5	138.4	4.029	415	172.5	265	1068	591	661	6.4	654	330.2	54.4	18.2
Fe SD	[μg/L]	0.7	0.1	0.008	4	0.7	2	13	2	9	0.1	3	0.1	0.8	0.5
K (OES)	[mg/L]	2.02	0.63	1.8	3.4	6	6.9	0.84	0.3	0.16	4	0.7	4.82	5.6	2.51
SD K	[mg/L]	0.06	0.06	0.1	0.1	0.1	0.2	0.06	0.1	0.05	0.1	0.1	0.09	0.1	0.04
Li (MS)	[μg/L]	7.94	3.87	6.3	13.4	16.1	21	3.59	1.92	1.94	11.61	5.04	2.95	19	10.3
Li SD	[μg/L]	0.08	0.07	0.1	0.1	0.2	0.3	0.07	0.03	0.04	0.08	0.08	0.06	0.3	0.01
Mg (OES)	[mg/L]	33.7	29.4	27.28	36	38.3	39.2	21.75	22.13	35.7	29.6	20.8	23.2	36.3	32.8
SD Mg	[mg/L]	0.4	0.3	0.07	1	0.5	0.8	0.03	0.08	0.2	0.2	0.1	0.3	0.3	0.1
Mn (MS)	[μg/L]	1158	357.2	504.5	1339	2464	7000	374.8	626	211.95	1095	1275	1285	1721	851
Mn SD	[μg/L]	9	0.8	0.5	1	8	49	0.2	12	0.07	12	13	0	25	9
Na (OES)	[mg/L]	43.7	40.9	36.6	48.8	49	52	16.7	16.34	43.7	35.1	16.7	21.8	47.7	33.3
SD Na	[mg/L]	0.3	0.2	0.4	0.6	1	1	0.2	0.05	0.6	0.2	0.3	0.5	0.7	0.3
Ni (MS)	[μg/L]	3.55	2.9	3.21	3.6	3.7	8.1	2.6	2.537	3.405	5.1	3.26	7.4	5.4	4.69
Ni SD	[μg/L]	0.05	0.2	0.07	0.2	0.2	0.2	0.1	0.002	0.002	0.4	0.05	0.3	0.3	0.09
P (OES)	[mg/L]	¡ 0,04	0.17	0.096	0.19	0.65	0.49	0.12	0.107	0.09	0.26	0.12	0.88	0.3	0.13
SD P	[mg/L]		0.02	0.007	0.01	0.01	0.02	0.01	0.004	0.01	0.01	0.02	0.02	0.01	0.01
Pb (MS)	[μg/L]	0.114	0.166	< 0,1	< 0,1	0.31	0.166	< 0,1	< 0,1	< 0,1	< 0,1	0.5045	< 0,1	< 0,1	0.107
Pb SD	[μg/L]	0.004	0			0.009	0.003					0.0007			0
S (OES)	[mg/L]	118	124	86.2	123	141.8	122	25.1	41.3	130.2	83	26.3	57	109	77.3
SD S	[mg/L]	1	3	0.9	1	0.3	1	0.3	0.3	0.7	2	0.4	2	2	0.5
Si (OES)	[mg/L]	4.87	5.2	5.07	5.45	5.7	5.8	4.53	4.97	4.92	5.5	4.94	4.2	5.09	4.675
SD Si	[mg/L]	0.08	0.2	0.04	0.08	0.1	0.2	0.04	0.07	0.04	0.04	0.01	0.1	0.06	0.004
Sr (OES)	[mg/L]	2.13	1.36	1.52	2.67	3.08	3.24	1.161	0.85	1.56	2.1	1.15	1.49	3.02	2.4
SD Sr	[mg/L]	0.03	0.04	0.01	0.05	0.09	0.08	0.008	0.01	0.01	0.01	0.005	0.04	0.02	0.01
Th (MS)	[μg/L]	4.2	2.26	1.52	1.24	1	0.8	0.662	0.53	0.55	<0,5	<0,5	<0,5	<0,5	<0,5
Th SD	[μg/L]	0.2	0.04	0.03	0.04	0.02	0.02	0.001	0.02	0.02					
Ti (MS)	[μg/L]	1	1.159	0.87	1.096	2.748	1.98	1.02	0.9	1.1	1.4	3.8	2.38	1.238	1
Ti SD	[μg/L]	0.1	0.007	0.01	0.007	0.001	0.08	0.01	0.1	0.3	0.1	0.2	0.08	0.007	0.2

U (MS)	[μg/L]	10.5	10.27	9.45	9.534	6.04	7.51	7.88	7.96	9.2	6.21	7.4	3.39	7.97	10.3
U SD	[μg/L]	0.1	0	0.07	0.008	0.04	0.1	0.07	0.1	0.1	0.06	0.1	0.03	0.1	0.2
V (MS)	[μg/L]	<0,2	0.21	<0,2	0.29	0.417	0.43	0.29	0.2285	<0,2	0.22	0.59	0.68	0.29	0.24
V SD	[μg/L]		0.01		0.05	0.004	0.02	0.05	0.0007		0.03	0.07	0.05	0.09	0.05
Zn (MS)	[μg/L]	10.1	4.8	10.6	15.8	7.9	15.04	24.845	2.8	2.9	17	9.5	20.3	11.6	33.7
Zn SD	[μg/L]	0.5	0.1	0.4	0.4	0.1	0.04	0.007	0.02	0.3	1	0.3	0.3	0.5	0.7
F (IC)	[mg/L]	<0,40	<0,40	<0,40	<0,40	<0,40	<0,40	<0,15	<0,15	<0,40	<0,15	0.22	<0,15	<0,40	<0,40
SD F	[mg/L]											0.01			
Cl(IC)	[mg/L]	52.1	39.8	33.7	71.7	81.9	88.3	2.2	1.57	24.7	53.6	2.37	23.2	72.3	37.5
SD Cl	[mg/L]	0.1	0.1	0.1	0.2	0.1	0.1	0.06	0.01	0.1	0.3	0.01	0.1	0.1	0.1
SO_4 (IC)	[mg/L]	346.4	366.5	250.8	370.9	376.6	378.5	74.3	121.3	380.8	252.5	78.1	160	326.2	237.1
SD SO_4	[mg/L]	0.3	0.2	0.2	0.5	0.5	0.5	0.1	0.2	0.1	0.1	0.1	0.2	0.3	0.2
NO_3 (IC)	[mg/L]	0.4	0.6	1.6	3.2	<0,40	3	<0,15	<0,15	<0,40	4.3	0.3	<0,15	5.6	51.8
SD NO_3	[mg/L]	0.1	0.1	0.1	0.1		0.1				0.1	0.1		0.1	0.1
Nitrit (Fotometer)	[mg/L]	<0,02	<0,02	0.05	0.241	0.021	0.099	<0,02	<0,02	<0,02	0.062	<0,02	0.122	0.097	0.149
Phosphat (Fotometer)	[mg/L]	0.05	0.48	0.24	0.5	1.93	1.42	0.27	0.25	0.17	0.75	0.27	2.39	0.9	0.26
Ammonium (ISE)	[mg/L]	0.15	0.61	0.18	0.71	4.98	1.84	0.43	0.34	0.1	0.5	0.32	5.51	0.77	0.63
HCO3 (Titration)	[mg/L]	497.2	531.1	521.4	484.4	528.8	501.7	593.7	574.6	766.3	437.4	622	459.4	474.5	541.7
Härte (berechnet)	[mmol/L]	7.77	7.94	6.97	7.87	8.14	8.01	5.56	5.95	8.70	6.32	5.71	5.23	7.45	7.11
	[°dH]	43.6	44.6	39.1	44.1	45.7	44.9	31.2	33.3	48.8	35.4	32.0	29.3	41.8	39.9
DOC	[mg/L]	1.69	2.55	2.39	2	4.94	2.9	6.4	4	4.2	4.08	4.19	8.2	4.5	3.67
SD DOC	[mg/L]	0.07	0.06	0.06	0.2	0.04	0.3	0.2	0.1	0.2	0.09	0.07	0.1	0.1	0.08

Table A.6 Groundwater chemical analysis of July-2010

Parameter	Unit	B1A04W	B1A14E	B2A03E	B2A13E	B3A02E	B3A02W	B3A05E	B3A13E	B3A13W	B3A16E	B4A02	B4A05
T	[°C]	17.3	16.2	15.7	15.7	16.4	16.8	20.0	15.9	16.1	17.1	15.0	15.0
LF	[μS/cm]	1478	1310	1694	1617	1071	1017	1513	1065	1602	1230	1508	1388
pH		7.09	7.11	7.05	7.01	7.15	7.10	7.24	7.07	7.10	7.12	7.01	7.04
UH	[mV]	100	380	0	360	170	110	230	130	100	70	360	300
O2	[mg/L]	0.2	3.8	2.6	2.8	3.2	2.6	3.6	2.8	2.9	1.9	3.0	2.8
O2	[%]	2	38	26	28	33	27	40	29	29	20	30	28
Al (MS)	[μg/L]	6.37	5.25	6.6	6.5	10.1	3.988	4.3	4.5	5.5	6.741	5.2	5.52
Al SD	[μg/L]	0.1	0.07	0.2	0.2	0.1	0.006	0.006	0.09	0.09	0.006	0.1	0.07
As (MS)	[μg/L]	10.9	<1	2.5	1	1.2	2.3	<1	1.17	1.99	2.7	<1	<1
As SD	[μg/L]	0.3		0.3	0.03	0.3	0.3		0.01	0.04	0.4		
B (MS)	[μg/L]	247.3	192	340	329	52.9	112	105.8	58	294	158.5	264	203.35
B SD	[μg/L]	0.3	1	3	7	0.3	1	0	1	4	0.3	4	0.07
Ba (MS)	[μg/L]	160.4	94.4	161.4	115.4	87.29	166	74.6	132	151.6	197.5	84	103.9
Ba SD	[μg/L]	1	0.02	0.8	0.1	0.06	1	0.2	1	0.4	0	1	0.9
Ca (OES)	[mg/L]	259	230	275	261	211	196.4	293	204	257	216	247	232
SD Ca	[mg/L]	5	3	2	3	1	0.9	3	2	2	2	3	4
Cd (MS)	[μg/L]	<0,2	<0,2	<0,2	<0,2	<0,2	<0,2	<0,2	<0,2	<0,2	<0,2	<0,2	<0,2
Cd SD	[μg/L]												
Co (MS)	[μg/L]	2.2	0.36	1.01	2.01	0.92	0.726	0.49	1.15	19.7	0.96	2.08	6.1
Co SD	[μg/L]	0.06	0.03	0.08	0.06	0.04	0.001	0.03	0.04	0.2	0.02	0.03	0.2
Cr (MS)	[μg/L]	< 0,3	< 0,3	< 0,3	< 0,3	< 0,3	< 0,3	< 0,3	< 0,3	< 0,3	< 0,3	< 0,3	< 0,3
Cr SD	[μg/L]												
Cs (MS)	[μg/L]	< 0,1	< 0,1	< 0,1	< 0,1	< 0,1	< 0,1	< 0,1	< 0,1	< 0,1	< 0,1	< 0,1	< 0,1
Cs SD	[μg/L]												
Cu (MS)	[μg/L]	0.75	1.2	2.7	0.87	0.59	0.55	1.18	0.61	4.5	0.48	1	1.98
Cu SD	[μg/L]	0.06	0.1	0.2	0.09	0.01	0.06	0.03	0.1	0.3	0.09	0.1	0.02

Fe (MS)	[μg/L]	8217	1.55	122	15.905	244	944	45.7	400	529	505	23.3	240.8
Fe SD	[μg/L]	13	0.07	1	0.007	3	10	0.5	6	3	7	0.4	0
K (OES)	[mg/L]	4.32	2.58	7.4	6.74	0.67	1.42	0.22	0.99	7.2	2.85	6.29	3.2
SD K	[mg/L]	0.01	0.07	0.1	0.09	0.08	0.08	0.05	0.06	0.1	0.08	0.08	0.1
Li (MS)	[μg/L]	11.8	10.14	18.33	24	2.781	4.446	2.99	5.802	16	4.47	21.4	13.64
Li SD	[μg/L]	0.2	0	0.05	0.4	0.003	0.007	0.03	0.003	0.1	0.03	0.2	0
Lu (MS)	[μg/L]	<0,05	<0,05	<0,05	<0,05	<0,05	<0,05	<0,05	<0,05	<0,05	<0,05	<0,05	<0,05
Lu SD	[μg/L]												
Mg (OES)	[mg/L]	36.2	29.3	40.4	40.5	23.1	23	35.2	21.9	37.4	29.6	37.5	33.6
SD Mg	[mg/L]	0.6	0.4	0.2	0.5	0.2	0.1	0.4	0.2	0.3	0.3	0.4	0.5
Mn (OES)	[mg/L]	1.8	0.88	2.4	1.96	0.388	0.401	0.073	1.17	18.8	1.6	0.87	1.71
SD Mn	[mg/L]	0.03	0.01	0.02	0.02	0.002	0.003	0.001	0.01	0.2	0.01	0.01	0.02
Na (OES)	[mg/L]	47.9	40.4	57.1	54.8	17.3	19.9	46.4	18.1	49.3	30.2	50.2	36.8
SD Na	[mg/L]	0.6	0.4	0.2	0.6	0.2	0.2	0.8	0.1	0.8	0.4	0.6	0.5
Ni (MS)	[μg/L]	1.51	2.27	1.9	4.19	1.6	1.44	1.7	1.923	12.7	2	2.62	3.08
Ni SD	[μg/L]	0.02	0.06	0.1	0.02	0.3	0.02	0.2	0.009	0.4	0.1	0.03	0.06
P (OES)	[mg/L]	0.18	¡ 0,04	1.41	0.136	0.08	0.302	0.0427	0.06	0.98	0.43	0.16	0.121
SD P	[mg/L]	0.01		0.02	0.009	0.02	0.009	0.0005	0.02	0.04	0.03	0.02	0.009
Pb (MS)	[μg/L]	< 0,1	< 0,1	< 0,1	< 0,1	< 0,1	< 0,1	< 0,1	< 0,1	0.268	< 0,1	< 0,1	< 0,1
Pb SD	[μg/L]									0.001			
S (OES)	[mg/L]	121	90	200	132	46.5	28.4	125.7	28.3	109	77	114.8	83.6
SD S	[mg/L]	1	1	5	4	0.7	0.3	0.7	0.03	2	1	0.4	0.4
Si (OES)	[mg/L]	5.45	5.21	6	5.64	5.13	5.06	5.41	5.27	5.11	4.97	5.1	4.9
SD Si	[mg/L]	0.04	0.008	0.1	0.01	0.01	0.03	0.02	0.04	0.07	0.04	0.07	0.09
Sr (OES)	[mg/L]	2.71	1.857	3.22	3.41	0.91	1.26	1.641	1.217	2.65	1.96	3.21	2.61
SD Sr	[mg/L]	0.04	0.008	0.05	0.04	0.01	0.009	0.009	0.005	0.08	0.02	0.05	0.03
Ti (OES)	[mg/L]	<0,003	<0,003	<0,003	<0,003	<0,003	<0,003	<0,003	<0,003	<0,003	<0,003	<0,003	<0,003
SD Ti	[mg/L]												

U (MS)	[μg/L]	12.39	9.8	6.533	8.7	9.22	7.88	9.31	7.25	8.37	5.79	8.911	10.2
U SD	[μg/L]	0.01	0.1	0.002	0.02	0.04	0.1	0.03	0.06	0.08	0.06	0.004	0.1
V (MS)	[μg/L]	1.55	<1	<1	<1	<1	<1	<1	<1	<1	<1	<1	<1
V SD	[μg/L]	0.01											
Zn (MS)	[μg/L]	35	29.4	57.21	10.1	3	43.6	20.1	1.7	45.79	18.6	10.8	22.9
Zn SD	[μg/L]	1	0.7	0.02	0.3	0.3	0.7	0.6	0.2	0.02	0.3	0.4	0.7
F (IC)	[mg/L]	<0,4	<0,4	<0,4	<0,4	<0,15	<0,15	<0,4	0.20	<0,4	0.18	<0,4	<0,4
SD F	[mg/L]								0.01		0.01		
Cl (IC)	[mg/L]	64.0	42.2	92.8	95.3	1.30	2.16	24.8	3.54	72.8	29.90	78.2	45.1
SD Cl	[mg/L]	0.1	0.1	0.1	0.1	0.06	0.03	0.1	0.01	0.2	0.02	0.1	0.1
Sulfat (IC)	[mg/L]	367.4	274.6	367.6	395.7	139.2	74.3	373.3	88	320.6	204.4	351.5	252.8
SD Sulfat	[mg/L]	0.3	0.2	0.5	0.1	0.1	0.1	0.2	0.4	0.2	0.1	0.1	0.1
NO_3 (IC)	[mg/L]	0.7	3.1	1.6	11.9	<0,15	<0,15	<0,4	0.4	2.1	<0,15	3.0	36.5
SD NO_3	[mg/L]	0.1	0.1	0.1	0.1				0.1	0.1		0.1	0.1
Nitrit (FM)	[mg/L]	<0,02	<0,02	1.08	0.042	<0,02	<0,02	<0,02	<0,02	0.090	<0,02	0.048	0.670
PO_4 (FM)	[mg/L]	0.06	0.07	3.44	0.29	0.14	0.62	0.08	0.37	2.03	1.23	0.46	0.45
Ammonium (ISE)	[mg/L]	0.53	0.09	9.19	0.50			0.11		5.52	3.92	0.60	1.06
Ammonium (FM)	[mg/L]					0.137	0.621		0.246				
HCO3 (Titration)	[mg/L]	Störung	522.3	582.1	483.6	609.2	637.7	622.9	661.6	622.3	589.3	498.4	553.2
Härte (berechnet)	[mmol/L]	7.95	6.94	8.52	8.18	6.21	5.85	8.76	5.99	7.95	6.61	7.71	7.17
	[°dH]	44.6	38.9	47.8	45.9	34.9	32.8	49.1	33.6	44.6	37.1	43.2	40.2
DOC	[mg/L]	3.4	3.6	20.5	3.95	5.02	7.50	4.6	5.8	23.0	4.6	4.4	3.7
SD DOC	[mg/L]	0.1	0.2	0.1	0.02	0.06	0.08	0.1	0.1	0.3	0.1	0.1	0.2

Table A.7 Groundwater chemical analysis of August-2010

Parameter	Unit	B1A04E	B1A04W	B1A14E	B1A14W	B2A03E	B2A13E	B2A16E	B3A02E	B3A02W	B3A05E	B3A13E	B3A13W	B3A16E	B4A02	B4A05
T	[°C]	14.3	14.6	14.6	14.6	14.1	13.5	14.2	14.5	14.7	15.2	14.7	14.6	14.6	14.1	13.9
LF	[μS/cm]	1512	1503	1576	1409	1711	1588	1753	1198	1456	1562	1239	1541	1496	1460	1449
pH		7.11	7.00	7.08	7.12	7.20	7.03	7.09	7.15	7.03	7.28	7.11	7.07	7.09	7.13	7.21
UH	[mV]	70	90	50	210	-110	370	-110	150	-100	140	40	120	-30	40	80
O2	[mg/L]	2.95	2.26	2.47	2.37	0.75	2.94	0.69	2.48	1.04	4.65	2.53	2.59	2.36	2.41	2.8
O2	[%]	29.5	22.9	25.1	23.6	7.3	29.8	7	25.4	10.6	47.6	23.6	26.6	24	24.3	28.3
Bemerkungen						H2S!		H2S!		H2S!						
Al (MS)	[μg/L]	7.5	6.035	9.6	26	5.8	3.1	15.2	1.1	10.9	1.8	3.4	12.2	9.77	10.47	8.7
Al SD	[μg/L]	0.2	0.008	0.04	0.2	0.2	0.3	0.2	0.1	0.1	0.05	0.3	0.6	0.03	0.02	0.7
As (MS)	[μg/L]	1	2.51	1.1	¡ 0,5	3.4	1	2.6	0.6	3.1	0.8	3.2	0.8	2	1.1	¡ 0,5
As SD	[μg/L]	0.1	0.05	0.4		0.5	0.2	0.02	0.2	0.5	0.03	0.04	0.2	0.7	0.5	
B (MS)	[μg/L]	250	278	365	258.3	395	385.7	415	88.1	144	133.4	108.5	295.6	314.25	297	266
B SD	[μg/L]	4	3	2	0.9	4	0.8	5	0.8	1	0.8	0.9	0.2	0.07	4	2
Ba (MS)	[μg/L]	86.8	78.4	100.7	81.12	160	110.3	208.1	83.2	190.95	61.7	162	99.9	203.05	104.65	122
Ba SD	[μg/L]	0.8	0.2	0.6	0.03	1	0.1	0.1	0.6	0.07	0.8	3	0.6	0.07	0.07	1
Ca (OES)	[mg/L]	274.4	255.8	255.5	241	249	250	225	218.491	228.4	285.44	222	247.1	240	228	223
SD Ca	[mg/L]	0.8	0.2	0.9	1	1	1	0.7	0.004	0.4	0.08	0.8	0.5	2	1	2
Cd (MS)	[μg/L]	<0,1	<0,1	<0,1	0.13	<0,1	0.14	<0,1	<0,1	<0,1	<0,1	<0,1	<0,1	<0,1	<0,1	<0,1
Cd SD	[μg/L]				0.02		0.04									
Co (MS)	[μg/L]	1.12	1.28	2.11	0.64	0.83	0.68	0.7	1.15	0.49	0.96	1.41	1.2	0.92	1.58	3.9
Co SD	[μg/L]	0.08	0.08	0.1	0.04	0.03	0.04	0.06	0.05	0.02	0.02	0.04	0.1	0.08	0.03	0.08
Cr (MS)	[μg/L]	<0,3	<0,3	<0,3	<0,3	<0,3	<0,3	<0,3	<0,3	<0,3	<0,3	<0,3	<0,3	<0,3	0.4	<0,3
Cr SD	[μg/L]														0.1	
Cs (MS)	[μg/L]	<0,05	<0,05	<0,05	<0,05	<0,05	<0,05	<0,05	<0,05	<0,05	<0,05	<0,05	<0,05	<0,05	<0,05	<0,05
Cs SD	[μg/L]															
Cu (MS)	[μg/L]	2.88	2.925	2.9	2.9	3.1605	2.8	3.4	2.68	2.6	2.5	2.01	2.3	1.82	2.19	2.57

Cu SD	[μg/L]	0.01	0.001	0.1	0.2	0.0007	0.1	0.1	0.07	0.3	0.1	0.1	0.1	0.01	0.09	0.05
Fe (MS)	[μg/L]	275.6	1216.5	396	3.6	20	6	44.5	104	143	272	756.2	46.88	403	136.75	42.19
Fe SD	[μg/L]	0.3	0.7	2	0.2	1	0.6	1	2	2	5	0.3	0.03	3	0.07	0.08
K (OES)	[mg/L]	1.26	2.742	4.80	1.938	10.62	6.40	19.52	0.37	5.20	0.4504	1.43	5.97	5.82	8.01	6.2
SD K	[mg/L]	0.03	0.007	0.04	0.005	0.07	0.07	0.03	0.04	0.09	0.0004	0.05	0.06	0.03	0.03	0.1
Li (MS)	[μg/L]	5.02	9.718	17.6	7.4	16.32	23.3	14	2.68	6.64	2.5	6.9	19.57	9	19.8	18.9
Li SD	[μg/L]	0.02	0.008	0.4	0.06	0.04	0.6	0.4	0.06	0.07	0.2	0.1	0.03	0.2	0.2	0.3
Mg (OES)	[mg/L]	31.39	35.9	38.847	30.15	38.5	40.21	37.35	25.44	27.87	35.98	26.156	38.3	36.375	36.917	36.25
SD Mg	[mg/L]	0.06	0.05	0.009	0.09	0.1	0.02	0.03	0.02	0.09	0.005	0.005	0.1	0.003	0.0003	0.08
Mn (MS)	[μg/L]	617	1024	2152	6174	2485	718.2	1067	483	802	321.85	1892	1818	1334.5	1669	7670
Mn SD	[μg/L]	10	0	12	53	9	0.3	4	10	6	0.07	13	12	0.7	16	83
Na (OES)	[mg/L]	50.57	52.1	56.3	47.67	56.8	58.4	53.7	25.3	30.25	51	27.5	52.4	49.44	49.8	46.552
SD Na	[mg/L]	0.09	0.1	0.3	0.02	0.4	0.3	0.2	0.1	0.06	0.1	0.06	0.2	0.07	0.2	0.0008
Ni (MS)	[μg/L]	1	0.91	1.45	5.5	3.6	2.99	13.75	1.55	1.4	1.47	1.07	2.9	2.2	1.4	4.4
Ni SD	[μg/L]	0.2	0.02	0.04	0.2	0.2	0.03	0.07	0.02	0.2	0.01	0.07	0.2	0.3	0.09	0.2
P (OES)	[mg/L]	0.253	0.35	0.52	0.12	3.06	0.19	7.16	0.077	2.52	0.09	0.2752	0.47	0.96	1.31	0.698
SD P	[mg/L]	0.002	0.05	0.05	0.05	0.02	0.01	0.08	0.005	0.06	0.03	0.0001	0.03	0.03	0.02	0.008
Pb (MS)	[μg/L]	<0,1	<0,1	0.142	<0,1	<0,1	<0,1	<0,1	<0,1	<0,1	<0,1	<0,1	0.119	<0,1	<0,1	<0,1
Pb SD	[μg/L]			0.001									0.003			0.006
S (OES)	[mg/L]	119.7	122.4	124.1	101.1	381	130.474	607.5	74	264	132.28	69.95	112.19	161.55	90.9	93.07
SD S	[mg/L]	0.4	0.6	0.6	0.5	2	0.005	0.6	1	3	0.02	0.01	0.06	0.09	0.3	0.03
Si (OES)	[mg/L]	5.80	5.111	5.65	5.280	6.46	5.633	5.29	5.168	5.82	5.2909	5.47888	5.31	5.098	5.24	5.03
SD Si	[mg/L]	0.02	0.009	0.02	0.003	0.03	0.0005	0.02	0.002	0.01	0.0009	0.00008	0.04	0.002	0.02	0.01
Sr (MS)	[μg/L]	1456	2199	2865	1619.5	2936	3306.5	2663	1002	1498	1522	1501	2832	2430	2935	2747
Sr SD	[μg/L]	4	17	10	0.7	32	0.7	24	1	16	18	0	31	5	15	1
Ti (MS)	[μg/L]	1.9	1.8	2.7	0.7	8.3	1.3	15.5	0.6	7.1	0.95	1.3	2.49	3	4.3	2.274
Ti SD	[μg/L]	0.2	0.4	0.4	0.2	0.2	0.4	0.8	0.2	0.3	0.02	0.3	0.07	0.1	0.09	0.001
U (MS)	[μg/L]	10.34	10.2	7.4	9.18	3.024	7.786	2.63	9.053	5.3	9.617	6.71	7.96	4.94	6.168	7.74

U SD	[μg/L]	0	0.05	0.1	0.06	0.001	0.003	0.01	0.009	0.1	0.004	0.09	0.04	0.05	0.002	0.009
V (MS)	[μg/L]	0.28	0.3	0.34	0.36	0.63	0.3	1.12	0.3	0.53	0.36	0.35	0.26	0.5	0.31	0.24
V SD	[μg/L]	0.02	0.06	0.09	0.07	0.002	0.1	0.02	0.1	0.03	0.05	0.05	0.05	0.06	0.05	0.06
Zn (OES)	[mg/L]	0.066	0.0703	0.0502	0.10101	0.083	0.1014	0.1013	0.0125	0.0307	0.0743	0.016	0.01701	0.0488	0.0113	0.0089
SD Zn	[mg/L]	0.001	0.0004	0.0005	0.00007	0.001	0.0004	0.0006	0.0002	0.0002	0.0003	0.0007	0.00004	0.0003	0.0007	0.0004
F (IC)	[mg/L]	<0,3	<0,3	<0,3	<0,3	<0,3	<0,3	<0,3	<0,3	<0,3	<0,3	<0,3	<0,3	<0,3	<0,3	<0,3
SD F	[mg/L]															
Cl (IC)	[mg/L]	52.7	63.8	79	56.1	86.5	96.4	72.8	24.9	38.6	22.1	32.7	83.1	60.5	69.6	71.8
SD Cl	[mg/L]	0.1	0.1	0.1	0.1	0.1	0.1	0.1	0.1	0.1	0.1	0.1	0.1	0.1	0.1	0.1
SO_4 (IC)	[mg/L]	354.6	367.8	373.8	306.2	187.7	384.8	54.7	203.5	100	388.5	187.3	340.6	301	275.3	283.9
SD SO_4	[mg/L]	0.4	0.1	0.3	0.1	0.2	0.3	0.3	0.1	0.1	0.3	0.4	0.1	0.2	0.1	0.1
NO_3 (IC)	[mg/L]	0.73	0.77	1.01	4.3	0.51	9.8	0.42	1.41	<0,4	<0,4	0.57	4.2	0.78	2	5.1
SD NO_3	[mg/L]	0.02	0.01	0.01	0.1	0.01	0.1	0.02	0.02			0.01	0.1	0.01	0.1	0.1
Nitrit (Fotometer)	[mg/L]	<0,02	0.045	<0,02	0.036	0.326	<0,02	0.099	0.089	<0,02	<0,02	<0,02	0.029	0.035	0.043	0.042
Phosphat (Fotometer)	[mg/L]	0.45	0.46	1.07	0.25	7.8	0.45	16.2	0.06	5.5	0.08	0.52	1.1	2.21	3.43	1.56
Ammonium (ISE)	[mg/L]	0.946	0.558	2.621	0.302	23.1	0.537	53.1	0.17	28.8	0.19	0.95	1.67	5.46	3.96	3.99
HCO3 (Titration)	[mg/L]	558.5	518.7	517.7	523.1	801.4	468.2	980.7	567.4	814.1	655.1	602.2	508.7	595.3	571.6	541.3
Härte (berechnet)	[mmol/L]	8.14	7.86	7.97	7.25	7.80	7.89	7.15	6.50	6.85	8.60	6.62	7.74	7.48	7.21	7.06
	[°dH]	45.6	44.1	44.7	40.7	43.7	44.3	40.1	36.4	38.4	48.2	37.1	43.4	42.0	40.4	39.6
DOC	[mg/L]	33	26.2	22.5	20.9	44	13.7	83	16	45	9.3	9.9	5.9	6.3	6.8	4
SD DOC	[mg/L]	2	0.9	0.6	0.8	1	0.3	2	2	1	0.4	0.4	0.1	0.3	0.3	0.1

Table A.8 Chloride concentration in soil profile in mg/L

Sample ID	7/6/2010	8/5/2010	8/19/2010	9/2/2010	9/14/2010	10/12/2010
B1 A05/30	0.32		0.50	< 0,20	< 0,20	0.42
B1 A06/30	0.25		0.20	< 0,20	0.22	< 0,20
B1 A16/30	0.42		0.47	< 0,20	0.37	< 0,20
B1 A17/30	1.67		0.54	< 0,20	0.31	0.52
B2 A01/10	0.75	9.78	5.08	0.62	0.90	
B2 A01/20	0.28	0.63	1.13	0.23	0.30	
B2 A01/30			0.60	0.42	0.54	
B2 A01/60			0.99	1.38		2.00
B2 A04/60	1.78		0.23	< 0,20	0.24	0.36
B2 A05/60	0.35		0.57	0.27	0.31	< 0,20
B2 A06/10	0.30	10.85	1.41	< 0,20	0.29	6.73
B2 A06/20	0.33	0.45	0.36	< 0,20	0.22	13.09
B2 A06/30	0.19		0.34	< 0,20	0.26	0.22
B2 A07/20	0.45		0.23	< 0,20	0.20	0.31
B2 A07/30	0.31		0.27	< 0,20	0.30	0.30
B2 A08/20	0.25		0.31	< 0,20	< 0,20	0.30
B2 A08/30	0.21		1.58	1.05	0.28	< 0,20
B2 A09/10	0.32	1.48	0.29	< 0,20	0.24	0.28
B2 A09/20	0.40		0.36	< 0,20	0.20	0.24
B2 A09/30	0.18		0.33	0.21	0.21	0.23
B2 A10/10		7.38	1.04	0.24	0.29	2.04
B2 A10/20		3.25		0.41	0.26	2.97
B2 A10/60	0.31		6.10	0.30		0.20
B2 A11/10		2.35	0.55	< 0,20	0.20	0.92
B2 A11/60	0.58		5.68	1.02		0.23
B2 A12/10	0.35	7.31	0.81	< 0,20	0.22	
B2 A12/20	0.20	1.19	0.15	< 0,20	0.24	
B2 A12/30	0.21	0.54	0.20	0.33	0.27	
B2 A12/60			0.28	0.48	0.51	5.88
B2 A15/60	0.25		0.38	0.32	0.41	0.25
B2 A16/10			0.35	< 0,20	0.20	0.91
B2 A16/20			0.37	0.23	0.24	< 0,20
B2 A16/30			0.58	< 0,20	0.29	0.20
B2 A16/60	2.91		0.78	0.34	0.35	0.20
B2 A17/10	0.30	8.04	1.88	0.41	0.32	4.66
B2 A17/20	0.34		0.93	0.24	0.34	3.39
B2 A17/30	0.35		0.58	0.28	0.33	0.35
B2 A18/10	0.32	4.08	0.72	0.31	0.27	1.13
B2 A18/20	0.29	1.77	0.38	0.22	0.28	0.51
B2 A19/10	0.32	10.51	2.04	0.72	0.88	9.11
B2 A19/20	0.27		1.05	0.25	0.30	2.60
B2 A19/30	0.38		0.50	0.21	< 0,20	0.35
B2 A20/10	0.23	2.52	0.42	< 0,20	0.45	0.44
B2 A20/20	0.44	1.35	0.37	< 0,20	0.22	< 0,20

Table A.9 Chloride concentration in soil profile in mg/L continued....

Sample ID	7/6/2010	8/5/2010	8/19/2010	9/2/2010	9/14/2010	10/12/2010
B2 A21/10		2.17	0.75	< 0,20	< 0,8	0.20
B2 A21/20		0.96	0.55	0.26	0.54	0.54
B2 A21/60	0.20		0.56	< 0,20		< 0,20
B2 A22/10		1.80	0.62	0.25	0.62	0.32
B2 A22/20			5.49	< 0,20	0.34	7.16
B2 A22/60	0.34		0.52	< 0,20		0.25
B3 A05/20	0.28		0.33	0.43	< 0,20	0.63
B3 A06/20	0.27		0.21	< 0,20	< 0,20	0.51
B3 A06/30	0.27		0.58	0.21	< 0,20	0.32
B3 A07/20		4.25	0.46	< 0,20	< 0,20	0.37
B3 A17/20	4.29		0.68	0.20	< 0,20	0.27
B3 A17/30	1.96		4.12	0.94	0.37	0.69
B3 A20/20		0.63	0.25	0.28	< 0,20	1.67
B3 A20/30			0.49	< 0,20	< 0,20	0.74
B3 A23/20		4.43	0.18	< 0,20	< 0,20	0.20

Appendix B

Soil texture

Aufschluss

Lokalität: Jenaer Experiment	Plot: B1A04_EAST	Datum: 15.06.2006
Bearbeiter: G.Büchel, Y. Kreutziger	Location coordinate in UTM:(0684445,5647631)	
Bodenprobennummer: 8	Eingebaute Rohre: 1 Schlitz & 2 Vollrohre	

Horizontbeschreibung

Nr.	Horizontgrenzen		Merkmale			Anmerkungen	Bildnr.(Meter)
	Untergrenze [cm]	Schärfe	Farbe	Stratifizierung : Auelehm - Sande - Kiese	KG		
1	37		braun		Slu	aAh-Horizont	B2-B4 (0-1)
2	140		hellbraun/ ocker		Slu		B5-B7 (1-2)
3	200				Slu - fS	Kernverlust in 200-225cm	B8-B10 (2-3)
4	290				fS – mS	FeMn-Fleckung, sehr feucht, in 260cm Wurzeln	
5	340				mS		
6	400				Kiese		

Aufschluss

Lokalität: Jenaer Experiment	Plot: B1A04_WEST	Datum: 15.06.2006
Bearbeiter: G.Büchel, Y. Kreutziger	Location coordinate in UTM:(0684422,5647628)	
Bodenprobennummer: 9	Eingebaute Rohre: 1 Schlitz & 2 Vollrohre	

Horizontbeschreibung

Nr.	Horizontgrenzen		Merkmale			Anmerkungen	Bildnr.(Meter)
	Untergrenze [cm]	Schärfe	Farbe	Stratifizierung : Auelehm - Sande - Kiese	KG		
1	40		braun		Slu	aAh-Horizont	B1-B3 (0-1)
2	140		hellbraun/ ocker		Slu		B4-B6 (1-2)
3	220				Slu - fS	durchsetzt mit Kiesen	B7-B9 (2-3)
4	290				fS – mS	Grundwasser bei ca. 260cm, Wurzeln in 220cm, FeMn-Fleckung in 250-260cm, zwischen 260-285 feinere organikreiche Lage (nicht getrennt beprobt)	
5	>290 bis ca. 340		graubraun		Kiese, Schotter		B10

$B_1A_{04}E$ and $B_1A_{04}W$

Aufschluss

Lokalität: Jenaer Experiment	Plot: B4A14_WEST	Datum: 15.06.2006
Bearbeiter: A. Grawunder, Y. Kreutziger	Location coordinate in UTM:(0684390,5647617)	
Bodenprobennummer: 11	Eingebaute Rohre: 1 Schlitz & 2 Vollrohre	

Horizontbeschreibung

Nr.	Horizontgrenzen		Merkmale			Anmerkungen	Bildnr.(Meter)
	Untergrenze [cm]	Schärfe	Farbe	Stratifizierung : Auelehm - Sande - Kiese	KG		
1	38		braun		Slu	aAh-Horizont, bis 20cm Krümmelgefüge	B23-B25 (0-1)
2	80		hellbraun		Slu		B26-B28 (1-2)
3	130		hellbraun		Slu - fS	durchsetzt mit Kiesen	B29-B31 (2-3)
4	225		hellbraun		fS – mS mit U	in 150cm Wurzeln	
5	245		hellbraun			Übergangsbereich	
6	285		grau		gS	Grundwasser bei ca. 250cm	B32
7	390				Kiese		

Aufschluss

Lokalität: Jenaer Experiment	Plot: B1A14_EAST	Datum: 15.06.2006
Bearbeiter: Ch.Lorenz, Y. Kreutziger	Location coordinate in UTM:(0684414,5647618)	
Bodenprobennummer: 10	Eingebaute Rohre: 1 Schlitz & 2 Vollrohre	

Horizontbeschreibung

Nr.	Horizontgrenzen		Merkmale			Anmerkungen	Bildnr.(Meter)
	Untergrenze [cm]	Schärfe	Farbe	Stratifizierung : Auelehm - Sande - Kiese	KG		
1	45		braun		Slu	aAh-Horizont	B12-B14 (0-1)
2	140		hellbraun		Slu		B15-B17 (1-2)
3	185		hellbraun/ ocker		Slu		B18-B20 (2-3)
4	232				Ls		
5	293		braun/ schwarz		mS	Grundwasser bei ca. 250cm, FeMn-Fleckung, teilweise organikeinschlüsse	
6	310		grau		gS,Kiese	,	B21+B22 (3,4-4,0)
7	400		grau		Kiese, Schotter		

$B_1A_{14}E$ $B_4A_{14}W$

Aufschluss

Lokalität: Jenaer Experiment	Plot: B2A03_West	Datum: 15.06.2006
Bearbeiter: A. Grawunder, Y. Kreutziger	Location coordinate in UTM:(0684350,5647607)	
Bodenprobennummer: 13	Eingebaute Rohre: 1 Schlitz & 2 Vollrohre	

Horizontbeschreibung

Nr.	Horizontgrenzen		Merkmale			Anmerkungen	Bildnr.(Meter)
	Untergrenze [cm]	Schärfe	Farbe	Stratifizierung : Auelehm - Sande - Kiese	KG		
1	45		braun		Lu	aAh-Horizont	B42-B44 (0-1)
2	120		hellbraun		Lu		
3	210		hellbraun		fS		B45-B47 (1-2)
4	225		hellbraun			Übergangsbereich	
5	270		hellbraun-ocker		mS	Grundwasser bei ca. 230cm, grau braun FeMn Fleckung	B48-B50 (2-3)
6	350		grau		gS		
7	350 - 400				Kiese		B51-B53 (3-4)

Aufschluss

Lokalität: Jenaer Experiment	Plot: B2A03_EAST	Datum: 15.06.2006
Bearbeiter: A. Grawunder, Y. Kreutziger	Location coordinate in UTM:(0684371,5647608)	
Bodenprobennummer: 12	Eingebaute Rohre: 1 Schlitz & 2 Vollrohre	

Horizontbeschreibung

Nr.	Horizontgrenzen		Merkmale			Anmerkungen	Bildnr.(Meter)
	Untergrenze [cm]	Schärfe	Farbe	Stratifizierung : Auelehm - Sande - Kiese	KG		
1	40		braun		Lu	aAh-Horizont	B33-B35 (0-1)
2	81		hellbraun		Lu	Regenwurm in 80cm	
3	90		hellbraun		Lu	durchsetzt mit gerundeten Kiesen	B36-B38 (1-2)
4	140		hellbraun		fS		
5	230		hellbraun		fS	sehr feucht	B39-B41 (2-3)
6	270		grau -braun		fS - mS	Altwassersedimente	
7	>270 - 400		bunt		G + Gerölle		

$B_2A_{03}E$ and $B_2A_{03}W$

Aufschluss

Lokalität: Jenaer Experiment	Plot: B1A17	Datum: 14.06.2006
Bearbeiter: Ch.Lorenz, Y. Kreutziger	Location coordinate in UTM:(0684438,5647687)	
Bodenprobennummer: ?	Eingebaute Rohre: 1 Schlitz & 1 Vollrohr	

Horizontbeschreibung

Nr.	Horizontgrenzen		Merkmale			Anmerkungen	Bildnr.(Meter)
	Untergrenze [cm]	Schärfe	Farbe	Stratifizierung : Auelehm - Sande - Kiese	KG		
1	40		dunkel-braun		Lu	aAh-Horizont	B8 (0-1)
2	100		braun		Lu	organikreich	B9 (1-2)
3	145		braun		Ut4	Übergangsbereich	B10 (2-3)
4	245		braun		Lu		B11 (3-4)
5	>245		grau-braun		MS, Kiese, Schotter	FeMn-Fleckung, sehr feucht	
	bis 380cm						

Aufschluss

Lokalität: Jenaer Experiment	Plot: B2A06_EAST	Datum: 16.06.2006
Bearbeiter: A. Grawunder, M. Lonschinski, Y. Kreutziger	Location coordinate in UTM:(0684396,5647675)	
Bodenprobennummer: 20	Eingebaute Rohre: 1 Schlitz & 1 Vollrohr	

Horizontbeschreibung

Nr.	Horizontgrenzen		Merkmale				Anmerkungen	Bildnr.(Meter)
	Untergrenze [cm]	Schärfe	Farbe	Farbe nach Munsel Farbtafel	Stratifizierung : Auelehm - Sande - Kiese	KG		
1	45		braun	10YR 4/2		Lu-Slu	aAh-Horizont	B34-B36 (0-1)
2	112		hellbraun	10YR4/4		Lu-Slu		
3	130		hellbraun	10YR4/4		fS mit Kiesen	ab 1,80m feucht, Wurzeln bei 150cm	B37-B39 (1-2)
4	228		hellbraun-grau	10YR4/2		fS	Grundwasser bei 230cm	
5	360		rostig grau-braun	10YR4/2		fS-mS-Kiese	Reduktionshorizont bei 280cm – 10 YR5/4	

$B_1A_{17}E$ and$B_2A_{06}E$

Aufschluss

Lokalität: Jenaer Experiment	Plot: B2A13_EAST	Datum: 15.06.2006
Bearbeiter: A. Grawunder, M. Lonschinski, Y. Kreutziger Location coordinate in UTM:(0684343,5647598)		
Bodenprobennummer: 14	Eingebaute Rohre: 1 Schlitz & 2 Vollrohre	

Horizontbeschreibung

Nr.	Horizontgrenzen		Merkmale			Anmerkungen	Bildnr.(Meter)
	Untergrenze [cm]	Schärfe	Farbe	Stratifizierung : Auelehm - Sande - Kiese	KG		
1	0		braun		Lu	aAh-Horizont	B54-B56 (0-1)
2	7		hellbraun/ ocker		Lu	ab ca. 80 cm gerundete Kiese	
3	6				fS	FeMn-Fleckung mit grauen tonigen Einlagen	B57-B60 (1-2)
4	5		grau-braun		mS-gS	feucht	
5	0		grau		gS-Kiese	Grundwasser bei ca. 220cm	B61-B63 (2-3)
6	5				mS-gS	260-275cm Reduktionshorizont	
7	0		braun-bunt		G		B68-B70 (3-4)
8	0		grau		gS-G		
9	0				G-gS	Muschelstücke keine Bodenproben	
10	0				mS-gS		
11	>380						

Aufschluss

Lokalität: Jenaer Experiment	Plot: B2A13_WEST	Datum: 16.06.2006
Bearbeiter: A. Grawunder, Y. Kreutziger Location coordinate in UTM:(0684323,5647588)		
Bodenprobennummer: 19	Eingebaute Rohre: 1 Schlitz & 2 Vollrohre	

Horizontbeschreibung

Nr.	Horizontgrenzen		Merkmale			Anmerkungen	Bildnr.(Meter)
	Untergrenze [cm]	Schärfe	Farbe	Stratifizierung : Auelehm - Sande - Kiese	KG		
1	47		braun		Lu	aAh-Horizont	B22-B24 (0-1)
2	87		hellbraun/ ocker/braun		Lu	mit Organik	
3	145		hellbraun		Ut4		B25-B27 (1-2)
4	187		grau-braun		fS		
5	230				mS-gS-Kiese	sehr feucht, FeMn-Fleckung, Grundwasser bei ca. 190cm	B28-B30 (2-3)
6	400		bunt		gS-Kiese-Schotter	260-275cm Reduktionshorizont	

$B_2A_{13}E$ and $B_2A_{13}W$

Aufschluss

Lokalität: Jenaer Experiment	Plot: B2A16	Datum: 14.06.2006
Bearbeiter: Ch. Lorenz, Y. Kreutziger	Location coordinate in UTM:(0684368,5647664)	
Bodenprobennummer: 19	Eingebaute Rohre: 1 Schlitz & 2 Vollrohre	

Horizontbeschreibung

Nr.	Horizontgrenzen		Merkmale			Anmerkungen	Bildnr.(Meter)
	Untergrenze [cm]	Schärfe	Farbe	Stratifizierung : Auelehm - Sande - Kiese	KG		
1	45		braun		Lu	aAh-Horizont	B12 (0-1)
2	140		ocker/braun		Lu		B13 (1-2)
3	200		grau-braun		mS,fS	FeMn-Fleckung, feucht	B14 (2-4)
4	300		grau		mS	mit Organikeinlagen	gestaucht
5	400		braun-grau		Kiese,gS	Grundwasser	

Aufschluss

Lokalität: Jenaer Experiment	Plot: B2A17_EAST	Datum: 16.06.2006
Bearbeiter: M.Lonschinski, Y. Kreutziger		
Bodenprobennummer: 22	Eingebaute Rohre: 1 Schlitz & 1 Vollrohr	

Horizontbeschreibung

Nr.	Horizontgrenzen		Merkmale			Anmerkungen	Bildnr.(Meter)
	Untergrenze [cm]	Schärfe	Farbe	Stratifizierung : Auelehm - Sande - Kiese	KG		
1	40		braun		Lu	aAh-Horizont	B49-B51 (0-1)
2	113		ocker/ hellbraun		Ut4		B53-B55 (1-2,2)
3	140				Ut4 mit Kiesen	wahrscheinlich anthropogen	
4	177		hellbraun		fS	FeMn-Fleckung	
5	220		grau		Kiese,gS, mS	Grundwasser bei ca. 180cm, keine Beprobung da zu wenig Material	

$B_2A_{16}E$ and $B_2A_{17}E$

Aufschluss

Lokalität:	Jenaer Experiment	Plot:	B3A02_WEST	Datum:	15.06.2006
Bearbeiter:	M.Lonschinski, A.Grawunder, Y. Kreutziger	Location coordinate in UTM:(06844284,5647586)			
Bodenprobennummer: 15		Eingebaute Rohre: 1 Schlitz & 1 Vollrohr			

Horizontbeschreibung

Nr.	Horizontgrenzen		Merkmale			Anmerkungen	Bildnr.(Meter)
	Untergrenze [cm]	Schärfe	Farbe	Stratifizierung : Auelehm - Sande - Kiese	KG		
1	30		braun		Lu	aAh-Horizont	B72-B74 (0-1)
2	135		ocker/ hellbraun		Lu		B75-B77 (1-2)
3	170		ocker/ hellbraun		fS mit Kiesen	sehr feucht	
4	350		grau		gS mit Kiesen		B78-B80 (2-3)

Aufschluss

Lokalität:	Jenaer Experiment	Plot:	B3A05_EAST	Datum:	16.06.2006
Bearbeiter:	M.Lonschinski, Y. Kreutziger	Location coordinate in UTM:(0684332,5647656)			
Bodenprobennummer: 21		Eingebaute Rohre: 1 Schlitz & 1 Vollrohr			

Horizontbeschreibung

Nr.	Horizontgrenzen		Merkmale			Anmerkungen	Bildnr.(Meter)
	Untergrenze [cm]	Schärfe	Farbe	Stratifizierung : Auelehm - Sande - Kiese	KG		
1	7		braun		Lu	aAh-Horizont	B43-B45 (0-1)
2	57		hellbraun		Ut4	Organikeinlagen	B46-B48 (1-2,5) überbohrt
3	86		hellbraun		fS, mS	sehr feucht	
4	250		grau/ hellbraun		gS, Kiese	mit Toneinlagen	

$B_3A_{02}W$ and $B_3A_{02}W$

Aufschluss

Lokalität:	Jenaer Experiment	Plot:	B3A13_EAST	Datum:	15.06.2006
Bearbeiter:	A.Grawunder, M. Lonschinski, Y. Kreutziger	Location coordinate in UTM:(0684274,5647577)			
Bodenprobennummer: 17			Eingebaute Rohre: 1 Schlitz & 2 Vollrohre		

Horizontbeschreibung

Nr.	Horizontgrenzen		Merkmale			Anmerkungen	Bildnr.(Meter)
	Untergrenze [cm]	Schärfe	Farbe	Stratifizierung : Auelehm - Sande - Kiese	KG		
1	40		braun		Lu	aAh-Horizont	B84-B86 (0-1)
2	112		hellbraun/ ocker		Ut4		B87-B89 (1-2)
3	160		braun		fS	FeMn-Fleckung, Grundwasser bei ca. 160cm	
4	350		grau		gS-mS-Kiese		B90-B92 (2-4) überbohrt

Aufschluss

Lokalität:	Jenaer Experiment	Plot:	B3A13_WEST	Datum:	16.06.2006
Bearbeiter:	A.Grawunder, Y. Kreutziger	Location coordinate in UTM:(0684254,5647575)			
Bodenprobennummer: 17			Eingebaute Rohre: 1 Schlitz & 2 Vollrohre		

Horizontbeschreibung

Nr.	Horizontgrenzen		Merkmale			Anmerkungen	Bildnr.(Meter)
	Untergrenze [cm]	Schärfe	Farbe	Stratifizierung : Auelehm - Sande - Kiese	KG		
1	37		braun		Ut4	aAh-Horizont	B1-B3 (0-1)
2	120		hellbraun		Ut4	Regenwurm in 70-80cm	B4-B6 (1-2)
3	150		Grau meliert		Ut4-fS	Übergangsbereich, organikreich	
4	190		Hellbraun, rostig, grau		fS-mS	FeMn-Fleckung, organikreich	
5	250				mS-gS-Kiese		
6	260		grau		Ton		B7-B9 (2-3)
7	350				Kiese, Schotter		

$B_3A_{13}E$ and $B_3A_{13}W$

Aufschluss

Lokalität: Jenaer Experiment	Plot: B3A16	Datum: 15.06.2006
Bearbeiter: Chr. Lorenz, Y. Kreutziger	Location coordinate in UTM:(0684297,5647647)	
Bodenprobennummer: ?	Eingebaute Rohre: 1 Schlitz & 2 Vollrohre	

Horizontbeschreibung

Nr.	Horizontgrenzen		Merkmale			Anmerkungen	Bildnr.(Meter)
	Untergrenze [cm]	Schärfe	Farbe	Stratifizierung : Auelehm - Sande - Kiese	KG		
1	25		dunkel-braun		Lu	aAh-Horizont	B15 (0-1)
2	80		braun		Lu		B16 (1-2)
3	155		hellbraun		fS-U	FeMn-Fleckung ab ca. 125cm, Wechsellagen, bis 140cm Wurzel ersichtlich	
4	250		grau/ocker		mS	feucht, mit organikeinschlüssen	B17
5	bis 4m		Bunte Mischung		mS-Kiese	Grundwasserbereich	B18 (2-4) überbohrt

Aufschluss

Lokalität: Jenaer Experiment	Plot: B4A02	Datum: 14.06.2006
Bearbeiter: Chr. Lorenz, Y. Kreutziger	Location coordinate in UTM:(0684234,5647621)	
Bodenprobennummer: ?	Eingebaute Rohre: 1 Schlitz & 2 Vollrohre	

Horizontbeschreibung

Nr.	Horizontgrenzen		Merkmale			Anmerkungen	Bildnr.(Meter)
	Untergrenze [cm]	Schärfe	Farbe	Stratifizierung : Auelehm - Sande - Kiese	KG		
1	40		braun		Ut4	aAh-Horizont	B19 (0-1)
2	145		hellbraun		Ut4		B20 (1-2)
3	200		graubraun		fS -mS	Organikeinschlüsse, Grundwasser bei ca. 170cm	
4	300		braun		mS		B21 (2-3)
5	350				mS, Kies, Schotter		B22 (3-3,5)

$B_3A_{16}E$ and B_4A_{02}

Aufschluss

Lokalität: Jenaer Experiment	Plot: B4A05	Datum: 14.06.2006
Bearbeiter: Chr. Lorenz, Y. Kreutziger	Location coordinate in UTM:(0684201,5647602)	
Bodenprobennummer: ?	Eingebaute Rohre: 1 Schlitz & 2 Vollrohre	

Horizontbeschreibung

Nr.	Horizontgrenzen		Merkmale			Anmerkungen	Bildnr.(Meter)
	Untergrenze [cm]	Schärfe	Farbe	Stratifizierung : Auelehm - Sande - Kiese	KG		
1	30		braun		Ut4	aAh-Horizont	B23 (0-1)
2	130		hellbraun		Ut4		B24 (1-2)
3	180		hellbraun		fS	FeMn-Fleckung in 170cm	
4	260		grau		mS	Grundwasser bei ca. 260cm, Wurzeln bei 240cm	B25 (2-3)
5	>260		bunt		Kiese		

Aufschluss

Lokalität: Jenaer Experiment	Plot: B4A13	Datum: 14.06.2006
Bearbeiter: Chr. Lorenz, Y. Kreutziger		
Bodenprobennummer: ?	Eingebaute Rohre: 1 Schlitz & 2 Vollrohre	

Horizontbeschreibung

Nr.	Horizontgrenzen		Merkmale			Anmerkungen	Bildnr.(Meter)
	Untergrenze [cm]	Schärfe	Farbe	Stratifizierung : Auelehm - Sande - Kiese	KG		
1	40		braun		Ut4	aAh-Horizont	B26 (0-1)
2	140		hellbraun		Ut4	ab 75cm FeMn-Fleckung	B27 (1-2)
3	240		hellbraun		fS mit U wechsel-lagig	feucht, Grundwasser bei ca. 200cm	
4	>240				mS-Kiese		B28 (2-3)

B_4A_{02} and B_4A_{13}

Aufschluss

Lokalität: Jenaer Experiment	Plot: B1A09_Zaun	Datum: 14.06.2006
Bearbeiter: Ch.Lorenz, Y. Kreutziger		
Bodenprobennummer: ?	Eingebaute Rohre: 1 Schlitz & 3 Vollrohre	

Horizontbeschreibung

Nr.	Horizontgrenzen		Merkmale			Anmerkungen	Bildnr.(Meter)
	Untergrenze [cm]	Schärfe	Farbe	Stratifizierung : Auelehm - Sande - Kiese	KG		
1	42		dunkel-braun		Slu	aAh-Horizont	B1 (0-1)
2	112		braun		Slu	organikreich	B2 (1-2)
3	130				Slu - fs	Übergangsbereich	
4	145				fs		
5	260		ocker-braun		Ts/fs	FeMn-Fleckung, sehr feucht	
6	365		grau-braun		fS - mS	Grundwasser,	B3 (2-3)
7	380				Kiese		B4
8	385		schwarz			Organische Lage	B5/6
9	>385		grau		Kiese	Pleistozäne Niederterasse	B7-fertige Messstelle

$B_1 A_{09}$

Sebständigkeitserklärung

Ich erkläre, daß ich die vorliegende Arbeit selbständig und unter Verwendug der angegebenen Hilfsmittel, persölichen Mitteilungen und Quellen angefertigt habe.

November 11, 2011, Jena

Sisay Girma Tessema

Curriculum Vitae

Marital status-Married

Birth date-1979

Birth place- Arsi (Assela), Ethiopia

Education

- **1998-2003**-Bachelor of Science in Chemical Engineering, Bahir dar University, Engineering Faculty, Bahir dar, Ethiopia
- **2005–2007**-Masters of Science in Environmental Science and Technology, IHE-Institute for water education Delft, The Netherlands

Experience

- **Apr 2003-Sep 2003**- Process foreman, Adami Tullu pesticide processing share company, Zeway, Ethiopia.
- **Sep 2003-2005**- Graduate Assistant, Bahir dar University Engineering faculty,Bahir dar, Ethiopia
- **2007-2008**-Assistant Lecturer, Bahir dar University Engineering faculty, Bahir dar, Ethiopia.
- **2008-Present**-PhD Student in University of Jena, Institute of Geoscience Jena,Germany.

Languages

English-Fluent, Amharic-Fluent, German-Basic

Acknowledgements

This work is financed by Helmholtz Initiative and Networking Fund through HI-GRADE (Helmholtz Interdisciplinary Graduate School for Environmental Research) theme.

I am sincerely and heartily grateful to my supervisor Prof. Dr. Georg Büchel for his guidance, advice, constructive criticisms, personal advices, encouragement and insight throughout my research. I also owe Georg unforgettable memory-Aloha Necklace from Hawaii. Thank you so much! I also would like to thank my second supervisor Prof. Dr. Sabine Attinger for her support and guidance.

I am much indebted to Jun. Prof. Dr. Anke Hilderbrandt and Dr. Dirk Merten for critical reading of this work, useful discussions and suggestions. It was multidisciplinary and helped me to see and understand my work in multiple direction. Thank you Anke for your time to read all the report, useful comments, and discussions. I would also like to thank Dr. Gerd Gleixner from Max-Planck Institute of Biogeochemistry for his useful suggestions and discussions on chemical composition of soil water. I owe sincere and earnest thankful to Dr. Jude Musuuza for many suggestions, discussions we had during my work. I am also grateful to Gerit Weinzierl, for lab analysis and for her tips of some useful German words in the lab. I also would like to thank Marc-André Allers from ETH Zürich for determination of groundwater oxygen and hydrogen isotopes.

I would also like to thank to Dr. Anja Grawunder, Dr. Martin Lonschinski an Daniel Mirgorodsky for introducing me to the field fork during my beginning of research; specially Daniel for his help (specially the hard water filtering in the summer) throughout my field work and feedback to know more about the background information about the study area. I also would like to thank Dr. Karin Eusterhues for her help in determining the x-ray diffraction of soil samples and Uta Gerighausen from Max-Planck Institute of Biogeochemistry for soil water sampling. I also would like to thank my officemate Delphine Ollivier for useful discussions we had.

I acknowledge the cooperativeness of TLUG (Thüringer Landesanstalt für Umwelt und Geologie), for providing me the river discharge data used in this study.

I would like to take this opportunity to thank Anahita, Tsilla, Getnet, Francissica, Brandlove, Sneha, Sathish and all other old Am Hernbergers. You enriched my knowledge of different cultures, and made my stay in Jena more beautiful. Thank you for being my friends. I also would like to thank my group for so many occasions we had together. I had the best experiences which I don't forget.

I would like to thank my parents brother, sister, and friends who have been encouraging and supporting me all thorough my carrier. Last but not least, I would like to thank my wife Hana, for her care, support and endless patience throughout my stay.

Propositions (Thesen)

- The study area was characterized in terms of groundwater and soil water geochemical processes and hydrogeology. Result of interpretation of the groundwater hydrochemical data using statistical technique shows that there are five dominant factors that account for about 90% of the variation of the chemical data set in the cold season (March, April, November) and the warm season (June, August). Groundwater-geological matrix interaction is the dominant factor.

- The spatial variation of the groundwater chemical composition of the experimental field was analyzed and the result showed that sampled plots (BIIIA02, BIIIA13) in block III have relatively different chemical composition from other plots. Hydrogen and oxygen isotope of the groundwater results also shows that most of the ground waters in wells of block III specially plots B3A13 and B3A02 are more enriched than that in other plots.

- we investigated the effect external factors (nearby river Saale, and an underground channel) on the groundwater of the study area. The results show that there is no significant effect of the river on the groundwater of the study area at mean river flow. However, Fe, K, Ca, Cl, Mg, Mn, SO_4^{2-} and NO_3^- concentrations of the groundwater are predicted to increase significantly when the influx of the river increases toward the groundwater of the study area. Chloride concentration (used as hydrologic tracer) measured at the inlet of the channel and in groundwater shows that the channel did not leak and therefore has no effect on the groundwater.

- The upward chloride transport during water stress, could not show a clear correlation between the aboveground diversity and water flow in the unsaturated zone. However, we could see a positive correlation of LAI (leaf area index) and chloride accumulation. Plots with a higher rate of evapotranspiration showed a higher accumulation of more chloride near the surface of the earth.